SYNTHESIS AND CHARACTERIZATION OF HOLE-TRANSPORTING AND ELECTROLUMINESCENT POLYMERS

Thesis by
Erika Bellmann

In Partial Fulfillment of the Requirements
for the Degree of
Doctor of Philosophy

California Institute of Technology
Pasadena, California

2000
(Submitted 12-6-99)

Acknowledgements

I would first like to thank Professor Robert H. Grubbs for the opportunity to be a member of his research group. I would also like to thank him for the opportunity to leave his group for extended periods of time in order to go to the University of Arizona or to various meetings and conferences. He always encouraged independence, the pursuit of one's own ideas, and collaboration efforts. I appreciate the fact that I have always enjoyed great freedom in determining the direction of my project. This has allowed me to explore and develop my own scientific interests. It has been sometimes a challenge and always a valuable learning experience.

The Grubbs group was a fun group to be part of. Many interesting and talented people have been my fellow-"Grubbies", and I would like to thank all the students and post-docs, with whom I overlapped, for upholding a productive but relaxed work environment in the group, and for always being helpful. I owe special thanks to Dr. Michael W. Wagaman, who helped me get started.

I also want to thank the members of my thesis committee—Professors Harry B. Gray, Dennis A. Dougherty and Nathan S. Lewis—for their support and constructive criticism. In particular, I would like to acknowledge Harry for always knowing how to take the pressure out of a situation and for writing several letters of recommendation for me. Nate gave me the opportunity to work in his group for a short time to explore a possible other application for the polymers that I have made. I appreciate that.

Next to chemistry, understanding of device physics and materials issues was just as crucial for the success of my research project. The cooperation with the groups of Nasser Peyghambarian (Optical Sciences Center, Univ. of Arizona) and Professor Seth R. Marder (Dept. of Chem., Univ. of Arizona) was essential throughout my graduate career, because it gave me the opportunity to acquire the necessary knowledge in the field of materials chemistry and device engineering. I am very much indebted to Dr. Sean E. Shaheen, Dr. Ghassan E. Jabbour, Dr. Steven Barlow and Dr. S. Thayumanavan, who were students and post-docs in these groups. They have taught me many valuable technical skills, were very patient in letting me use their equipment, and discussions with them were a tremendous help in furthering my research.

I also would like to thank all the other members of The Center for Advanced Multifunctional Polymers (CAMP) for their expert advice and support. CAMP was an ONR funded cooperation effort and a great source of information and interdisciplinary expertise.

Finally, I would like to thank the magic forces of market economy for causing all that competition between the long-distance telephone companies. The cheapest available rate for calls to Germany decreased from 46 cents in September 1995 to 9 cents in October 1999. This helped to closely stay in touch with my parents in Berlin, whom I can not thank enough for all their love, encouragement and understanding. Local or Zone 3 family support was provided by my friend Debby. I thank her for it.

Abstract

This thesis describes research on synthesis and characterization of electroluminescent and hole-transporting polymers for applications in organic light-emitting diodes (OLEDs). The first part of the project focuses on the synthesis of derivatives of the electroluminescent polymer poly(*para*-phenylenevinylene) (PPV) using ring-opening metathesis polymerization (ROMP) of substituted barrelenes. Barrelenes (a certain kind of bicyclic olefins) have been prepared through multi-step synthetic procedures, and the existing synthetic route was extended to barrelenes without electron-withdrawing groups. ROMP of barrelenes was explored because this polymerization can be living, which allows the preparation of well-defined polymeric products. A new version of a soluble PPV derivative was prepared *via* this route.

The second part of the project focuses on hole-transporting (HT) polymers. A range of HT polymers were prepared *via* ROMP and anionic polymerization to explore the influence of different hole mobility and different ionization potential on the performance of a two-layer OLED. OLED devices were fabricated using spin-casting and vacuum vapor deposition, and were characterized in terms of current-voltage behavior and light output. A photo-crosslinkable hole transport layer was demonstrated. The HT polymers have been found to yield improved OLEDs by comparison to analogous small-molecule materials due to better film coverage and better film morphology. The device performance has been found to improve with increasing ionization potential of the hole transport polymer. An optimized device was fabricated,

which showed 20 Lm/W efficiency. The best HT polymer was modified further to improve the operational stability of the device by improving the interfacial contact to the anode. A better adhesion to the conducting glass was achieved by preparing trimethoxysilane-containing copolymers *via* radical polymerization, and developing a procedure to cross-link these copolymers to the anode surface.

The appendix describes a project unrelated to the general topic of materials for OLEDs. It presents a study on four chiral molybdenum-based ROMP-initiators with regard to their ability to yield highly stereoregular polymers.

Table of Contents

List of Illustrations

List of Tables

Chapter 1:

Introduction – Organic Materials for Light-Emitting Diodes

A. Organic Light-Emitting Diodes – General Overview

Electroluminescence of an organic material has first been demonstrated in 1963.[1] Pope *et al.* have build a prototype of an organic light-emitting diode (OLED) by placing anthracene crystals between two electrodes. However, the efficiency was extremely low, and the minimum voltage, which was required for the detection of electroluminescence, exceeded 400 V. Therefore, a commercial use of the OLED concept seemed impossible, which resulted in very little attention being paid to this effect at that time.

One major breakthrough in OLED technology was the introduction of the two-layer structure[2] by Tang and Van Slyke in 1987 resulting in OLEDs with substantially improved external quantum efficiency. In a two-layer device, a hole-transport layer (HTL) is placed between the anode and the electroluminescent layer (EL) (Figure 1.1). The HTL consists of an organic material, which is easily and reversibly oxidized. This facilitates the injection of holes from the anode and enables hole transport from the anode to the HTL/EL interface. At the same time, the reduction of the hole transport material is not a favorable process. Consequently, the transport of electrons towards the anode is disfavored. In contrast, the HOMO/LUMO characteristics of the electroluminescent

material are such that the energy barrier for electron injection from the cathode is low, but the hole injection from the HTL is hindered. Such mismatch in energy levels at the HTL/EL interface leads to a better balance of hole transport and electron transport rates resulting in higher probability of exciton formation, and consequently, higher external quantum efficiency. Most of the photons are generated within a 5 nm thin layer at the HTL/EL interface, which is the region where both electron and hole transport are relatively slow.

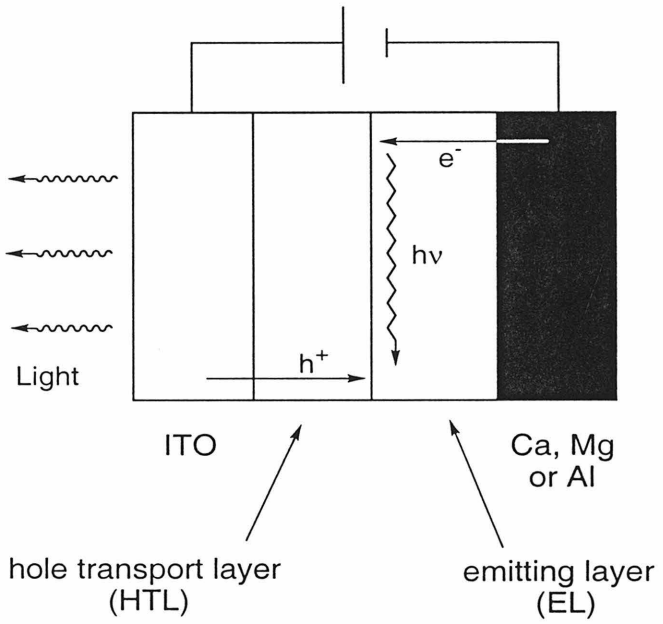

Figure 1.1: Schematic representation of a two-layer OLED.

An other remarkable achievement was the fabrication of a polymeric OLED using poly(*para*-phenylenevinylene) (PPV).[3] The highly conjugated polymer PPV acts as both the charge transport material and the electroluminescent material. The device configuration is that of a one-layer OLED, which can be fabricated conveniently through spin-casting of a soluble PPV precursor. Figure 1.2 shows the device configuration and the structure of PPV.

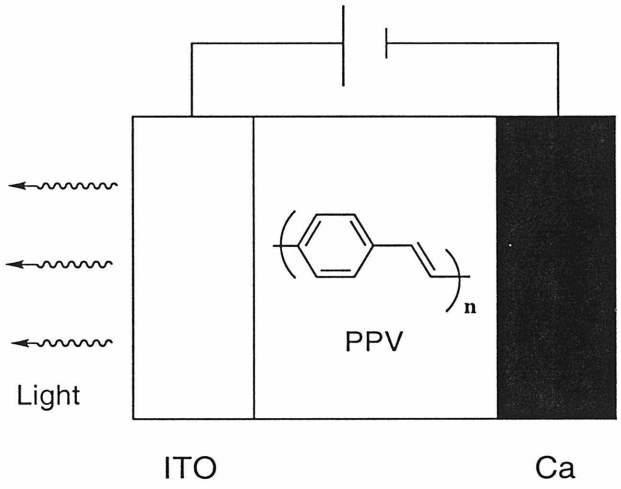

Figure 1.2: Schematic representation of a PPV-based OLED.

Even though PPV was not the first polymer used in an OLED,[4] this work together with the work of Tang and Van Slyke inspired many research activities in the field, and the performance of OLEDs is now approaching commercially viable levels.

The anode material commonly used in OLEDs is glass coated with indium tin oxide (ITO) (wok function ϕ_w ~ 4.7 eV). The hole transport material is often a triarylamine derivative (Figure 1.3). Photoconductivity and the hole-transporting properties of triarylamines have been studied extensively.[5] The emitting layer consists of a dye with electron transport capability or of an electron transport material with an emissive dopant (Figure 1.3).[6] Very well established is the use of tris(8-quinolinato)aluminum[7] (Alq, IP = 5.93 eV) which acts as an electron transport material and emits green light. The cathode is commonly fabricated by vacuum vapor deposition of a low-work-function metal such as calcium (ϕ_w = 2.9 eV) or magnesium (ϕ_w = 3.7 eV). More recent work is geared towards the use of the more environmentally stable aluminum.[8]

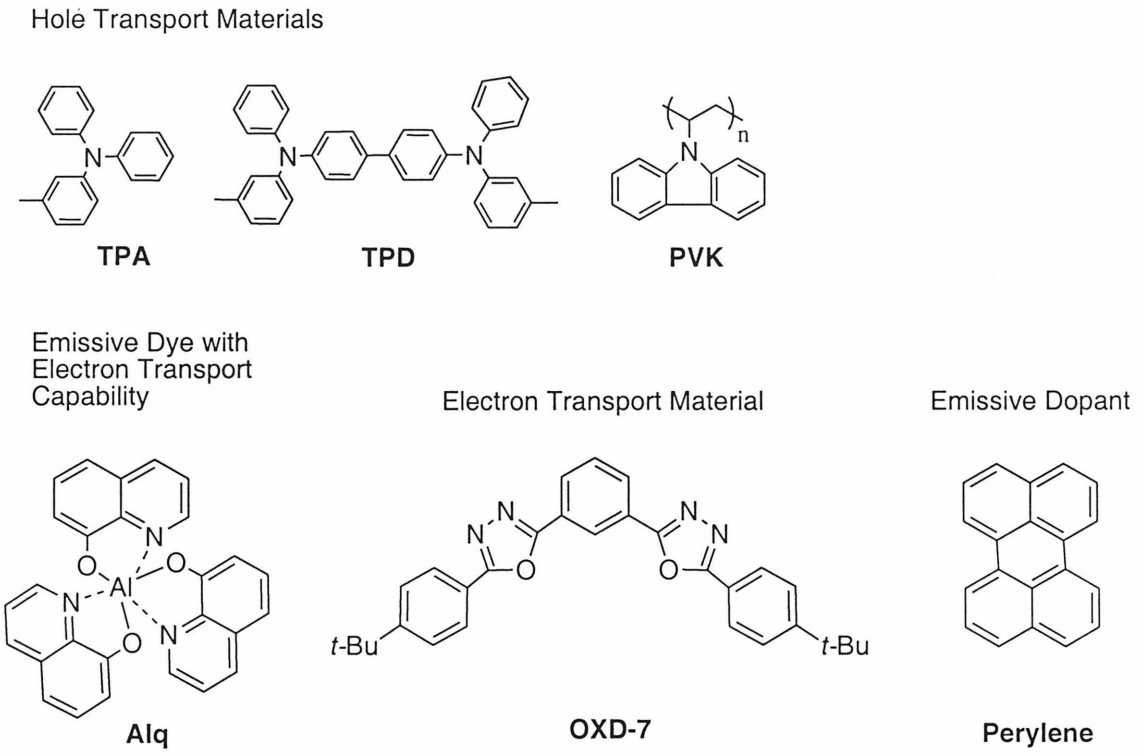

Figure 1.3: Examples of organic materials commonly used in OLEDs.

B. Working Mechanism and Characterization of an OLED

OLEDs are made of materials which are considered insulators. Typical resistivities are of the order of 10^{15} Ω cm. No electronic charge is present in the device without charge injection from the electrodes. All injected charges are assumed to behave as space charges, and no local charge neutrality is expected within the device during operation. In contrast to inorganic semiconductors, organic charge transport materials are not described in terms of valence band and conduction band. Their behavior is best modeled assuming a large number of distinct sites with a Gaussian distribution of site energies.[5e] The charge transport proceeds through hopping between these sites.

Charge recombination results in the formation of neutral excited states, and emission is due to emissive transitions from the neutral excited states to ground states. Most commonly, light emission in OLEDs is due to fluorescence only, e. g. emissive transitions from singlet excited states. However, 75 % of excitons formed through charge recombination are triplet excited states[9] and deactivate without light emission. This limits the quantum efficiency of an OLED to a theoretical maximum of 25 %.[10] The internal quantum efficiency is defined by the number of photons produced within the device divided by an apparent number of charges injected. For a fluorescence-based device the internal quantum efficiency η is given by

$$\eta = \gamma * \eta_r * \phi_r \qquad (1)$$

γ charge-balance factor
η_r efficiency of production of singlet excitons (maximum 0.25)
ϕ_r fluorescence quantum efficiency.

Consequently, materials with high fluorescence quantum efficiencies will potentially yield more efficient OLEDs. The charge-balance factor γ describes the ratio between charges used for recombination and charges passing through the device as current. Figure 1.4 illustrates the meaning of γ. The charge-balance factor can be adjusted through variation of the energetic barriers for hole and electron injection. Higher values for γ are achieved in multi-layer devices.[11]

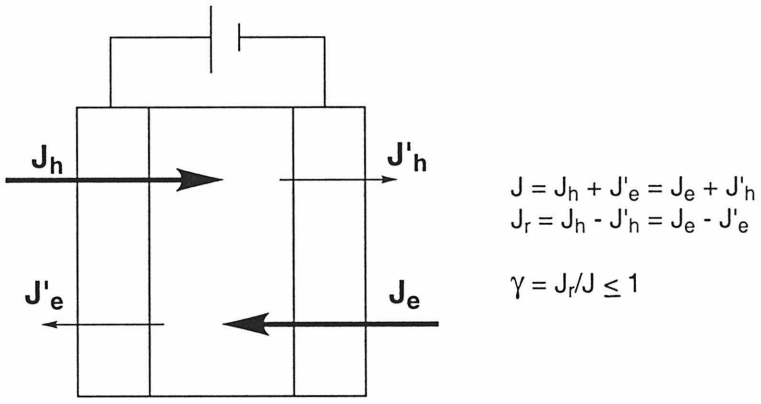

Figure 1.4: Charge-balance factor γ in relation to the positive and negative charges injected and passed through an electroluminescent device.

Not all of the emitted light leaves the device through the transparent anode. The refractive index n of the materials determines the ratio between external emission and internal light dissipation. Equation (2) shows the relationship between external and internal quantum efficiency. Experimentally the external quantum efficiency is determined by measuring the number of emitted photons using a calibrated silicon photodetector and dividing this number by the number of injected charges, which is calculated from the circuit current J.

$$\eta \text{ (ext.)} = 1/(2n^2) * \eta \qquad (2)$$

Equations (1) and (2) express quantum efficiency independently from the energy of emitted photons and the applied electric power. Consequently, voltage losses due to charge injection barriers and charge transport resistance, as well as excess energy consumed for thermal relaxation of singlet excitons are not accounted for. In order to take these effects into consideration efficiency is sometimes reported as the ratio of

emitted light power to the electric power applied. This parameter is called "energy efficiency" and relates to the internal quantum efficiency η as follows:

$$\eta_E = \eta * \varepsilon_p/eV \quad (3)$$

ε_p photon energy of emitted light
e elemental charge
V applied voltage.

For practical purposes, efficiency is also reported in photometric units "lumens per Watt" (lm/W). The lumen is evaluated with reference to visual sensation and is routinely used to characterize artificial lighting. The human eye is most sensitive to the wavelength of 555 nm. At other wavelengths the sensitivity of the eye is less, and a light source would appear less bright even if the same number of photons is emitted. Since OLEDs are most likely to be applied in flat-panel displays, characterization of OLED efficiency with respect to visual perception is relevant. Similar purpose is served by reporting OLED brightness in cd/m^2 (cd = candela = one lumen per steradian).

Another practically relevant parameter is the operating voltage, which is the voltage at which a particular brightness is achieved. The operating voltage should be as low as possible. For commercial use a brightness of 100 – 150 cd/m^2 (brightness of a computer monitor) should be achieved at a voltage below 4 V.

C. Synthesis of PPV

The original synthesis of poly(*para*-phenylenevinylene) (PPV) involves the preparation of a soluble polymeric precursor (Scheme 1.1). A film of the precursor can be fabricated through spin-casting, and the insoluble product PPV is formed after processing into the desired shape through heating of the precursor to 300 °C.

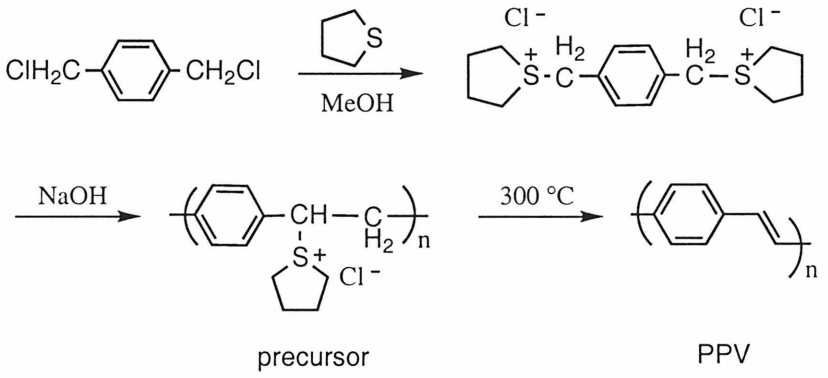

Scheme 1.1: Original synthesis of PPV.

This synthetic route requires rather harsh conditions and allows little control over molecular weight and amount of defects. Since the first report of a PPV-based light-emitting diode[3] a number of other synthetic procedures to prepare PPV and PPV derivatives have been developed. Of particular interest is the preparation of PPV bearing long alkyl chains, and PPV with electron-withdrawing or electron-donating substituents. Alkyl-substituted PPV has the advantage of being soluble in organic solvents.[12] Electron-donating and electron-withdrawing substituents cause a shift in the energy levels resulting in a different color of electroluminescence.[13] Steric effects are also very important since twisting of the PPV chains due to bulky substituents results in decreased effective conjugation length, which in turn influences the electroluminescence color.

Synthetic procedures to shorten the conjugation length in PPV through incomplete conversion of a precursor polymer have been described.[14]

In our research group, we have developed a synthetic route for the preparation of PPV *via* ring-opening metathesis polymerization (ROMP)[15] of substituted barrelenes. This route allows the synthesis of PPV under mild conditions. The polymerization is living, which provides for a high degree of control over the molecular weight and for the possibility to prepare block-copolymers. A range of PPV derivatives with different substitution patterns have been prepared by this method.[16] Chapter 2 describes my contribution to this project.

D. Characteristics of Organic Hole Transport Materials

Organic hole transport materials are an important part of a two-layer or a multi-layer OLED (Figure 1.1). One or several hole transport layers (HTL) are placed between the anode and the electroluminescent material (EL) to increase the charge-balance factor γ (Equation 1). Consequently, HTL-containing OLEDs usually show higher quantum efficiency.

The ionization potential of the hole transport material determines the energetic barriers for charge transfer across the anode/HTL and the HTL/EL interfaces, and is, therefore, a crucial parameter for the performance of an OLED. High hole mobility is desired to ensure movement of the positive charges across the HTL.

The aromatic diamine TPD (Figure 1.3) shows excellent hole injection (IP ~ 5.4 eV) and hole transport capability (~ 10^{-2} cm^2/Vs), and exhibits good electron-blocking

characteristics at the HTL/EL interface.[5] It is, therefore, widely used as HTL material. TPD films are fabricated through vacuum vapor deposition. The two *meta*-methyl groups introduce asymmetry which is necessary to suppress crystallization. Crystallization of the HTL can cause a breakdown of charge transport through formation of deep traps at grain boundaries, and it increases internal losses through scattering of the emitted light by the crystallites. Therefore, organic hole transport materials must be amorphous. One of the disadvantages of TPD is its low glass transition temperature. A phase transition occurs at 71 °C, which limits the thermal and operational stability of TPD-based devices. Starburst triarylamines,[17] TPD-oligomers,[18] and naphthyl-substituted TPD[19] have been explored to improve the properties.

A polymeric HTL material offers several advantages over TPD and its small-molecule analogues: i) A polymer film can be formed by spin-casting or spray-coating, which is a more efficient way of device fabrication compared to vacuum vapor deposition. ii) Many polymers have an intrinsically low tendency to crystallize. iii) Polymers can have a high glass transition temperature. iv) Polymers can be cross-linkable. Cross-linking of the hole transport material would allow spin-casting of a polymeric electroluminescent material on top of the insoluble cross-linked HTL, which would further simplify device fabrication. Cross-linking could also result in additional improvement of thermal and operational stability.

Chapter 3 describes the synthesis of a series of photo-crosslinkable hole transport polymers by ring-opening metathesis polymerization of triarylamine-substituted norbornenes. The hole transport moiety in this study is not varied ensuring constant ionization potential and consequently, comparable charge injection rates at the interfaces.

The linkers between the triarylamine and the norbornene have different polarity and length, which influences hole mobility through broadening of the Gaussian distribution of site energies and through changing the degree of orientational disorder.[5e] The effect of these structural differences and cross-linking on the performance of a two-layer OLED was explored.

Chapter 4 describes the synthesis of a series of hole transport polymers with high glass transition temperatures and different ionization potentials (IP). The choice of the polymer backbone was based on conclusions from Chapter 3, and the backbone remained constant within this series. Variations in ionization potential were achieved through changing the substituents on the hole-transporting moiety. Two-layer OLEDs were fabricated to study the effect of the ionization potential on the device performance.

The HTL polymer with the optimized IP was further modified to enhance adhesion to the anode material. This modification yielded OLEDs with decreased operating voltage and improved lifetime characteristics. These results are described in Chapter 5.

The work presented in this thesis focuses on the application of organic hole transport materials in light-emitting diodes. Other applications in the field of electronic devices include photorefractive materials,[20] organic transistors[21] and solar cells.[22]

E. References and Notes

(1) Pope, M.; Kallmann, H. P.; Magnante, P. *J. Chem. Phys.* **1963**, *38*, 2042.

(2) Tang, C. W.; Van Slyke, S. A. *Appl. Phys. Lett.* **1987**, *51*, 913.

(3) Burroughes, J. H.; Bradley, D. D. C.; Brown, A. R.; Marks, R. N.; Mackay, K.; Friend, R. H.; Burns, P. L.; Holmes, A. B. *Nature* **1990,** *347,* 539.

(4) Partridge R., H. *Polymer* **1983**, *24*, 748.

(5) a. Van der Auweraer, M.; De Schryver, F. C.; Borsenberger, P. M.; Fitzgerald, J. J. *J. Phys. Chem.* **1993**, *97*, 8808. b. Borsenberger, P. M.; Pautmeier, L.; Richert, R.; Bässler, H. *J. Chem. Phys.* **1991**, *94*, 8276. c. Gruenbaum, W. T.; Sorriero, L. J.; Borsenberger, P. M.; Zumbulyadis, N. *Jpn. J. Appl. Phys.* **1996**, *35*, 2714. d. Heun, S.; Borsenberger, P. M. *Physica B* **1995**, *216*, 43. e. Bässler, H. *Phys. Status Solidi (b)* **1993**, *175*, 15 and references therein. f. Adachi, S.; Tokito, S.; Tsutsui, T.; Saito, S. *Jpn. J. Appl. Phys.* **1988**, *27*, L269.

(6) a. Hamada, Y.; Adachi, C.; Tsutsui, T.; Saito, S. *Jpn. J. Appl. Phys.* **1992**, 31, 1812. b. Tokuhisa, H.; Era, M.; Tsutsui, T.; Saito, S. Appl. Phys. Lett. 1995, 66, 3433. c. Tang, C. W.; Van Slyke, S. A.; Chen, C. H. *J. Appl. Phys.* **1989**, *65*, 3610.

(7) Naito, K.; Miura, A. *J. Phys. Chem.* **1993**, *97*, 6240.

(8) a. Hung, L. S.; Liao, L. S.; Lee, C. S.; Lee, S. T. *J. Appl. Phys.* **1999**, 86, 4607. b. Cao, Y.; Yu, G.; Heeger, A. J. *Synth. Met.* **1999**, *102*, 881. c. Jabbour, G. E.; Kawabe, Y.; Shaheen, S. E.; Wang, J. F.; Morrell, M. M.; Kippelen, B.; Peyghambarian, N. *Appl. Phys. Lett.* **1997**, *71*, 1762.

(9) According to spin statistics, the ratio of triplet to singlet excitons formed by charge recombination is always 3 to 1. Consequently, the maximum value for the efficiency of production of singlet excitons is 0.25. Helfrich, W.; Schneider, W. G. *J. Chem. Phys.* **1966**, *44*, 2902.

(10) More recently, OLEDs which make use of phosphorescence, e. g. emissive transitions from triplet states, have been demonstrated: a. Blumstengel, S.; Dorsinville, R. *Jpn. J. Appl. Phys. 2* **1999**, *38*, L403. b. Hishino, S.; Suzuki, H. *Appl. Phys. Lett.* **1996**, *69*, 224. c. O'Brien, D. F.; Baldo, M. A.; Thompson, M. E.; Forrest, S. R. *Appl. Phys. Lett.* **1999**, *74*, 224.

(11) Tsutsui, T.; Aminaka, E.; Saito, S. *J. Appl. Phys.* **1996**, *79*, 8808.

(12) Braun, D.; Heeger, A. J. *Appl. Phys. Lett.* **1991**, *58*, 1982.

(13) a. Greenham, N. C.; Moratti, S. C.; Bradley, D. D. C.; Friend, R. H.; Holmes, A. B. *Nature* **1993,** *365,* 628. b. Chan, W.-K.; Yu, L. *Macromolecules* **1995**, *28*, 6410. c. Gurge, R. G.; Sarker, A.; Lahti, P. M.; Hu, B.; Karasz, F. E. *Macromolecules* **1996**, *29*, 4287. d. Gurge, R. G.; Sarker, A.; Lahti, P. M.; Hu, B.; Karasz, F. E. *Macromolecules* **1997**, *30*, 8286.

(14) a. Burn, P. L.; Holmes, A. B.; Kraft, A.; Bradley, D. D. C.; Brown, A. R.; Friend, R. H. J. Chem. Soc., Chem. Commun. 1992, 32. b. Zhang, C.; Braun, D.; Heeger, A. J. *J. Appl. Phys.* **1993**, *73*, 5177.

(15) a. Grubbs, R. H.; Tumas, W. *Science* **1989**, *243*, 907. b. Schrock, R. R. *Acc. Chem. Res.* **1990**, *23*, 158.

(16) a. Wagaman, M. W.; Grubbs, R. H. *Macromolecules* **1997**, *30*, 3978. b. Wagaman, M. W.; Grubbs, R. H. *Synth. Met.* **1997**, *84*, 327. c. Pu, L.;

Wagaman, M. W.; Grubbs, R. H. *Macromolecules* **1996**, *29*, 1138. d. Conticello, V. P.; Gin, D. L.; Grubbs, R. H. *J. Am. Chem. Soc.* **1992,** *114,* 9708. e. Gin, D. L; Conticello, V. P.; Grubbs, R. H. *J. Am. Chem. Soc.* **1994,** *116,* 10507. f. Gin, D. L; Conticello, V. P.; Grubbs, R. H. *J. Am. Chem. Soc.* **1994,** *116,* 10934.

(17) a. Shirota, Y.; Kuwabara, Y.; Inada. H.; Wakimoto, T.; Nakada, H.; Yonemoto, Y.; Kawami, S.; Imai, K. *Appl. Phys. Lett.* **1994**, *65*, 807. b. Thelakkat, M.; Schmidt, H.-W. *Adv. Mater.* **1998**, *10*, 219. c. Katsuma, K.; Shirota, Y. *Adv. Mater.* **1998**, *10*, 223.

(18) a. Adachi, C.; Nagai, K.; Tamoto, N. *Appl. Phys. Lett.* **1994**, *66*, 2679. b. Tanaka, H.; Tokito, S.; Taga, Y.; Okada, A. *J. Chem. Soc., Chem. Commun.* **1996**, 2175.

(19) Van Slyke, S. A.; Chen, C. H.; Tang, C. W. *Appl. Phys. Lett.* **1996**, *69*, 2160.

(20) Kippelen, B.; Meerholz, K.; Peyghambarian, N. *Introduction to Photorefractive Polymers* in Nalwa, H. S.; Miyata, S. (Eds.) *Nonlinear Optics of Organic Molecules and Polymers* CRC Press, New York, 1997.

(21) a. Dimitrakopoulos, C. D.; Furman, B. K.; Graham, T.; Hedge, S.; Purushothaman, S. *Synth. Met.* **1998**, *92*, 47. b. Horowitz, G. *Adv. Mater.* **1998**, *10*, 365. c. Dimitrakopoulos, C. D.; Purushothaman, S.; Kymissis, J.; Callegari, A.; Shaw, J. M. *Science* **1999**, *283*, 822.

(22) Bach, U.; Lupo, D.; Comte, P.; Moser, J. E.; Weissörtel, F.; Salbeck, J.; Spreitzer, H.; Grätzel, M. *Nature* **1998**, *395*, 583.

Chapter 2:

Synthesis of Electroluminescent Polymers by Ring-Opening Metathesis Polymerization

A. Introduction

Synthesis of electroluminescent polymers by ring-opening metathesis polymerization (ROMP)[1,2] was an ongoing project in the group of Professor Robert H. Grubbs when I joined Caltech. ROMP is the polymerization of a strained cyclic olefin initiated by a transition metal complex. First-generation initiators were ill-defined multicomponent mixtures or heterogeneous systems, which only polymerized strained cyclic olefins in a non-living fashion.[1] More recently, a series of well-defined soluble transition metal complexes has been developed,[3] which initiate ROMP according to a well-understood mechanism.[4]

The mechanism of the polymerization was determined to be as illustrated in Figure 2.1. First a cyclic olefin reacts with a transition metal carbene to form a metallocyclobutane intermediate. This intermediate can disassociate in a non-productive fashion to yield the starting materials, or it can undergo a productive rearrangement to generate a new carbene, the propagating carbene, which contains the ring-opened olefin inserted into the original metal-carbon bond. Repeated reactions of the cyclo-olefinic monomers with the propagating carbene result in growth of the polymer chain. The

polymerization is enthalpically driven through release of ring strain. A propagating carbene is regenerated after each insertion of a new monomer unit, and the polymerization is living in many cases. The polymerization is terminated through deliberate destruction of the propagating species *via* addition of benzaldehyde (for molybdenum-based initiators) or ethylvinylether (for ruthenium-based initiators).

Compared to the initially reported systems, the new well-defined initiators also have the advantage of being more reactive towards olefins and less sensitive towards other functional groups. Most recent research efforts are geared towards extending the scope of ROMP and other olefin metathesis reactions through the development of more active and more stable initiators.[5]

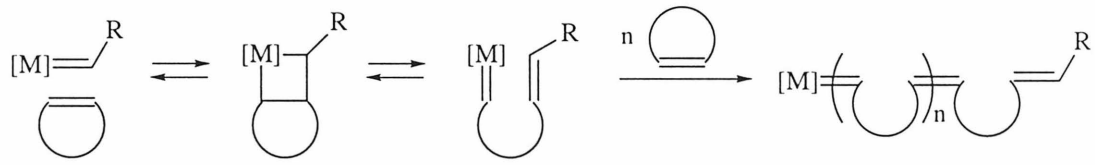

Examples of ROMP Initiators

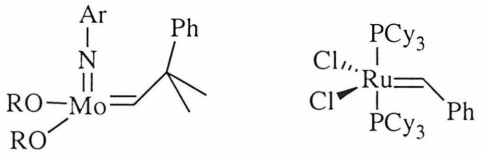

R = $C(CH_3)_2CF_3$

1

2

Figure 2.1: Mechanism of ring-opening metathesis polymerization (ROMP).

Because of its living nature, the use of ROMP to prepare electroluminescent polymers allows a high degree of control over the polymer's molecular weight and molecular weight distribution, and enables the synthesis of well-defined block-

copolymers. Since new initiators show increased tolerance towards functional groups, preparation of polymers bearing different kinds of substituents is possible.

The electroluminescent polymers poly(1,4-naphthylenevinylenes) (PNVs) can be prepared from benzobarrelenes,[6] such as **3** and **4** (Scheme 2.1), using the molybdenum complex **1** (Figure 2.1) as ROMP initiator. A compound analogous to **1** with R = $C(CH_3)(CF_3)_2$ will also polymerize benzobarrelenes. As illustrated in Scheme 2.1, non-conjugated precursor polymers **5** and **6** are formed at first. Oxidation with 2,3-dichloro-5,6-dicyanoquinone (DDQ) yields the target polymers PNV (**8**) and Cl-PNV (**7**). An efficient method to prepare the monomers involves the benzyne addition of tetrachlorobenzene and benzene[7] (Scheme 2.1). This approach easily yields tetrachloro-benzobarrelene **3**, which can be reduced to benzobarrelene **4**.

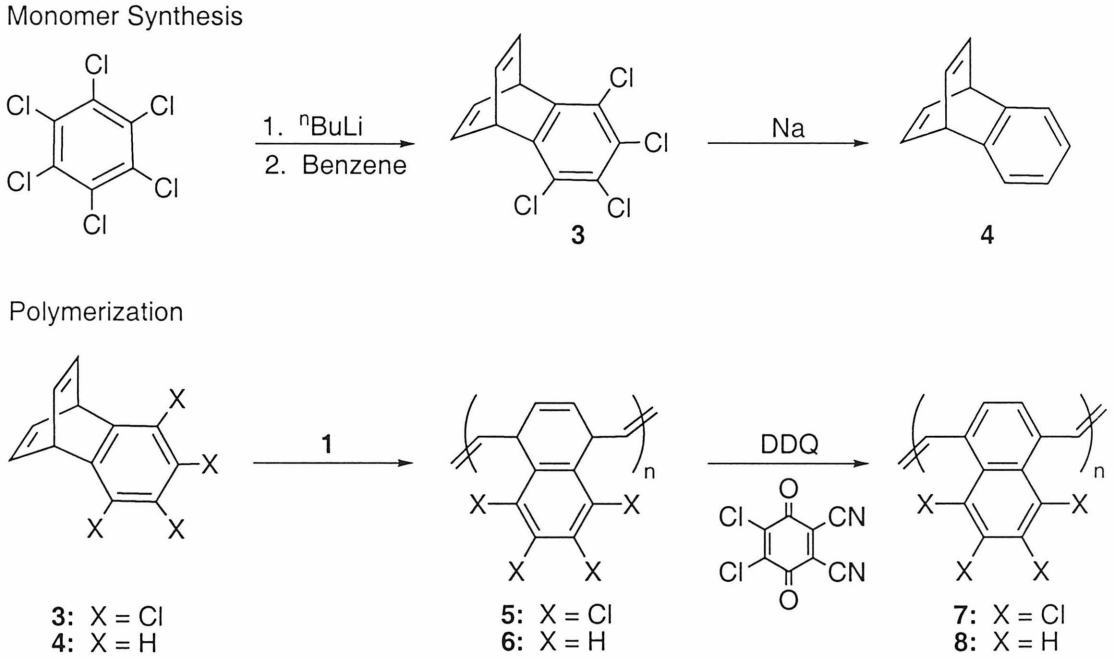

Scheme 2.1: Synthesis of poly(1,4-naphthylenevinylenes) by ring-opening metathesis polymerization of benzobarrelenes.

The resulting polymers **7** and **8** have the disadvantage of being intractable, which makes the study of their electroluminescence properties very difficult. In the case of the chlorinated derivative, the solubility of the precursor polymer **5** is also poor resulting in problems during polymer synthesis. The solubility of the polymers **5** – **8** would improve if they contained alkyl substituents. In order to keep the monomer synthesis short and efficient, introduction of solubility-enhancing substituents through alkylation of **3** would be desirable. However, alkylation of **3** was originally difficult to achieve. A more complex multi-step synthetic procedure has been developed to obtain alkylated benzobarrelene,[6] while attempts to synthesize alkylated chlorobenzobarrelene using Grignard reagents remained unsuccessful.

I have explored a different way to alkylate compound **3**. As a result, derivatives of **3** bearing linear and branched alkyl substituents have been prepared and polymerized to yield alkylated Cl-PNVs with improved solubility. This work is presented in part **B** of this chapter.

A different kind of electroluminescent polymers, poly(1,4-phenylenevinylenes) (PPVs), can also be prepared *via* ROMP using barrelenes as the cyclo-olefinic monomers. As illustrated in Scheme 2.2, the polymerization procedure for barrelenes (**10**) is analogous to ROMP of benzobarrelenes (Scheme 2.1), the monomer synthesis, however, is more challenging. The synthetic procedure developed by Michael W. Wagaman involves a Diels-Alder addition of diol **9** to an acceptor-substituted acetylene. Subsequently, the OH-groups are converted to the thiocarbonate using (thiocarbonyl)diimidazole (TCDI), and the treatment of the thiocarbonate with 1,3-

dimethyl-2-phenyl-1,3,2-diazaphospholidine (DPD)[8] results in formation of the barrelene monomer **10**.

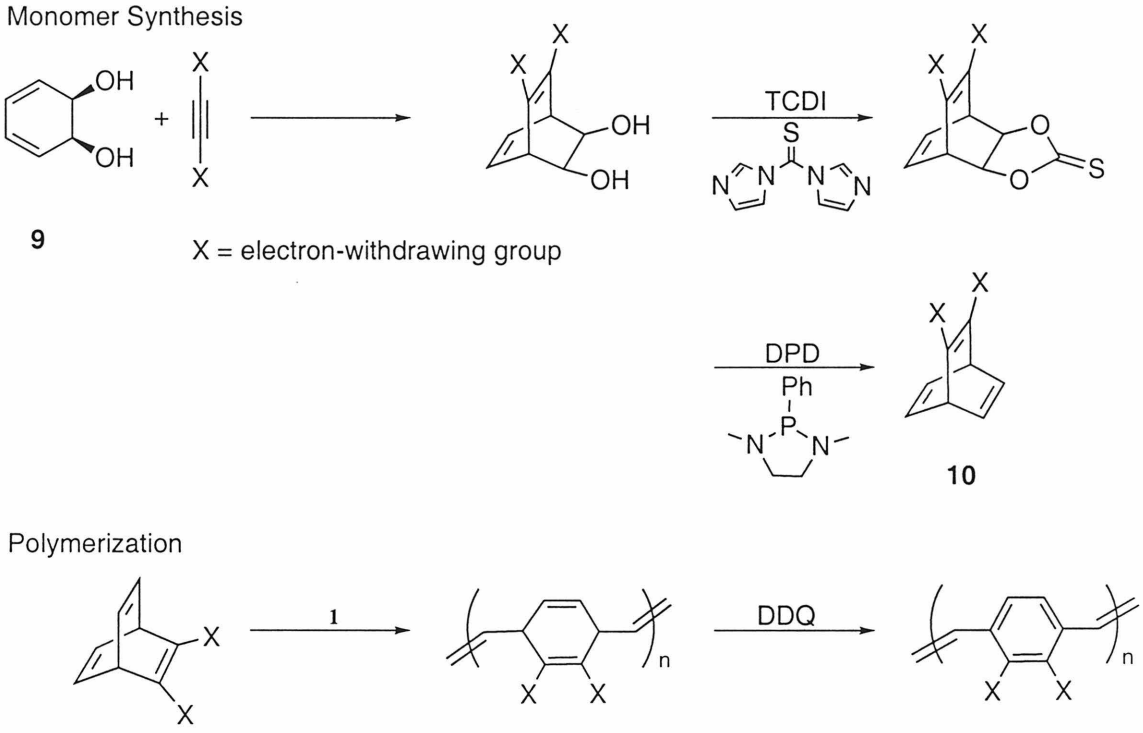

Scheme 2.2: Synthesis of poly(1,4-phenylenevinylenes) by ring-opening metathesis polymerization of barrelenes.

Since the first step of the monomer synthesis requires activation of the triple-bond by two strongly electron-withdrawing groups, the resulting monomers and polymers are functionalized with two strong electron acceptors. I have explored reactions to extend the methodology presented in Scheme 2.2 to the synthesis of barrelenes without electron-withdrawing groups. As a result, mono-alkylated barrelene was prepared and polymerized to yield a soluble PPV-derivative. The fluorescence color of this derivative is red-shifted by comparison to acceptor-substituted PPV. This work is presented in part **C** of this chapter.

B. Synthesis and Polymerization of Alkyltrichlorobenzobarrelenes

Chlorinated PNV (**7**, Scheme 2.1) is a potentially interesting electroluminescent material. However, its insolubility in organic solvents greatly limits applications. In order to improve processibility, attempts have been made to introduce solubility-enhancing alkyl substituents. Alkylation of the monomer tetrachlorobenzobarrelene (**3**, Scheme 2.1 and Scheme 2.3) using Grignard reagents failed. The successful alkylation procedure is described below. It uses *n*-butyllithium and an excess of an alkyliodide (Scheme 2.3).

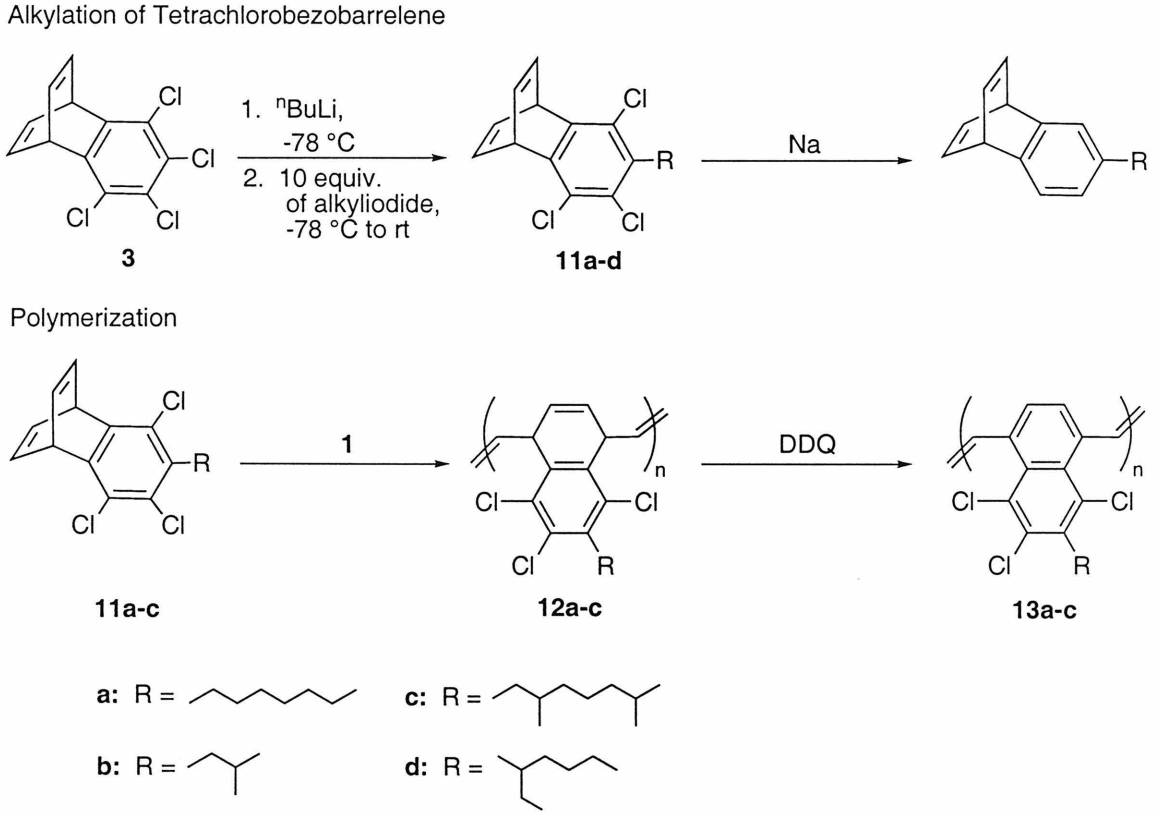

Scheme 2.3: Synthesis and polymerization of 5-alkyltrichlorobenzobarrelenes.

This alkylation method yields alkyltrichlorobenzobarrelenes such as **11a-d**. The corresponding non-halogenated alkylbenzobarrelenes can be obtained from these compounds by removal of the chlorines through reduction with sodium metal as reported earlier for tetrachlorobenzobarrelene.[7] Comparison of ^{1}H NMR spectra of octylbenzobarrelene prepared by this route and by the previously reported method,[3] which can only yield 5-alkylbenzobarrelenes, shows that the new procedure also results in benzobarrelenes alkylated only in the 5 position.

The monomers **11a-c** were polymerized using the iniator **1** (Figure 2.1). As previously seen for other benzobarrelene monomers, addition of 15 equivalents of hexafluoro-*t*-butanol (HFB) to activate the catalyst improved the reaction. Under these conditions, the propagating carbene was observed by ^{1}H NMR, and the polymerization appeared living yielding the precursor polymers **12a-c** (Scheme 2.3) with PDIs of 1.13 to 1.15. The polymerization is substantially slower than the polymerization of non-halogenated benzobarrelene and requires 6 h at room temperature to go to completion. For comparison, polymerization of the non-chlorinated octylbenzobarrelene takes 35 min and yields a polymer with a PDI of 1.7.[6b] The difference in reaction rate is due to the electron-withdrawing effect of the chlorine substituents. The substituents also alter the ratio of initiation rate to propagation rate. In case of the chlorinated monomer, initiation is fast compared to propagation resulting in complete initiation and consequently, a low PDI. For benzobarrelene monomers without electron-withdrawing substituents, initiation is slow relative to propagation, and incomplete initiation (75 – 80 %) causes a broadening of the molecular weight distribution.

The aromatization reaction (Scheme 2.3) is also affected by the chlorine substituents. To obtain alkyltrichloro-PNVs **13a-c**, the precursor polymers have to be treated with DDQ for 12 h at 120 °C in bromobenzene. For comparison, oxidation of non-chlorinated PNV-precursors takes 2 h at room temperature.[6b]

Whereas octyl-PNV is sufficiently soluble in organic solvents, the solubility of octyltrichloro-PNV **13a** is poor. In hopes that a branched alkyl substituent will give a greater increase in solubility, the alkylation of **3** was performed using a number of branched alkyliodides. Table 2.1 summarizes the alkylation results.

Table 2.1: Yields for the synthesis of various alkyltrichlorobenzobarrelenes.

Compound	Yield of the Alkylation (%)
11a	78[a]
11b	86[a]
11c	90[a]
11d	10[b]

[a]isolated yield after distillation of excess iodide and column chromatography
[b]yield determined on crude reaction mixture by GC-MS

Monomers **11a-c** have been prepared in high yields. However, the alkylation using an α-branched alkyl-iodide afforded the desired product **11d** in only 10 % yield. Apparently, elimination competes with the desired reaction in this case. The compound **11d** was not further investigated due to the difficulty to synthesize it in good yield.

The precursor polymers **12a-c** all show good solubilities. This is an advantage over the tetrachloro-polymer **5** because the polymerization goes to completion, the

polymer PDIs are narrow, and the preparation of block-copolymers is no longer hindered through poor solubility of the chlorinated segment. PNV-block-copolymers have been prepared in a subsequent study.[9] While the tetrachloro-PNV **7** is intractable, the polymers **13a-c** are somewhat soluble in organic solvents. The solubility of **13a-c**, however, is still quite poor for the purposes of spin-casting. The possibility to convert the compounds **11a-c** to 5-alkylbenzobarrelenes allows to synthesize alkylated benzobarrelenes *via* a new and more efficient route. All of the 5-alkylbenzobarrelenes show satisfactory solubility in organic solvents allowing their use in devices, which are fabricated through spin-casting.[10]

C. Synthesis and Luminescence Properties of Octyl-PPV

PPV derivatives have been synthesized in our group *via* ROMP of barrelenes (Scheme 2.2). Compared to previously reported procedures for the preparation of barrelenes,[11] our synthetic route towards barrelene monomers is shorter and results in higher yields.[12] However, originally our method was limited to the preparation of barrelenes with two strong electron acceptors. This part describes the extension of the methodology to the synthesis of barrelenes without electron-withdrawing substituents. More specifically, it is focused on the synthesis of octyl-barrelene (2-octylbicyclo-[2.2.2]octatriene) because its polymerization yields the soluble octyl-PPV.

It has been observed that the diol **9** (Scheme 2.2) undergoes Diels-Alder additions more smoothly if it is protected as acetonide **14**[6a,13] (Scheme 2.4). In this case, substitution of the acetylene with two electron-withdrawing groups is not required, and

sufficient activation of the triple-bond is achieved by one *p*-toluenesulfone substituent. The *p*-toluenesulfone group can be subsequently removed by reductive desulfonylation.[14]

Scheme 2.4 illustrates the synthetic route. Acetylene **15** was prepared according to a published procedure.[15] Heating of a 1:1 mixture of **14** and **15** without solvent to 60 °C for 3 days afforded the Diels-Alder product **16** in 70 % yield. Reductions of the *p*-toluenesulfone group have been investigated previously, and treatment with SmI_2 and HMPA has been found to remove the *p*-toluenesulfone group selectively in the presence of olefinic bonds.[14] This method was also successful in our case affording compound **17** in 67 % yield.

To remove the acetonide protecting group, several methods were tested. The optimized procedure involves treatment of compound **17** with methanol and pyridinium *p*-toluenesulfonate (PPTS) at 60 °C for 3 days. HCl would deprotect an acetonide faster, but in the case of compound **17**, decomposition was observed upon exposure to aqueous hydrochloric acid. Finally, conversion of **18** to the desired product **19** was achieved using the previously investigated reaction sequence.

The ring-opening metathesis polymerization of monomer **19** using HFB-activated initiator **1** at a monomer to initiator ratio of 40 to 1 was complete within 7 h at room temperature. The precursor polymer readily converts to octyl-PPV immediately upon addition of DDQ at room temperature. Both the precursor polymer and the octyl-PPV are readily soluble in organic solvents.

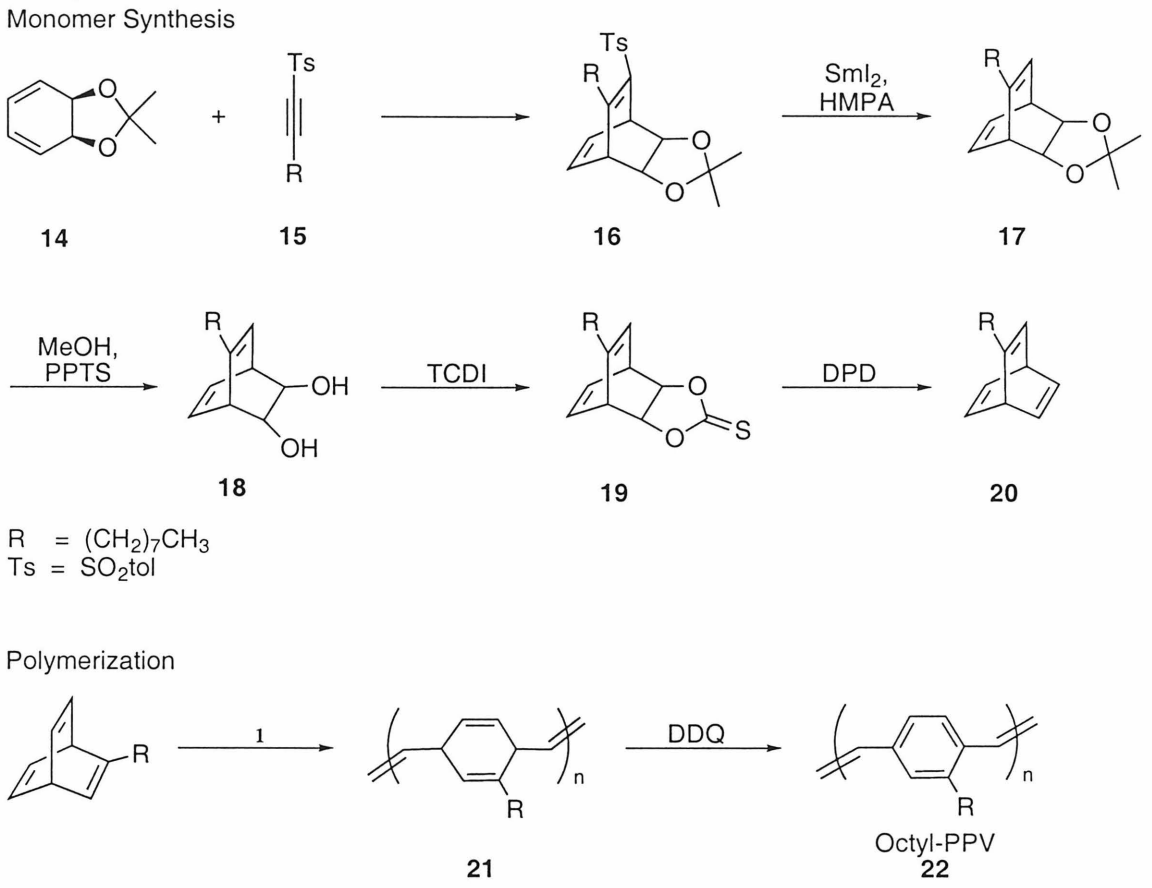

Scheme 2.4: Synthesis and polymerization of octyl-barrelene (2-octylbicyclo[2.2.2]-octatriene).

Fluorescence spectra of the PPV-derivative **22** were taken in methylene chloride solution and in solid state as a film (Figure 2.2). The excitation wavelengths correspond to the absorbtion maximum in each case as determined by absorbtion spectroscopy. The luminescence of the film is red-shifted compared to the luminescence in solution. This is generally observed in luminescent polymers,[16] since polymer chains resume a more planar conformation in the solid state leading to an extension of the effective conjugation length.

PPVs tend to decompose oxidatively when irradiated in the presence of oxigen. In order to test the stability, a film of octyl-PPV was exposed to the excitation beam of the spectrometer in air for 1 h. After that the film was still luminescent with 59 % of the original intensity.

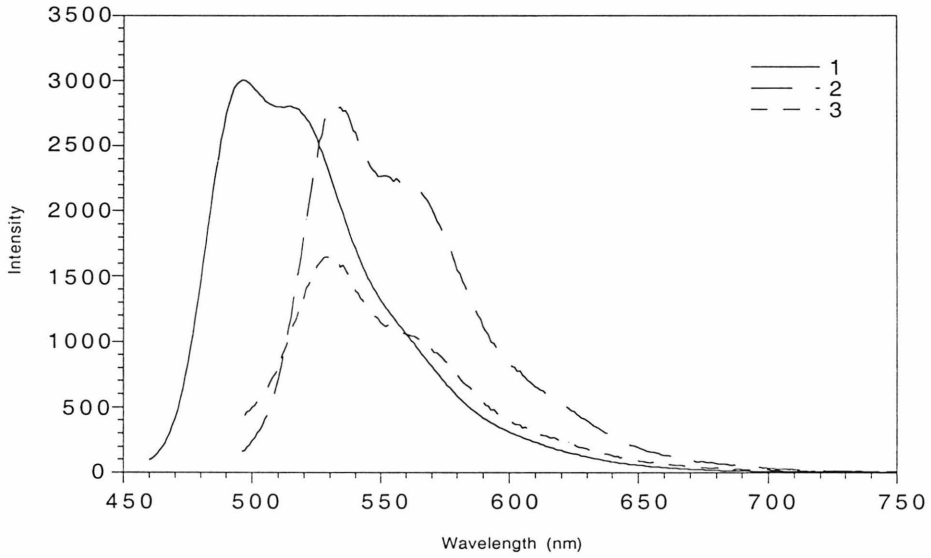

Figure 2.2: Fluorescence spectra of octyl-PPV.
1: 2.4 x 10^{-7} M solution in CH_2Cl_2; excitation wavelength 446 nm.
2: thin film on glass plate; original spectrum; excitation wavelength 478 nm.
3: thin film on glass plate; after irradiation for 1 h; excitation wavelength 478 nm.

In summary, the methodology for the synthesis of PPV-derivatives by ROMP was extended to PPVs without electron-withdrawing substituents. Octyl-PPV has been synthesized, which is a new soluble luminescent polymer.

D. Experimental Section

General: NMR spectra were recorded on a QE Plus-300 MHz (300.1 MHz ^{1}H; 75.49 MHz ^{13}C) spectrometer or a Jeol JNM-GX400 (399.78 MHz ^{1}H, 100.53 MHz ^{13}C) spectrometer. Argon was purified by passage through columns of BASF R3-11 catalyst (Chemalog) and 4 Å molecular sieves (Linde). Fluorescence spectra were taken on a spectrofluorometer SML 8000 using a 2.4 x 10^{-7} M solution of **22** in degassed Omnisolve spectroscopy grade CH_2Cl_2. Elemental analyses were performed by Caltech Analytical Labs or Mid-West Microlab. High resolution mass spectra were obtained from UC Riverside Mass Spectrometry Facility.

Materials: THF and toluene were dried by passing through activated alumina columns. Tetrachlorobenzobarrelene,[7] acetylene **15**,[15] and protected diol **14**[13] were prepared according to literature procedures. Hexamethylphosphoramide (HMPA) was purchased from Aldrich and dried over calcium hydride and then distilled under reduced pressure prior to use. *Cis*-3,5-cyclohexadiene-1,2-diol was obtained from ICI. All other materials were purchased from Aldrich and used without further purification except where noted otherwise.

General procedure for the alkylation of tetrachlorobenzobarrelene (3): A 0.25 molar solution of **3** in dry THF was cooled to - 78 °C under Ar. 1.05 equivalents of *n*-buthyl lithium (1.5 M in hexane) were added slowly. The solution turned purple. 10 equivalents of the alkyliodide (purified by drying over $MgSO_4$ and distillation) were added, and the solution was allowed to warm up and stir at room temperature over night. The yellow reaction mixture was quenched with little water. After removal of solvent, the residue was redissolved in a 1 : 2 mixture of water and diethylether, and the aqueous

phase was extracted with diethylether. The organic phase was dried over Na_2SO_4 and the solvent was removed under reduced pressure. Excess iodide was removed by applying full vacuum at room temperature over night. Flash column chromatography on silica gel with hexane afforded pure products as colorless viscous liquids in 80 – 90 % yield. Data presented is for octyl substituted **11a**. Compounds **11b-d** were also prepared by this method and had nearly identical NMR spectra except for the alkyl region of the spectrum. ^{1}H NMR ($CDCl_3$) δ 6.91 (m, 4H), 5.43 (m, 2H), 2.83 (t, J = 9 Hz, 2H), 1.25 (bs, 12 H), 0.88 (t, J = 7.5 Hz, 3H).

Preparation of 6-octylbicyclo[2.2.2]octa-5,7-diene-2,3-dimethylacetal-5-toluenesulfonate (16). 100 mg (0.342 mmol) of **14** and 52 mg (0.342 mmol) of **15** were heated neat under argon for 3 days. Flash chromatography on silica gel (10% ethyl acetate/hexane) yielded **16** (106 mg, 0.24 mmol, 70%) as a colorless oil. ^{1}H NMR (300 MHz, $CDCl_3$) δ 7.68 (d, *J* = 8.0 Hz, 2H), 7.30 (d, *J* = 8.0 Hz, 2H), 6.19 (m, 2H), 4.19 (m, 2H), 4.07 (m, 1H), 3.82 (m, 1H), 2.73 (t, *J* = 6.9 Hz, 2 H), 2.42 (s, 3H), 1.26 (br d, 17H), 1.20 (s, 3H), 0.88 (t, *J* = 6.3 Hz, 3H); ^{13}C NMR (75 MHz, $CDCl_3$) δ 158.4, 144.1, 138.0, 136.6, 131.9, 130.8, 129.8, 127.4, 113.1, 78.7, 78.0, 50.4, 44.0, 31.8, 31.4, 29.6, 29.4, 29.2, 27.4, 25.7, 25.6, 22.7, 21.6, 14.1; HRMS calcd. for $C_{26}H_{36}O_4S$ $(M+H)^+$ 445.2413, found 445.2426. Anal. Calcd. for $C_{26}H_{36}O_4S$: C, 70.24; H, 8.16. Found: C, 70.12; H, 8.16.

Preparation of 5-octylbicyclo[2.2.2]octa-5,7-diene-2,3-dimethylacetal (17). To 3.6 g (8.1 mmol) of **16**, dissolved in 4 mL of dry THF, was added under argon 420 mL SmI_2 solution (0.1 M in THF). The mixture was cooled to -20 °C and 26.5 mL HMPA

was added to yield a dark purple solution. The reaction was kept at - 20 °C for 1.5 h, treated with 42 mL saturated NH_4Cl solution and allowed to warm up to rt during which time the solution turned yellow and a white precipitate formed. The precipitate was filtered off and washed with diethyl ether several times, and then solvent was removed under vacuum. 20 mL brine was added to the remaining mixture and it was then extracted with diethyl ether. The ether was removed under reduced pressure and the product purified by passing through a plug of silica gel. HMPA was removed first by eluting with hexane and then **17** was eluted using 10% ethyl acetate/hexane. Removal of solvent yielded 1.57 g (5.43 mmol, 67%) of **17** as a colorless liquid. ^{1}H NMR (300 MHz, $CDCl_3$) δ 6.30 (m, 2H), 5.72 (dd, J = 6.3, 1.8 Hz, 1H), 4.19 (m, 2H), 3.69 (m, 1H), 3.54 (m, 1H), 2.06 (td, J = 7.5, 0.75 Hz, 2 H), 1.31 (s, 3H), 1.24 (br d, 15H), 0.86 (t, J = 7.2 Hz, 3H); ^{13}C NMR (75 MHz, $CDCl_3$) δ 147.8, 132.8, 131.7, 124.7, 112.5, 79.4, 78.7, 46.4, 42.0, 34.0, 31.9, 29.43, 29.32, 29.27, 27.2, 26.0, 25.6, 22.7, 21.6, 14.1; HRMS calcd. for $C_{19}H_{30}O_2$ $(M+H)^+$ 291.2324, found 291.2317.

Preparation of 5-octylbicyclo[2.2.2]octa-5,7-diene-2,3-diol (18). **17** (1.57 g, 5.43 mmol) and pyridinium *p*-toluene sulfonate (0.3 g, 1.1 mmol) were dissolved in 100 mL of methanol and heated to 60 °C in an open flask for 3 days. Methanol was removed under reduced pressure and the product purified by flash column chromatography on silica gel (50% ethyl acetate/hexane). Removal of solvent under vacuum yielded 1 g of **17** (4 mmol, 74%) as a colorless liquid. ^{1}H NMR (300 MHz, $CDCl_3$) δ 6.39 (m, 2H), 5.72 (m, 1H), 3.68 (m, 3H), 3.54 (m, 1H), 2.64 (s, 2H), 2.08 (t, J = 7.8 Hz, 2 H), 1.25 (br d, 12H), 0.87 (t, J = 7.5 Hz, 3H); ^{13}C NMR (75 MHz, $CDCl_3$) δ 147.2, 133.3, 132.6,

124.1, 68.4, 67.8, 48.9, 44.6, 33.9, 31.9, 29.47, 29.35, 29.30, 27.2, 22.7, 14.2; HRMS calcd. for $C_{16}H_{26}O_2$ $(M+H)^+$ 249.1855, found 249.1859.

Preparation of 5-octylbicyclo[2.2.2]octa-5,7-diene-2,3-thiocarbonate (19). 18 (1 g, 4 mmol) and TCDI (0.87 g, 4.4 mmol) were refluxed in 20 mL toluene for 30 min. The reaction mixture was eluted through a plug of silica with 30% ethyl acetate/hexane to afford 1.15 g (3.9 mmol, 98%) of **19** as a white crystalline solid. ^{1}H NMR (300 MHz, $CDCl_3$) δ 6.42 (m, 2H), 5.79 (dd, J_1=6.3 Hz, J_2 =1.5 Hz, 1H), 4.85 (m, 2H), 4.06 (m, 1H), 3.90 (m, 1H), 2.12 (t, J = 7.5 Hz, 2 H), 1.24 (br d, 12H), 0.86 (t, J = 6.9 Hz, 3H); ^{13}C NMR (75 MHz, $CDCl_3$) δ 192.64, 147.4, 132.6, 131.6, 128.2, 123.8, 82.6, 82.2, 45.0, 40.7, 33.9, 31.9, 29.3, 29.2, 27.0, 22.7, 14.1; HRMS calcd. for $C_{17}H_{24}O_2S$ 292.1497, found 292.1504.

Preparation of 2-octylbicyclo[2.2.2]octa-2,5,7-triene (20). 19 (1.15 g, 3.9 mmol) was suspended in DPD (0.76 g, 11.7 mmol) and heated at 40 °C under argon for 5 days. The reaction mixture was purified by flash column chromatography on silica gel (10% ethyl acetate/hexane) to yield 168 mg (0.78 mmol, 25%) of **20** as a colorless liquid. ^{1}H NMR (300 MHz, $CDCl_3$) δ 6.76 (m, 4H), 6.17 (dd, J = 6.1, 1.8 Hz, 1H), 4.68 (m, 1H), 4.49 (m, 1H), 2.06 (td, J =7.1, 1.8 Hz, 2 H), 1.25 (br d, 12H), 0.88 (t, J = 7.3 Hz, 3H); ^{13}C NMR (75 MHz, $CDCl_3$) δ 155.4, 141.0, 139.9, 131.5, 52.5, 47.8, 33.7, 31.9, 29.5, 29.3, 29.1, 27.2, 22.7, 14.1; HRMS calcd. for $C_{19}H_{30}O_2$ $(M+H)^+$ 216.1877, found 216.1878.

General procedure for the preparation of the precursor polymers 12a-c and 21: Under inert gas atmosphere, 40 equivalents of the monomer and 15 equivalents of

hexafluoro-*t*-butanol were dissolved in benzene. The reaction was initiated through addition of 1 equivalent of initiator **1** under vigorous stirring. The reaction was monitored by ^{1}H-NMR and terminated upon completion through addition of benzaldehyde. The polymer was precipitated into degassed methanol and purified by repeated precipitation from methylene chloride into methanol. All solvents used for reprecipatation were degassed, since the precursor polymers are susceptible to oxidation and partial oxidation through air oxygen needed to be avoided. After reprecipitation, the polymers were dried *in vacuo* and stored under argon.

Polymer **12a**: Reaction time: 6 h. Yield: quantitative. ^{1}H NMR (C_6D_6, all peaks were broad) δ 6.02 (2H), 5.65 (2H), 4.37 (2H), 3.03 (2H), 1.62 + 1.29 (12H), 0.93 (3H); carbene signal observed during the reaction at δ 11.97. M_w = 36700. PDI = 1.13. Data presented is for octyl substituted **12a**. Polymers **12b-c** were also prepared by this method and had nearly identical NMR spectra except for the alkyl region of the spectrum.

Polymer **21**: Reaction time: 7 h. Yield: quantitative. ^{1}H NMR ($C_6D_4Cl_2$) δ 5.46, 5.23, 4.95, 3.64, 3.55, 3.13, 3.03, 1.84, 1.00, 0.62.

General procedure for the oxidation of precursor polymers 12a-c and 21: 1 equivalent of the precursor polymer is reacted with 1 equivalent of 2,3-dichloro-5,6-dicyano-1,4-benzochinone (DDQ) in dichlorobenzene or bromobenzene respectively. The reaction mixture is heated if necessary. The reaction can be followed by ^{1}H NMR. As the reaction progresses, yellow precipitate of hydroxy-DDQ forms, and the polymer solution becomes flourescent. Pouring of the reaction mixture into methanol results in dissolving of hydroxy-DDQ and precipitation of the product. Purification is achieved by repeated precipitation into methanol from methylene chloride.

Polymer **13a**: Reaction conditions: 5 h at 120 °C in bromobenzene. Yield: 95 %. ^{1}H NMR (toluene-d_8): Poor solubility caused some difficulty in obtaining a good spectrum. Broad peaks were observed at δ 7.8 - 6.6 and 1.3 – 0.93. UV/VIS (chloroform) λ_{max} = 437 nm.

Polymer **22**: Reaction conditions: 1 min at room temperature in dichlorobenzene. Yield: 96 %. ^{1}H NMR ($C_6D_4Cl_2$) δ 6.81, 6.47, 6.35, 2.25, 1.21, 0.94, 0.61.

E. References and Notes

A majority of the work in this chapter has been previously published: a. Wagaman, M. W.; Bellmann, E.; Grubbs, R. H. *Phil. Trans. R. Soc. Lond. A* **1997**, *355*, 727. b. Wagaman, M. W.; Bellmann, E.; Cucullu, M.; Grubbs, R. H. *J. Org. Chem.* **1997**, *62*, 9076.

(1) For a general introduction to olefin metathesis, see Ivin, K. J. *Olefin Metathesis* Academic Press, London, 1996.

(2) a. Grubbs, R. H.; Tumas, W. *Science* **1989**, *243*, 907. b. Schrock, R. R. *Acc. Chem. Res.* **1990**, *23*, 158.

(3) Titanium-based initiators: a. Cannizzo, L. F.; Grubbs, R. H. J. *Org. Chem.* **1985**, *50*, 2386. b. Gilliom, L. R.; Grubbs, R. H. *Organometallics* **1986**, *5*, 721. Ruthenium-based initiators: c. Nguyen, S. T.; Grubbs, R. H.; Ziller, J. W. *J. Am. Chem. Soc.* **1993,** *115,* 9858. d. Schwab, P. E.; Grubbs, R.H.; Ziller, J. W. *J. Am. Chem. Soc.* **1996,** *188,* 100. Molybdenum-based initiators: e. Schrock, R.

R.; DePue, R. T.; Feldman, J.; Schaverein, C. J.; Dewan, J. C.; Liu, A. H. *J. Am. Chem. Soc.* **1988,** *110,* 1423. f. Schrock, R. R.; Murdzek, J. S.; Bazan, G. C.; Robbins, J.; DiMare, M.; O'Regan, M.*J. Am. Chem. Soc.* **1990,** *112,* 3875.

(4) The metallocyclobutane-mechanism was first suggested by a. Herisson, J.-L.; Chauvin, Y. *Makromol. Chem.* **1971**, *141*, 161. For mechanistic studies involving well-defined transition-metal carbenes, see b. Dias, E. L.; Nguyen, S. T.; Grubbs, R. H. *J. Am. Chem. Soc.* **1997**, *119*, 3887. c. Tallarico, J. A.; Bonitatebus, P. J.; Snapper, M. L. *J. Am. Chem. Soc.* **1997**, *119*, 7157.

(5) a. Scholl, M.; Trnka, T. M.; Morgan, J. P.; Grubbs, R. H. *Tetrahedron Lett.* **1999**, *40*, 2247. b. Weskamp, T.; Kohl, F. J.; Hieringer, W.; Gleich, D.; Herrmann, W. A. *Angew. Chem., Int. Ed.* **1999**, *38*, 2416. c. Chang, S.; Jones, L.; Wang, C. M.; Henling, L. M.; Grubbs, R. H. *Organometallics* **1998**, *17*, 3460. d. Lynn, D. M.; Mohr, B.; Grubbs, R. H. *J. Am. Chem. Soc.* **1998**, *120*, 1627.

(6) a. Pu, L.; Grubbs, R. H. *J. Org. Chem.* **1994**, *59*, 1351. b. Pu, L.; Wagaman, M. W.; Grubbs, R. H. *Macromolecules* **1996**, *29*, 1138.

(7) Hales, N. J.; Heaney, H.; Hollinshead, J. H.; Singh, P. *Org. Syn.* **1979,** *59,* 71.

(8) a. Corey, e. J.; Carey, F. A.; Winter, R. A. E. *J. Am. Chem. Soc.* 1965, 87, 934. b. Corey, E. J.; Hopkins, P. B. *Tetrahedron Lett.* **1982,** *23,* 1979.

(9) Wagaman, M. W.; Grubbs, R. H. *Synth. Met.* **1997**, *84*, 327.

(10) An example for fabrication of OLEDs using soluble PNV: Tasch, S.; Graupner, W.; Leising, G.; Pu, L.; Wagaman, M. W.; Grubbs R. H. *Adv. Mater.* **1995**, *7*, 903.

(11) a. Zimmerman, H. E.; Paufler, R. M. *J. Am. Chem. Soc.* **1960**, *82*, 1514. b. Zimmerman, H. E.; Grunewald, G. L.; Paufler, R. M.; Sherwin, M. A. *J. Am. Chem. Soc.* **1969**, *91*, 2330. c. Liu, R.. H.; Krespan, C. G. *J. Org. Chem.* **1969**, *34*, 1271. d. Stapersma, J.; Rood, I. D. C.; Klumpp, G. W. *Tetrahedron* **1982**, *18*, 191. e. Lightner, D. A.; Paquette, L. A.; Chayangkoon, P.; Lin, H. S.; Peterson, J. R. *J. Org. Chem.* **1988**, *53*, 1969. f. Cossu, S.; Battaggia, S.; DeLucchi, O. *J. Org. Chem.* **1997**, *62*, 4162.

(12) Wagaman, M. W.; Grubbs, R. H. *Macromolecules* **1997**, *30*, 3978.

(13) Cotterill, I. C.; Roberts, S. M. Williams, J. O. *J. Chem. Soc., Chem. Commun.* **1988**, 1628.

(14) a. Künzer, H.; Stahnke, M.; Sauer, G.; Wiechert, R. *Tetrahedron Lett.* **1991,** *32,* 1949. Previously reported methods for reductive cleavage of the *p*-toluene-sulphone group use sodium amalgam or aluminum amalgam. Under these conditions, reduction of the olefinic double-bond can result in low yield of the desired compound: b. Pascali, V.; Umani-Ronchi, A. *J. Chem. Soc., Chem. Commun.* **1973**, 351. c. Davis, A. P.; Whitham, G. H. *J. Chem. Soc., Chem. Commun.* **1980**, 639. More recently, reductive desulfonylation procedures using SmI_2 and DMPU instead of the highly carcinogenic HMPA have been suggested: d. Keck, G. E.; Savin, K. A.; Weglarz, M. A. *J. Org. Chem.* **1995**, *60*, 3194.

(15) a. Back, T. G.; Collins, S. *Tetrahedron Lett.* **1980,** *21,* 2213. b. Back, T. G.; Collins, S.; Kerr, R. G. *J. Org. Chem.* **1983,** *48,* 3077.

(16) Skotheim, T. A., Ed. *Handbook of Conducting Polymers* Marcel Dekker, New York, 1986.

Chapter 3:

New Triarylamine-Containing Polymers as Hole Transport Materials in Organic Light-Emitting Diodes: Effect of Polymer Structure and Cross-linking on Device Characteristics

A. Introduction

Organic hole transport materials find applications in organic light-emitting diodes (OLEDs), where they substantially increase device performance, if placed as hole transport layer (HTL) between the anode and the luminescent layer. An organic material is a potential hole transporter, if it can reversibly form radical cations, e. g. accept and donate positive charges without decomposition. The triarylamine functionality is known to fulfill this requirement and constitutes a key feature of many organic hole transport materials.[1]

Figure 3.1 shows the structures of two widely studied triarylamines. Their hole transport properties have been investigated,[2-6] and they have been used in OLEDs.[1,7-20] Triarylamine-based HTLs are most commonly prepared by vacuum vapor deposition of the molecular material.[1,7-14] Polymeric host-guest systems[1,15] and covalent incorporation of triarylamine into polymers[16-20] have also been reported.

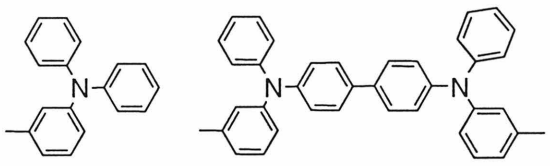

TPA TPD

Figure 3.1: Structures of commonly used organic hole transport materials.

These previous studies showed that physical properties of the systems such as glass transition temperature (T_g), crystallization, phase separation or structure of the polymeric host are as crucial for the device performance as the favorable reversible oxidation potential of triarylamine. This motivated the synthesis of a series of analogous triarylamine-containing polymers with systematic variation in T_g, linker length and linker polarity in order to study the effect of these structural differences on the performance of two-layer OLED devices.

The synthesis and investigation of new hole-transporting polymers is of particular interest, since device fabrication through spin-casting a polymer offers a desirable alternative to vacuum vapor deposition of a molecular material. Large-area and flexible OLEDs can be fabricated using polymer films.[21] Furthermore, covalent incorporation of the hole conducting moiety onto the polymer chain prevents phase separation, a problem seen in many host-guest systems.[1]

Another challenge is the development of cross-linkable hole transport polymers. If the hole-transporting polymer remains soluble, the emissive layer (EL) must be vacuum vapor deposited to prevent destruction of the first layer through exposure to solvents. Making the HTL insoluble by cross-linking would allow to spin cast a luminescent polymer, thereby further enabling flexibility in device fabrication.

This chapter describes the synthesis of a series of cross-linkable triarylamine-containing poly(norbornenes) by ring-opening metathesis polymerization (ROMP)[22,23] and their application in organic LEDs. ROMP allows one to convert a large number of substituted cyclic olefins to the corresponding macromolecules under mild conditions[24-32] providing a variety of comparable polymers. Initiator **1** (Figure 3.2) was shown to be remarkably tolerant towards functional groups[33,34] and to yield living polymerization in many cases.[24,25]

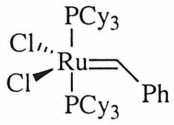

1

Figure 3.2: Structure of the ruthenium-based ROMP-initiator used in this study.

B. Experimental Section

General: Argon was purified by passage through columns of BASF R-11 catalyst (Chemalog) and 4 Å molecular sieves (Linde). NMR spectra were recorded on GE QE-300 Plus (300 MHz for ^{1}H; 75 MHz for ^{13}C) spectrometer. Gel permeation chromatograms were obtained on a HPLC system using an Altex model 110A pump, a Rheodyne model 7125 injector with a 100 μL injection loop, American Polymer Standards 10 micron mixed bed columns, a Knauer differential refractometer and CH_2Cl_2 as eluent at a 1.0 mL/min flow rate. Differential scanning calorimetry was carried out on a Perkin-Elmer DSC-7 with a scan rate of 10 °C/min. High resolution mass spectra were provided

by the Southern California Mass Spectrometry Facility (University of California at Riverside). Elemental analysis was performed by Midwest Microlabs.

Materials: Methylene chloride used in polymerization experiments was distilled from CaH_2 and degassed by freeze-pumping the liquid several times. Toluene and tetrahydrofuran were distilled from Na/benzophenone. All other reagents and starting materials were purchased from Aldrich Chemical Company and used as received unless otherwise noted.

Preparation of 1-bromo-4-(*m*-tolylphenylamino)benzene (2): Tris(dibenzylideneacetone)dipalladium(0) (Pd_2dba_3) (4.00 g, 4.37 mmol), 1,1'-bis(diphenylphosphino)ferrocene (dppf) (3.63 g, 6.55 mmol) and 1,4-dibromobenzene (206 g, 873 mmol) were dissolved in 400 mL dry toluene and stirred for 15 min. Sodium *tert*-butoxide (41.9 g, 436 mmol) and *m*-tolylphenylamine (50 mL, 290 mmol) were then added. The reaction mixture was warmed to 100 °C for 16 h. Thereafter, the reaction mixture was poured into water (1 L) and ether (500 mL), and the aqueous layer was extracted with ether. The combined organics were dried over $MgSO_4$, and the solvent evaporated under reduced pressure. Column chromatography (silica, hexanes) afforded 63.4 g (64%) of product **2**. ^{1}H NMR ($CDCl_3$) δ 7.33-7.23 (m, 4H), 7.15 (t, 1H, J = 7.7 Hz), 7.08-6.86 (m, 8H), 2.27 (s, 3H); ^{13}C NMR ($CDCl_3$) δ 147.5, 147.3, 147.1, 139.3, 132.1, 129.3, 129.2, 125.2, 125.0, 124.3, 124.2, 123.0, 121.8, 114.6, 21.4; HRMS calcd. for $C_{19}H_{16}BrN$ [M^+] 339.0446, found 339.0452; Anal. calcd. for $C_{19}H_{16}BrN$: C 67.47, H 4.77, N 4.14. Found: C 67.42, H 4.71, N 4.18.

Preparation of 1-(hex-5-enyl)-4-(*m*-tolylphenylamino)benzene (3): 12 g (35 mmol) of **2** were dissolved in 500 mL THF and treated with 2 equivalents of *tert*-BuLi

(1.66 M solution in hexanes, 45 mL) at -78 °C under inert gas atmosphere. 14.5 g (89 mmol) of 6-bromohexene were added, and the solution was allowed to slowly warm up to RT. After 5 h water was added to the reaction mixture. The mixture was extracted with ether. After drying the organic phase over $MgSO_4$, the solvent and excess of 6-bromohexene were removed under reduced pressure yielding 11.4 g (94 %) of colorless oil. ^1H NMR (CD_2Cl_2) δ 7.3-6.8 (m, 13H), 5.85 (m, 1H), 5.00 (m, 2H), 2.58 (t, 2H, J = 7.7 Hz), 2.25 (s, 3H), 2.12 (m, 2H), 1.65 (m, 2H), 1.47 (m, 2H); ^{13}C NMR (CD_2Cl_2) δ 147.9, 147.7, 145.2, 138.8, 138.7, 137.2, 128.8, 128.7, 128.6, 124.3, 124.2, 123.2, 123.0, 121.8, 120.8, 113.8, 34.8, 33.3, 30.7, 28.3, 20.8; HRMS calcd. for $C_{25}H_{27}N$ [M^+] 341.2139, found 341.2143; Anal. calcd. for $C_{25}H_{27}N$: C 87.93, H 7.97, N 4.10. Found: C 87.85, H 7.89, N 3.97.

Preparation of 1-(6-hydroxyhexyl)-4-(*m*-tolylphenylamino)benzene (4): 11.4 g (33.3 mmol) of **3** were placed into a 500 mL flask and 150 mL of a 0.5 M solution of 9-borabicyclo[3.3.1]nonane (9-BBN) in THF were added under inert gas atmosphere. The reaction mixture was stirred at RT for 24 h and cooled to 0 °C. 26 mL of 3M NaOH and 22 mL of H_2O_2-solution (30 %) were added slowly. The reaction mixture was warmed up to 50 °C and kept at 50 °C for 2 h. The aqueous phase was extracted with ether, and the product was purified by column chromatography (silica, 30 % ethylacetate in hexanes). Yield: 8.8 g, 74 %. ^1H NMR (CD_2Cl_2) δ 7.3-6.8 (m, 13H), 3.60 (t, 2H, J = 6.5 Hz), 2.58 (t, 2H, J = 7.7 Hz), 2.25 (s, 3H), 1.7-1.5 (m, 4H), 1.5-1.3 (m, 4H); ^{13}C NMR (CD_2Cl_2) δ 147.9, 147.7, 145.2, 139.1, 137.8, 128.8, 128.7, 128.6, 124.3, 124.2, 123.5,

123.4, 121.8, 120.8, 62.8, 35.3, 32.8, 31.6, 29.2, 25.7, 20.8; HRMS calcd. for $C_{25}H_{29}NO$ [MH^+] 360.2318, found 360.2327.

Preparation of 1-(2-hydroxyethyl)-4-(*m*-tolylphenylamino)benzene (5): 4-bromophenethanol was protected with a triphenylmethyl (trityl) group by stirring a solution of 4-bromophenethanol (20.3 g, 0.101 mol), trityl chloride (30.97 g, 0.111 mol), and 4-dimethylaminopyridine (200 mg) in pyridine (200 mL) under nitrogen atmosphere at 70 °C for 33 h. The protected compound was purified by phase separation between methylene chloride and water and flash column chromatography (silica, 10 % ethylacetate in hexanes). The yield of the trityl protected 4-bromophenethanol was 74 %. The protected 4-bromophenethanol (31.10 g, 70.16 mmol) was coupled to *m*-anisidine (13.3 mL, 77.2 mmol) following the procedure for Pd-catalyzed amination as described for **2**. The reaction time needed was 24 h at 90 °C. The reaction mixture was cooled down to RT and separated between ether and water layers. The combined organic layer was concentrated *in vacuo*. Column chromatography (silica, 20 % methylene chloride in hexanes) afforded a mixture of starting materials and the product. This mixture was dissolved in diethyl ether (150 mL) and treated with 98 % formic acid (200 mL). The resultant solution was stirred at RT for 90 min. After 90 min, the reaction mixture was separated between ether and water layers, and the ether layer was washed with water and saturated aqueous sodium bicarbonate solution. Concentration of the organic layer and column chromatography (silica, 30 % ethyl acetate in hexanes) yielded 9.6 g (45 % over 2 steps) of a very viscous material. ^1H NMR (CD_2Cl_2) δ 7.25-6.95 (m, 10H), 6.89 (s, 1H), 6.82 (d, 2H, J = 7.7 Hz), 3.81 (q, 2H, J = 6.3 Hz), 2.79 (t, 2H, J = 6.5 Hz), 2.24 (s,

3H), 1.45 (t, 1H, J = 5.8 Hz); ^{13}C NMR (CD_2Cl_2) δ 148.4, 148.2, 146.6, 139.5, 133.6, 130.2, 129.5, 129.4, 125.1, 124.7, 124.1, 123.9, 122.7, 121.6, 63.8, 38.9, 21.5; HRMS calcd. for $C_{21}H_{22}NO$ [MH^+] 304.1701, found 304.1696.

Preparation of 1-methoxy-3-(*m*-tolylphenylamino)benzene (6): 3-Bromoanisole was reacted with 1 equivalent of *m*-tolylphenylamine in analogy to the procedure described for **2**. The reaction time needed was 8 h at 95 °C. The yield after purification (silica gel column, 5 % ethylacetate in hexanes) was 83 %. ^{1}H NMR (CD_2Cl_2) δ 7.3-6.85 (m, 10H), 6.65-6.55 (m, 3H), 3.70 (s, 1H), 2.27 (s, 1H); ^{13}C NMR (CD_2Cl_2) δ 161.1, 149.8, 148.4, 148.2, 139.7, 130.3, 129.7, 129.6, 125.8, 124.8, 124.4, 123.2, 122.3, 116.8, 110.2, 108.3, 55.7, 21.7; HRMS calcd. for $C_{20}H_{19}NO$ [M^+] 289.1467, found 289.1469; Anal. calcd. for $C_{20}H_{19}NO$: C 83.01, H 6.62, N 4.84. Found: C 82.89, H 6.76, N 4.66.

Preparation of 1-hydroxy-3-(*m*-tolylphenylamino)benzene (7): 13.3 g (53.1 mmol) of BBr_3 were added to a solution of **6** (12.8 g, 44.2 mmol) in 200 mL dry CH_2Cl_2 at -78 °C under inert gas atmosphere. The solution was stirred at -78 °C for 5 min and at RT for 3 h. 150 mL of ice water were added, and the reaction mixture was stirred for another 3 h. Extraction with CH_2Cl_2 followed by column chromatography (silica, 10 % ethylacetate in hexanes) afforded 8.3 g (68 %) of **7**. ^{1}H NMR (CD_2Cl_2) δ 7.3-6.85 (m, 10H), 6.62 (m, 1H), 6.50 (t, 1H, J = 2.1 Hz), 6.45 (m, 1H), 5.04 (bd s, 1H), 2.27 (s, 3H); ^{13}C NMR (CD_2Cl_2) δ 156.9, 150.0, 148.3, 148.1, 130.6, 129.8, 129.7, 126.1, 125.1, 124.7, 123.5, 122.6, 116.4, 110.8, 109.8, 21.7; HRMS calcd. for $C_{19}H_{17}NO$ [M^+]

275.1310, found 275.1312; Anal. calcd. for $C_{19}H_{17}NO$: C 82.88, H 6.22, N 5.09. Found: C 82.92, H 6.21, N 5.13.

Preparation of the ester monomers 8, 9 and 10: To a solution of the respective alcohol **4**, **5** or **7** in THF were added 1 equivalent of norborn-2-ene-5-carbonyl-chloride[35] and 2 equivalents of triethylamine. The reaction mixture was heated to 50 °C for 5 h in the case of **8** and **9** or stirred at RT for 2 h in the case of **10**. The triethylaminehydro-chloride was filtered off, the solvent removed under reduced pressure and the products purified by column chromatography (silica, 5 % ethylacetate in hexanes). Yields: 95-100 %.

8 (mixture of endo and exo): ^{1}H NMR (CD_2Cl_2) δ 7.3-6.8 (m, 13H), 2H: 6.20 (dd, J_1 = 3.0 Hz, J_2 = 5.7 Hz) + 6.15 (m) + 5.94 (dd, J_1 = 3.0 Hz, J_2 = 5.7 Hz), 4.04 (m, 2H), 2H: 3.21 (bd s) + 3.04 (bd s) + 2.95 (m), 2.58 (t, 2H, J = 7.7 Hz), 2.25 (s and m, 4H), 1.7-1.2 (m, 12H); ^{13}C NMR (CD_2Cl_2) δ 174.5, 147.9, 147.7, 145.2, 139.2, 138.0, 137.7, 135.8, 132.4, 128.8, 128.7, 128.6, 124.3, 124.2, 123.2, 123.0, 121.8, 120.8, 64.5, 64.2, 49.6, 46.7, 46.3, 45.8, 43.3, 43.2, 42.7, 41.7, 35.3, 31.5, 30.3, 29.0, 28.7, 25.9, 20.8; HRMS calcd. for $C_{33}H_{37}NO_2$ [MH^+] 480.2899, found 480.2902.

9 (mixture of endo and exo): ^{1}H NMR (CD_2Cl_2) δ 7.3-6.8 (m, 13H), 2H: 6.15 (dd, J_1 = 3.0 Hz, J_2 = 5.7 Hz and m) + 5.76 (dd, J_1 = 3.0 Hz, J_2 = 5.7 Hz), 4.23 (m, 2H), 4H: 3.15 (bd s) + 3.0-2.8 (m), 2.25 (s, 3H), 1.9 (m, 1H), 1.5-1.3 (m, 4H); ^{13}C NMR (CD_2Cl_2) δ 174.0, 147.9, 147.7, 146.0, 138.8, 137.7, 137.3, 132.4, 130.7, 128.8, 128.7, 128.6, 124.3, 124.2, 123.2, 123.0, 121.8, 120.8, 64.5, 64.2, 49.3, 46.7, 46.3, 45.5, 43.0, 42.9, 42.3, 41.4, 34.2, 30.0, 30.3, 28.7, 20.8; HRMS calcd. for $C_{29}H_{29}NO_2$ [MH^+]

424.2261, found 424.2276; Anal. calcd. for $C_{29}H_{29}NO_2$: C 82.24, H 6.90, N 3.31. Found: C 81.86, H 6.96, N 3.32.

10 (mixture of endo and exo): ^{1}H NMR (CD_2Cl_2) δ 7.3-6.6 (m, 13H), 2H: 6.22 (dd, J_1 = 3.0 Hz, J_2 = 5.7 Hz) + 6.15 (m) + 5.98 (dd, J_1 = 3.0 Hz, J_2 = 5.7 Hz), 2H: 3.32 (bd s) + 3.12 (m) + 2.94 (bd s), 2.25 (s, 3H), 1.95 (m, 1H), 1.6-1.2 (m, 4H); ^{13}C NMR (CD_2Cl_2) δ 173.7, 152.2, 149.6, 148.1, 147.9, 139.8, 138.9, 138.8, 136.3, 132.8, 130.2, 129.92, 129.90, 126.1, 125.2, 124.9, 123.7, 122.7, 121.0, 120.9, 116.8, 115.8, 64.5, 64.4, 50.3, 47.4, 47.0, 46.5, 44.2, 43.9, 43.3, 42.4, 29.9, 20.8; HRMS calcd. for $C_{27}H_{25}NO_2$ [MH^+] 396.1968, found 396.1964; Anal. calcd. for $C_{27}H_{25}NO_2$: C 82.00, H 6.37, N 3.54. Found: C 82.06, H 6.51, N 3.58.

Preparation of 1-(6-iodohexyl)-4-(*m*-tolylphenylamino)benzene (11): A solution of triphenylphosphine (8.76 g, 33.4 mmol) and imidazole (2.32 g, 33.4 mmol) in acetonitrile/ether (1:3, 80 mL) was cooled to 0 °C and iodine (8.48 g, 33.4 mmol) was added slowly under vigorous stirring, yielding a yellow slurry. The ice bath was removed and the reaction mixture stirred at RT for 15 min. A solution of **4** (4 g, 11 mmol) in 20 mL of the acetonitrile/ether solvent mixture was then added dropwise, and the reaction mixture stirred for 1h. Filtration through a plug of silica with 5 % ethylacetate in hexanes as eluent afforded 5.07 g (97 %) of pure product. ^{1}H NMR (CD_2Cl_2) δ 7.3-6.8 (m, 13H), 3.22 (t, 2H, J = 6.9 Hz), 2.58 (t, 2H, J = 7.7 Hz), 2.25 (s, 3H), 1.85 (m, 2H), 1.65 (m, 2H), 1.42 (m, 4H); ^{13}C NMR (CD_2Cl_2) δ 147.9, 147.7, 145.2, 139.1, 137.6, 128.8, 128.7, 128.6, 124.3, 124.2, 123.5, 123.4, 121.8, 120.8, 35.2, 33.6, 31.4, 30.4, 28.3, 20.8, 7.6; HRMS calcd. for $C_{25}H_{28}NI$ [M^+] 469.1279, found 469.1267; Anal. calcd. for $C_{25}H_{28}NI$:

C 63.97, H 6.01, N 2.98. Found: C 63.93, H 5.96, N 2.80.

Preparation of 1-(2-iodoethyl)-4-(*m*-tolylphenylamino)benzene (12): 12 was prepared in analogy to **11** in 97 % yield. ^{1}H NMR (CD_2Cl_2) δ 7.3-6.8 (m, 13H), 3.35 (t, 2H, J = 7.2 Hz), 3.12 (t, 2H, J = 7.2 Hz), 2.25 (s, 3H); ^{13}C NMR (CD_2Cl_2) δ 147.9, 147.7, 146.7, 139.3, 135.0, 129.18, 129.16, 129.0, 125.0, 124.0, 123.8, 122.6, 121.5, 39.8, 20.8, 6.3; HRMS calcd. for $C_{21}H_{20}NI$ [MH^+] 414.0726, found 414.0719; Anal. calcd. for $C_{21}H_{20}NI$: C 61.03, H 4.88, N 3.39. Found: C 61.06, H 4.96, N 3.28.

Preparation of 1-(6-(norborn-2-ene-5-methoxy)hexyl)-4-(*m*-tolylphenylamino)benzene (13): Norborn-2-ene-5-methanol (0.53 g, 4.3 mmol) was dissolved in 20 mL THF and treated with NaH (0.15 g, 6.4 mmol) at 0 °C. After stirring for 15 min, a solution of **11** (4 g, 4.3 mmol) in THF (10 mL) was added dropwise. The reaction mixture was allowed to slowly warm up to RT and stirred for 6 h. Water was added and the reaction mixture extracted with ether. Removing the solvent under reduced pressure and column chromatography afforded 0.44 g (22 %) of the desired product as a mixture of endo- and exo-isomers. ^{1}H NMR (CD_2Cl_2) δ 7.3-6.8 (m, 13H), 2H: 6.12 (dd, J_1 = 3.0 Hz, J_2 = 5.7 Hz) + 6.09 (m) + 5.95 (dd, J_1 = 3.0 Hz, J_2 = 5.7 Hz), 4H: 3.37 (m) + 3.23 (t, J = 7.2 Hz) + 3.13 (dd, J_1 = 6.6 Hz, J_2 = 9.3 Hz) + 3.00 (t, J = 9.0 Hz), 3H: 2.90 (bd s) + 2.79 (bd s) + 2.74 (bd s) + 2.34 (m), 2.58 (t, 2H, J = 7.7 Hz), 2.25 (s, 3H), 12H: 1.83 (m) + 1.7-1.5 (m) + 0.51 (m); ^{13}C NMR (CD_2Cl_2) δ 147.9, 147.7, 145.2, 138.8, 137.5, 136.7, 136.3, 132.4, 128.8, 128.7, 128.6, 124.3, 124.2, 123.2, 123.0, 121.8, 120.8, 75.1, 74.2, 70.6, 70.4, 49.1, 44.7, 43.8, 43.5, 42.0, 41.3, 48.71, 48.57, 35.0, 33.3, 31.3, 20.1, 29.5, 29.3, 29.0, 28.8, 25.8, 25.0, 20.8, 7.1; HRMS calcd. for $C_{33}H_{39}NO$ [M^+] 465.3032,

found 465.3028.

Preparation of 1-(norborn-2-ene-5-methoxy)-3-(m-tolylphenylamino)-benzene (14): A solution of norborn-2-ene-5-methanol (1.8 g, 14.5 mmol), **7** (4 g, 14.5 mmol) and triphenylphosphine (5.7 g, 22 mmol) in 250 mL THF was cooled to 0 °C. 2.53 g (14.5 mmol) diethyl azodicarboxylate (DEAD) were added dropwise, and the solution stirred at RT for 6 h. After addition of water the reaction mixture was extracted with ether. Purification by column chromatography (silica, 5 % ethylacetate in hexanes) yielded 2.64 g (48 %) of product as a mixture of endo- and exo-isomers. ^{1}H NMR (CD_2Cl_2) δ 13H: 7.3-6.85 (m) + 6.75-6.55 (m), 2H: 6.18 (dd, J_1 = 3.0 Hz, J_2 = 5.7 Hz) + 6.15 (m) + 5.98 (dd, J_1 = 3.0 Hz, J_2 = 5.7 Hz), 2H: 4.00 ($_d$d, J1 = 6.*0* Hz, J2 = 9.$_3$ Hz) $_+$ 3.79 (t, J = 9.0 Hz) + 3.66 (dd, J1 = 6.3 Hz, J2 = 9.0 Hz) + 3.15 (^{t}, J $_=$ 9.0 Hz), 7H: 3.05 (bd s) + 2.89 (m) + 2.55 (m) + 1.92 (m) + 1.51 (m) + 1.45-1.2 (m) + 0.63 (m), 2.30 (s, 3H); 13C NMR (CD2Cl2) δ 160.6, 149.8, 149.7, 148.5, 148.3, 139.6, 138.1, 137.4, 137.1, 133.0, 130.4, 130.3, 129.8, 129.6, 125.8, 124.9, 124.4, 123.2, 122.4, 117.1, 111.2, 111.1, 109.1, 72.8, 72.0, 50.1, 45.7, 44.5, 44.3, 42.9, 42.2, 39.2, 39.0, 30.2, 29.7, 22.1; HRMS calcd. for $C_{27}H_{27}NO$ [MH^+] 382.2171, found 382.2175; Anal. calcd. for $C_{27}H_{27}NO$: C 85.00, H 7.13, N 3.67. Found: C 84.78, H 7.18, N 3.68.

General polymerization procedure: In a nitrogene filled dry box, a solution of the monomer and a solution of the initiator **1**[33] in CH_2Cl_2 were prepared. (1 mL solvent was used for every 100 mg monomer. The initiator was dissolved in minimum amount of solvent. Monomer to initiator ratio was 100.) The reaction was initiated by adding the initiator solution to the vigorously stirred monomer solution. The reaction mixture was

stirred for 2.5 h. Outside the dry box, the reaction was terminated by adding a small amount of ethylvinylether and poured into methanol to precipitate the polymer. The polymer was purified by dissolving in CH_2Cl_2 and reprecipitating into methanol several times and drying *in vacuo*. Isolated yields ranged from 85 to 95 % (100 % by NMR).

Poly-8: ^{1}H NMR ($CDCl_3$) δ 7.3-6.8 (bd m, 13H), 5.6-5.2 (bd, 2H), 4.0 (bd s, 2H), 5H: 3.2 (bd) + 2.9 (bd) + 2.6 (2 broad signals overlap), 2.2 (bd, 3H), 12H: 2.0 (bd) + 1.7 (bd) + 1.4 (bd) + 1.2 (bd).

Poly-9: ^{1}H NMR ($CDCl_3$) δ 7.3-6.8 (bd m, 13H), 5.6-5.2 (bd, 2H), 4.0 (bd s, 2H), 5H: 3.2 (bd) + 2.9 (2 broad signals overlap) + 2.5 (bd), 2.2 (bd, 3H), 4H: 2.0 (bd) + 1.8 (bd) + 1.4 (bd).

Poly-10: ^{1}H NMR ($CDCl_3$) δ 7.3-6.6 (bd m, 13H), 5.6-5.2 (bd, 2H), 3.2-2.3 (bd, 3H), 2.2 (bd, 3H), 4H: 2.1-1.6 (bd) + 1.4 (bd).

Poly-13: ^{1}H NMR ($CDCl_3$) δ 7.3-6.8 (bd m, 13H), 5.6-5.2 (bd, 2H), 4H: 3.4 (bd) + 3.2 (bd), 3.0-2.4 (bd, 5H), 2.2 (bd, 3H), 12H: 1.9 (bd) + 1.6 (bd) + 1.4 (bd) + 1.2 (bd).

Poly-14: ^{1}H NMR ($CDCl_3$) δ 7.3-6.8 (bd m, 13H), 5.6-5.2 (bd, 2H), 2H: 3.8 (bd) + 3.6 (bd), 3.0-2.2 (bd, 3H), 2.2 (bd, 3H), 4H: 2.0-1.5 (bd) + 1.2 (bd).

Fabrication and characterization of light-emitting devices: Devices were fabricated on ITO coated glass substrates with a sheet resistance of 20 ohms/sq (Donnelly Corporation) which had been ultrasonicated in acetone and methanol, dried in a stream of nitrogen, and then plasma etched for 60 seconds. Polymer layers were formed by spin casting from chlorobenzene solutions (10 g/L). The second layer consisted of vacuum vapor deposited Alq (50 nm), which had been purified by recrystallization and

sublimation prior to deposition. Mg cathodes (200 nm) were thermally deposited at a rate of 8 Å/s through a shadow mask to create devices 3 x 5 mm in area. Current-voltage and light output characteristics of the devices were measured in forward bias. Device emission was measured using a silicon photodetector at a fixed distance from the sample (12 cm). The response of the detector had been calibrated using several test devices, for which the total power emitted in the forward direction was measured with a NIST traceable integrating sphere (Labsphere). Photometric units of cd/m^2 were calculated using the forward output power and the electroluminescence spectra of the devices. Efficiencies were measured in units of external quantum efficiency (% photons/electron). Cathode deposition and device characterization were performed in a nitrogen dry box (VAC).

Cross-linking procedure: Polymer films were placed 7 inches away from a 150 W Hg:Xe lamp with a glass diffuser in between for uniform exposure and irradiated for 1 hour.

C. Results and Discussion

Synthesis: The monomers employed in this study are norbornenes linked to a tri-arylamine. The linkers contain either an ester- or an ether-functionality, which varies the polarity around the triarylamine group. Increases in linker length result in a greater number of degrees of freedom for the TPA functionality in the polymer.

The key step of the monomer synthesis is the assembly of a suitably functionalized triarylamine moiety through Pd-catalyzed coupling of a substituted

bromobenzene with *m*-tolylphenylamine (Scheme 3.1). Using the chemistry developed by Buchwald and Hartwig,[36-39] the different triarylamines have been obtained in yields of 64 % to 83 %.

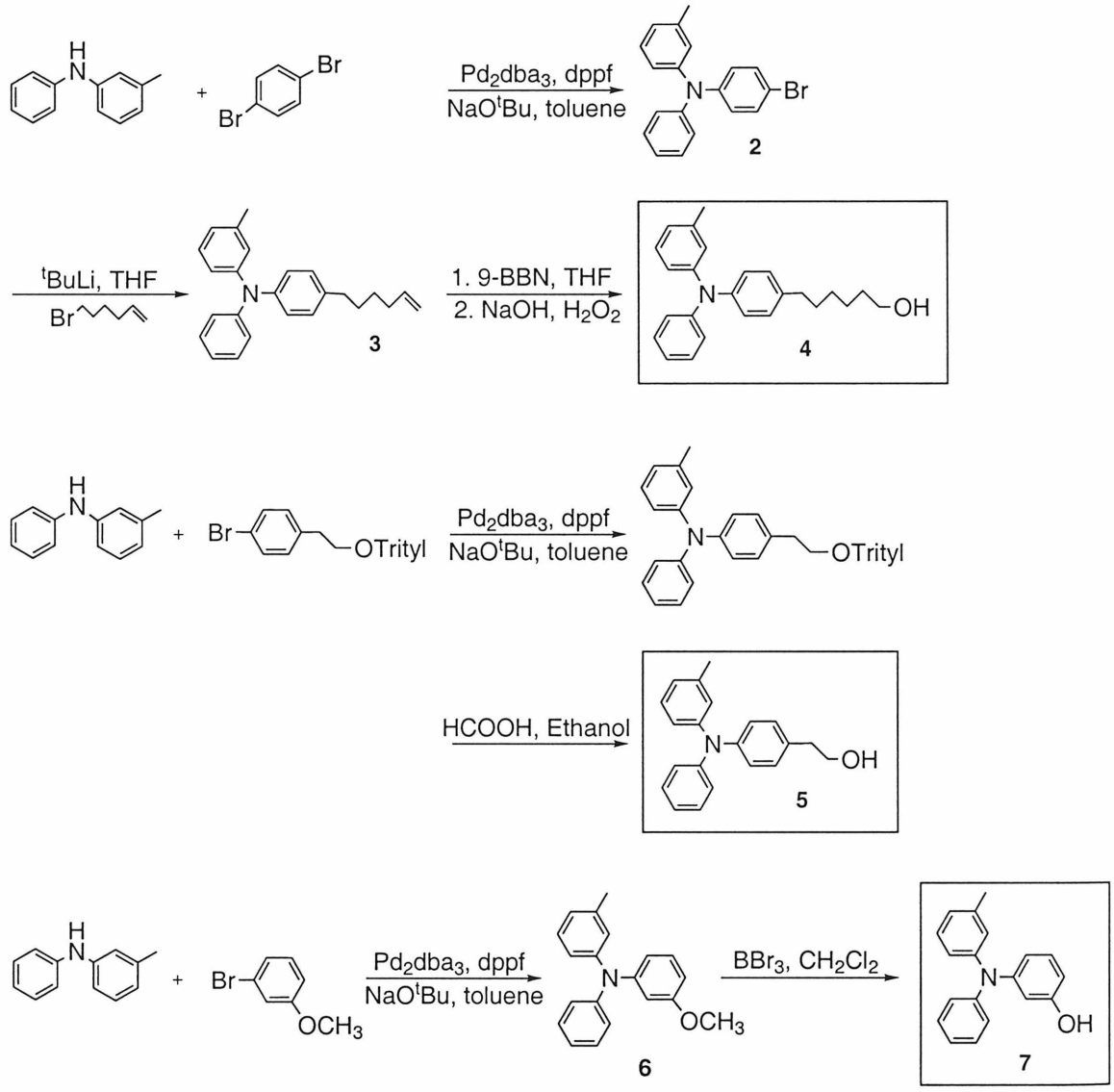

Scheme 3.1: Synthesis of functionalized triarylamines bearing alkyl linkers of different lengths.

Alkylation of 1-bromo-4-(*m*-tolylphenylamino)benzene (**2**) with 6-bromohexene followed by reaction with 9-BBN afforded a triarylamine bearing a C_6-alkyl linker (**4**) (Scheme 3.1).

Attempts to synthesize C_4-, C_3- and C_2-analogues of **4** from 1-bromo-4-(*m*-tolylphenylamino)benzene failed. 4-Bromobutene and TBS-protected 4-bromobutanol have been tested as C_4-alkylating agents under conditions similar to the synthesis of **3**. In both cases, only *m*-tolyldiphenylamine was isolated, suggesting that elimination to butadiene is favored over the desired reaction pathway. Reaction of allylbromide with **2** under lithiation conditions and reaction of allyl-MgBr with **2** in the presence of a Ni-catalyst[40,41] did not result in formation of the C_3-analogue of **3**. Similarly, reaction of vinyl-MgBr with **2** did not yield the desired product.

As illustrated in Scheme 3.1, a triarylamine bearing a C_2-linker (**5**) was prepared from 4-bromophenethanol and compound **7** (C_0-linker) was obtained via Pd-coupling of *m*-bromoanisidine to *m*-tolylphenylamine.

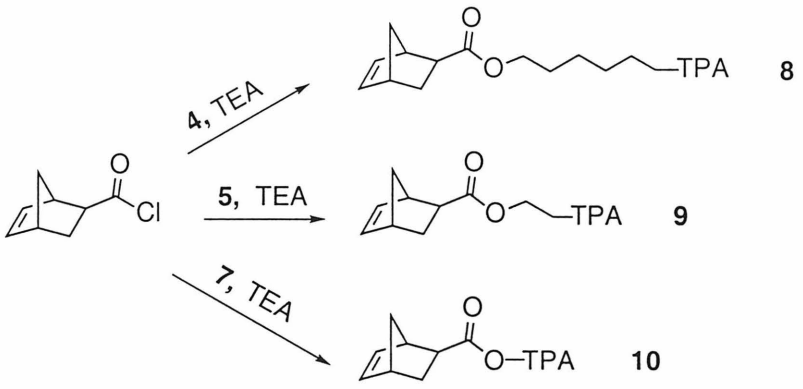

Scheme 3.2: Synthesis of the monomers containing ester groups.

As shown in Schemes 3.2 and 3.3, compound **7** can be directly attached to a norbornene acid chloride or norbornene alcohol to produce monomers with a C_0-linker. A *para*-alkoxy-substituent would significantly alter the oxidation potential of triaryl-amine.[42] Therefore, *meta*-substituted phenol **7** was prepared to ensure that the resulting C_0-polymers are comparable to the polymers bearing C_2- or C_6-linkers.

The ester monomers **8, 9** and **10** have been synthesized from the alcohols **4, 5** and **7** as shown in Scheme 3.2.

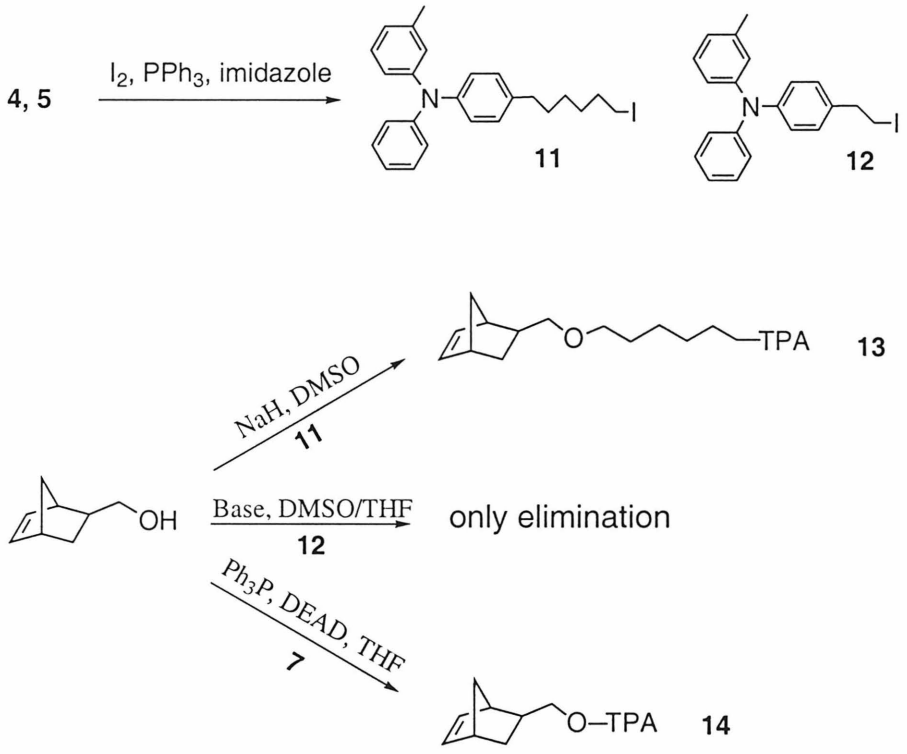

Scheme 3.3: Synthesis of the monomers containing ether groups.

To prepare the less polar ether monomers, the alcohols **4** and **5** have been transformed to the corresponding iodides[43] **11** and **12** and reacted with norborn-2-ene-5-methanol as shown in Scheme 3.3. In both cases, elimination interfered with ether

formation. In the case of **11**, the desired product **13** was isolated in 22 % yield along with the elimination product **3**. In the case of **12**, only 1-vinyl-4-(*m*-tolylphenylamino)-benzene[44] was obtained in 60 % yield. It has been found, that NaH does not react with **11** and **12**, but the elimination is caused by the deprotonated norborn-2-ene-5-methanol. Changing the base therefore had no effect on the ratio of ether formation to elimination. Employing different solvents and lowering the reaction temperature did not improve the yield of the ether. Reaction of alcohols **4** and **5** with norborn-2-ene-5-methyliodide have been tried, but resulted only in decomposition.

The C_0-monomer **14** was obtained through coupling of the phenol **7** to norborn-2-ene-5-methanol using Mitsunobu conditions[45] (Scheme 3.3).

Initiator **1** was used to polymerize the monomers **8, 9, 10, 13** and **14**. The polymerization reaction was allowed to proceed for 2.5 h at room temperature in dichloromethane. Treatment with ethylvinylether cleaved the initiator from the polymer chain. The polymers were then isolated and purified by repeated precipitation from methanol. All polymers were prepared using a monomer to initiator ratio of 100. Polydispersities ranged between 1.14 and 1.22 (Table 3.1). The general structure of the polymers is shown in Figure 3.3.

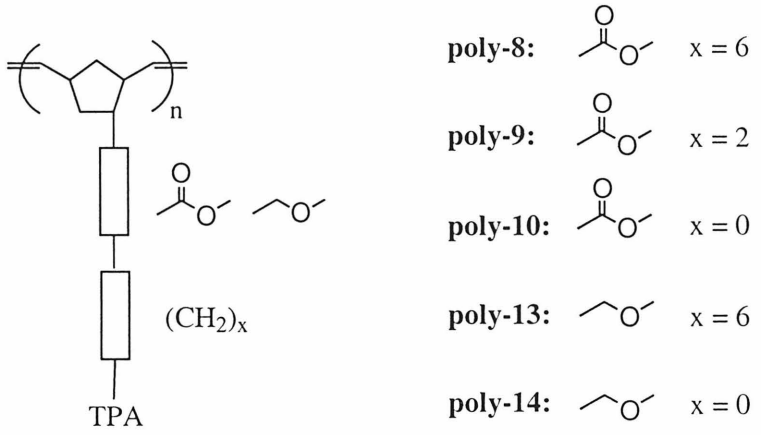

Figure 3.3: General structure of the hole-transporting polymers.

Table 3.1: Polymerization results.

polymer	M_n[a]	PDI[a]
poly-8	48 000	1.22
poly-9	38 000	1.16
poly-10	46 000	1.13
poly-13	62 000	1.22
poly-14	58 000	1.17

[a] Determined by gel permeation chromatography in CH_2Cl_2 relative to monodispersed polystyrene standards.

As previously observed with liquid crystalline ROMP polymers,[24] the T_g decreases with increasing linker length indicating that the triarylamine side group should have higher mobility (Table 3.2). Furthermore, the T_g of the ester polymers was found to be significantly higher compared to their ether analogues.

Table 3.2: Glass transition temperatures for the different triarylamine-substituted poly-(norbornenes).

-COO-polymer	T_g (°C)	-CH_2-O-polymer	T_g (°C)
poly-8	37.6	**poly-13**	23.4
poly-9	72.6		
poly-10	84.0	**poly-14**	68.3

All polymers cross-link upon exposure to UV-light. For thin films, irradiation with a 150 W Hg:Xe lamp for 1 h causes the films to become completely insoluble in organic solvents. Addition of a sensitizer is not necessary and does not shorten the time needed for cross-linking. We presume, that the triarylamine substituents, which have their absorption maximum at 303 nm, sensitize a photochemical reaction of the carbon-carbon double bonds in the backbone. The UV-irradiated films remain colorless, transparent and retain their blue fluorescence.

Fabrication and Characterization of Light-Emitting Devices: Two-layer OLEDs have been prepared with **poly-8, poly-9, poly-10, poly-13** and **poly-14** as the hole-transporting layer (HTL). Indium tin oxide (ITO) was used as the anode, Mg as the cathode (200 nm) and tris(8-quinolinato)aluminum (Alq) as electron-transporting and emitting layer (50 nm). The light emission corresponded to the typical Alq emission spectrum[7,8] resulting in green OLEDs.

All of the studied polymers have very good solubilities in organic solvents, and spin casting from chlorobenzene yielded uniform thin films of good quality. Thinner HTL results in decreased device operating voltage. However, when the HTL gets too

thin, the external quantum efficiency starts to decrease (Table 3.3). The device data reported in Table 3.4 and Figures 3.4 and 3.5 refer to 20 nm thick HTL films, which showed the highest external power efficiency.

Table 3.4 and Figures 3.4 and 3.5 summarize the device data for the hole transporting poly(norbornenes). All of the studied polymers exhibit high quantum efficiencies. The small structural differences between the five polymers have a large impact on the device performance, showing that reducing the polarity and length of the linker greatly improves the characteristics (compare **poly-8** (C_6/ester) to **poly-14** (C_0/ether)).

Table 3.3: ITO/**poly-14**/Alq/Mg: Dependence of the device performance on the thickness of the hole transport layer.

thickness of the HTL-film (nm)[a]	operating voltage (V)[b]	max. ext. quantum eff. (% photons/ electron)	max. light output (cd/m^2)	max. ext. power eff. (Lm/W)
30	5.25	0.81	1690 @ 11 V	1.21
20	4.25	0.77	2580 @ 8 V	1.30
15	3.25	0.62	3150 @ 7 V	1.23

[a] Determined by TINCOR alpha-step profilometer. [b] Light output at this voltage equals 5 cd/m^2.

Poly-10 (C_0/ester) decomposed rapidly under device operating conditions. Separation of the carbonyl group from the triarylamine functionality by an alkyl segment results in increased stability of the device **(poly-9, poly-8)**. The ether polymers **poly-13** and **poly-14** show best stabilities, presumably since they lack the carbonyl group as a reaction center, which reduces the number of possible decomposition pathways.

Substitution of the ester functionality by the less polar ether linkage causes the external quantum efficiency to increase and the operating voltage to decrease significantly (Table 3.4, Figure 3.4). In the case of **poly-13** and **poly-8** a threefold increase in external quantum efficiency has been achieved by substituting carbonyl groups with the non-polar methylene groups.

Table 3.4: ITO/poly(norbornene)-TPA/Alq/Mg: Device performance for different hole-transporting polymers.

HTL-polymer		operating voltage (V)[a]	max. ext. quantum eff. (% photons/ electron)	max. light output (cd/m^2)	max. ext. power eff. (Lm/W)
-COO-	**poly-8**	6.75	0.20	240 @ 11 V	0.26
	poly-9	5.50	0.63	800 @ 10 V	0.84
	poly-10	(8)[b]	(0.42)[b]	(1030 @ 14 V)[b]	(0.54)[b]
-CH_2-O-	**poly-13**	5.50	0.65	850 @ 8 V	0.96
	poly-14	4.25	0.77	2580 @ 8 V	1.30
x-linked	**poly-14**	5.25	0.37	880 @ 9 V	0.61

All data refers to 20 nm thick HTL films. Cross-linking of **poly-14** was achieved by UV-irradiation after spin-casting on ITO. [a]Light output at this voltage equals 5 cd/m^2. [b]Degradation interfered with measurement.

Based on disorder formalism developed by Bässler and Borsenberger[2,3,6] the hole mobilities in the less polar polymers, that is polymers with linkers containing an ether functionality, should be higher. The disorder model assumes that the charge transport occurs through hopping between localized electronic states, which show a Gaussian-shaped distribution. According to the model, energetical disorder, e.g. the presence of several functional groups with different polarities, results in broadening of the

distribution of states and, consequently, in lower charge mobilities. Thus, these results on two-layer devices using a hole transport layer and Alq as an emitting layer suggest that the quantum efficiency can be improved and the operating voltage decreased by increasing the hole mobility of the HTL. One caveat of this analysis is the possible influence of the polymer structure on the charge transfer reactions at the anode/HTL and HTL/EL interfaces. The polymer structure could have affected the position of the highest occupied molecular orbital (HOMO) of the triaryl moiety, or it could have altered the film quality, namely the degree of surface coverage and the strength of adhesion at the interfaces.

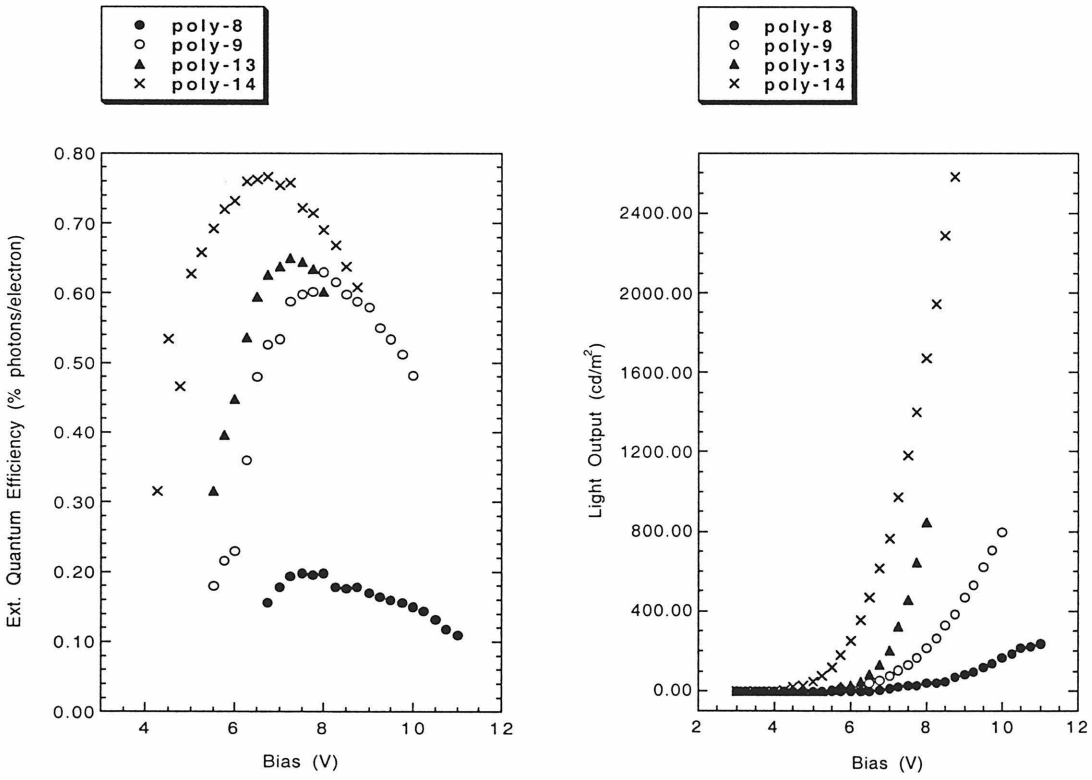

Figure 3.4: ITO/poly(norbornene)-TPA/Alq/Mg: External quantum efficiency and light output *versus* bias voltage for different triarylamine-substituted poly(norbornenes) as the hole transport layer.

By introducing longer alkyl linkers, the number of degrees of freedom available to the triarylamine side groups has been increased. It has been previously found for carbazole containing polymers, that increased mobility of the hole conducting side groups enhances the hole mobility.[46] An optimum linker length has been shown to exist in that study. In this system, however, a decrease in efficiency and an increase in operating voltage with increasing linker length is observed (**poly-8** vs. **poly-9** and **poly-13** vs. **poly-14**). The polymers with the shortest linkers show best performance. If side group mobility promotes hole transport in this system, this influence is overcompensated by the fact, that longer alkyl linkers correspond to more insulating matter around the hole-transporting functionalities. Thus, with increasing linker length the density of triaryl-amine groups becomes lower resulting in less efficient charge transport and decreased device performance.

All of the studied polymers can be cross-linked by a simple procedure, which does not require addition of other reagents or removal of byproducts. Cross-linked devices show poorer performance relative to the ones with the original soluble films (Table 3.4, Figure 3.5). Possible explanations are partial decomposition of the polymers in UV and decreased film quality as a consequence of slight volume changes upon cross-linking. Decreased mobility of the triarylamine side groups may also contribute to a reduced charge transport capability. A cross-linkable HTL will allow the fabrication of two-layer devices with a spin-casted polymer as an emitting layer.

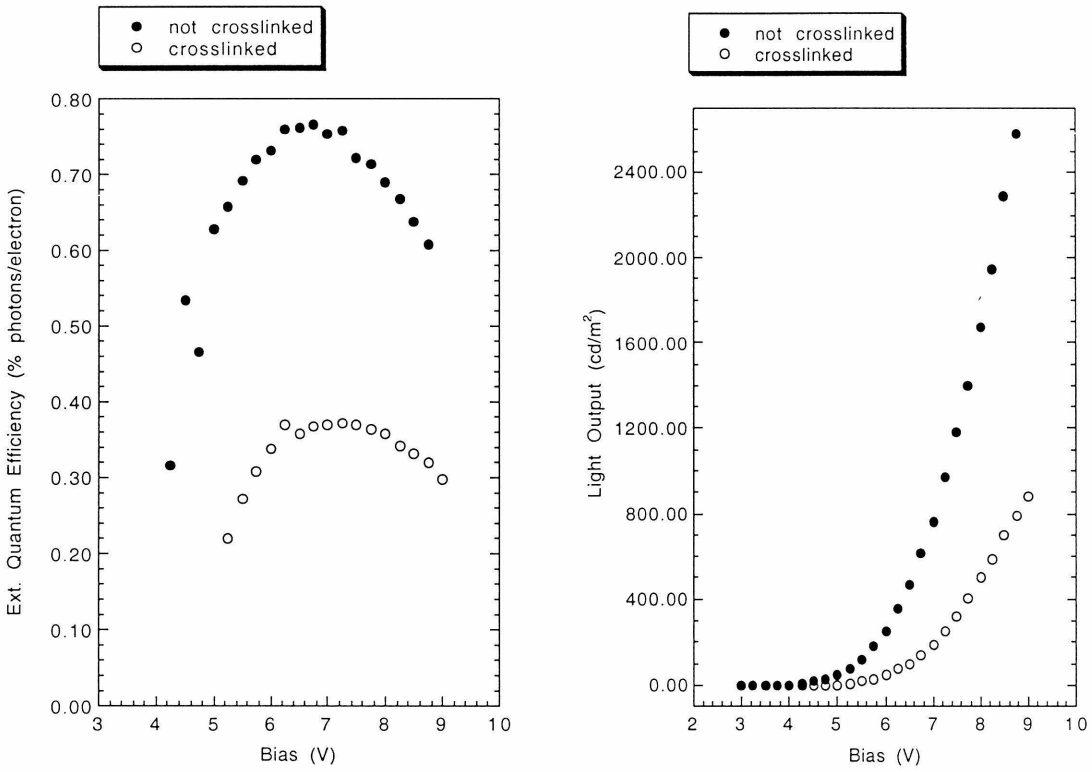

Figure 3.5: ITO/**poly-14**/Alq/Mg: Effect of cross-linking of the hole transport layer on the external quantum efficiency and light output.

D. Summary and Conclusions

A series of cross-linkable polymeric hole transport materials has been synthesized, and the influence of structural changes within this series on the performance of organic two-layer LEDs (ITO/poly(norbornene)-TPA/Alq/Mg) has been investigated. Poly(norbornenes) with pendent triarylamine groups have proven to yield devices with high external quantum efficiencies and light output. The device performance improved as a result of slight changes in the polymer backbone. The least polar polymer with the

shortest linker showed the highest external quantum efficiency (0.77 %), the lowest operating voltage (4.25 V), and best device stability.

The film formation properties of these poly(norbornenes) are excellent allowing efficient fabrication of thin (20 nm and thinner) HTL-films through spin-casting. The HTL-films can be easily cross-linked by UV-irradiation. Cross-linking, however, has been found to decrease device performance. The maximum external quantum efficiency for the best material dropped from 0.77 % to 0.37 %.

For future work, it is to be concluded, that avoiding polar functional groups and long spacers in the polymer backbone will yield promising hole transport materials for OLED and laser applications.

E. References and Notes

A majority of the work in this chapter has been previously published: Bellmann, E.; Shaheen, S. E.; Thayumanavan, S.; Barlow, S; Grubbs, R. H.; Marder, S. R.; Kippelen, B.; Peyghambarian, N. *Chem. Mater.* **1998**, *10*, 1668.

(1) Tsutsui, T. *MRS Bulletin* **June 1997**, 39.

(2) Van der Auweraer, M.; De Schryver, F. C.; Borsenberger, P. M.; Fitzgerald, J. J. *J. Phys. Chem.* **1993**, *97*, 8808.

(3) Borsenberger, P. M.; Pautmeier, L.; Richert, R.; Bässler, H. *J. Chem. Phys.* **1991**, *94*, 8276.

(4) Gruenbaum, W. T.; Sorriero, L. J.; Borsenberger, P. M.; Zumbulyadis, N. *Jpn. J. Appl. Phys.* **1996**, *35*, 2714.

(5) Heun, S.; Borsenberger, P. M. *Physica B* **1995**, *216*, 43.

(6) Bässler, H. *Phys. Status Solidi (b)* **1993**, *175*, 15 and references therein.

(7) Tang, C. W.; VanSlyke, S. A. *Appl. Phys. Lett.* **1987**, *51*, 913.

(8) Tang, C. W.; VanSlyke, S. A.; Cheng, C. H. *J. Appl. Phys.* **1989**, *65*, 3610.

(9) Kalinowski, J.; Di Marco, P.; Cocchi, M.; Fattori, V.; Camaioni, N.; Duff, J *Appl. Phys. Lett.* **1996**, *68*, 2317.

(10) Tanaka, K.; Tokito, S.; Taga, Y; Okada, A. *J. Chem Soc., Chem. Commun.* **1996**, 2175.

(11) Tokito, S.; Tanaka, H.; Okada, A.; Taga, Y. *Appl. Phys. Lett.* **1996**, *69*, 878.

(12) Adachi, C.; Tokito, S.; Tsutsui, T.; Saito, S. *Jpn. J. Appl. Phys.* **1988**, *27*, L269.

(13) Mori, T.; Obata, K.; Imaizumi, K.; Mizutani, T. *Appl. Phys. Lett.* **1996**, *69*, 3309.

(14) Burrows, P. E.; Shen, Z.; Bulovic, V.; McCarty, D. M.; Forrest, S. R.; Cronin, J. A.; Thompson, M. E. *J. Appl. Phys.* **1996**, *79*, 7991.

(15) Lin, C. P.; Tsutsui, T.; Saito, S. *New Polymeric Mater.* **1995**, *4*, 277.

(16) Kim, D. U.; Aminaka, E.; Tsutsui, T.; Saito, S. *Jpn. J. Appl. Phys.* **1995**, *34*, 6255.

(17) Kim, D. U.; Tsutsui, T. *J. Appl. Phys.* **1996**, *80*, 4785.

(18) Kolb, E. S.; Gaudiana, R. A.; Mehta, P. G. *Macromolecules* **1996**, *29*, 2359.

(19) Hosokawa, C.; Kawasaki, N.; Sakamoto, S.; Kusumoto, T. *Appl. Phys. Lett.* **1992**, *61*, 2503.

(20) Kraft, A.; Burn, P. L.; Holmes, A. B.; Bradley, D. D. C.; Friend, R. H.; Martens, J. H. F. *Synthetic Metals* **1993**, *55*, 4163.

(21) Gustaffson, G.; Cao, Y.; Treacy, G. M.; Klavetter, F.; Colaneri, N.; Heeger, A. J. *Nature* **1992**, *357*, 477.

(22) Grubbs, R. H.; Tumas, W. *Science* **1989**, *243*, 907.

(23) Schrock, R. R. *Acc. Chem. Res.* **1990**, *23*, 158.

(24) Maughon, B. R.; Weck, M.; Mohr, B.; Grubbs, R. H. *Macromolecules* **1997**, *30*, 257.

(25) Maughon, B. R.; Grubbs, R. H. *Macromolecules* **1997**, *30*, 3459.

(26) Boyd, T. J.; Geerts, Y.; Lee, J.; Fogg, D. E.; Lavoie, G. G.; Schrock, R. R.; Rubner, M. F. *Macromolecules* **1997**, *30*, 3553.

(27) Percec, V.; Schlueter, D. *Macromolecules* **1997**, *30*, 5783.

(28) Biagini, S. C. G.; Gibson, V. C.; Giles, M. R.; Marshall, E. L.; North, M. *J. Chem. Soc., Chem. Commun.* **1997**, 1097.

(29) Gibson, V. C.; Marshall, E. L.; North, M.; Robson, D. A.; Williams, P. J. *J. Chem. Soc., Chem. Commun.* **1997**, 1095.

(30) Gratt, J.; Cohen, R. E. *Macromolecules* **1997**, *30*, 3137.

(31) Wagaman, M. W.; Bellmann, E.; Grubbs, R. H. *Phil. Trans. R. Soc. Lond. A* **1997**, *355*, 727.

(32) Schneider, M. F.; Lucas, N.; Velder, J.; Blechert, S. *Angew. Chem., Int. Ed. Eng.* **1997**, *36*, 257.

(33) Schwab, P.; Grubbs, R. H.; Ziller, J. W. *J. Am. Chem. Soc.* **1996**, *118*, 100.

(34) Schwab, P.; France, M. B.; Ziller, J. W.; Grubbs, R. H. *Angew. Chem., Int. Ed. Eng.* **1995**, *34*, 2039.

(35) Jacobine, A. F.; Glaser, D. M.; Nakos, S. T. *Polym. Mater. Sci. Eng.* **1989**, *60*, 211.

(36) Wolfe, J. P.; Rennels, R. A.; Buchwald, S. L. *Tetrahedron* **1996**, *52*, 7525.

(37) Wolfe, J. P.; Wagaw, S.; Buchwald, S. L. *J. Am. Chem. Soc.* **1996**, *118*, 7215.

(38) Driver, M. S.; Hartwig, J. F. *J. Am. Chem. Soc.* **1996**, *118*, 7217.

(39) Thayumanavan, S.; Barlow, S.; Marder, S. R. *Chem. Mater.* **1997**, *9*, 3231.

(40) Tamao, K.; Sumitani, K.; Kumada, M. *J. Am. Chem. Soc.* **1972**, *94*, 4374.

(41) Nugent, W. A.; McKinney, R. J. *J. Org. Chem.* **1985**, *50*, 5370.

(42) Barlow, S.; Thayumanavan, S.; Marder, S. R. unpublished results.

(43) Millar, J. G.; Underhill, E. W. *J. Org. Chem.* **1986**, *51*, 4727.

(44) An efficient synthesis of 1-vinyl-4-(*m*-tolylphenylamino)benzene, its anionic polymerization and applications of the polymer as hole transport material is described in Chapter 4.

(45) Nakano, J.; Mimura, M.; Hayashida, M.; Kimura, K.; Nakanishi, T. *Heterocycles* **1983**, *20*, 1975.

(46) Domes, H.; Fischer, R.; Haarer, D.; Strohriegl, P. *Makromol. Chem.* **1989**, *190*, 165.

Chapter 4:

Organic Two-Layer Light-Emitting Diodes Based on High-T_g Hole-Transporting Polymers with Different Redox Potentials

A. Introduction

Many organic light-emitting diodes (OLEDs) are two-layer devices with a film of a hole-transporting material (HTL) between the anode (most commonly ITO = indium tin oxide) and the electroluminescent layer (EL). The hole-transporting material traps the electrons inside EL but allows hole injection into the EL. This facilitates exciton formation inside the EL or at the HTL/EL interface consequently improving the overall device characteristics. Three key properties of the hole transport material impact the device performance: i) hole mobility within the material, ii) its redox potential, and iii) its thermal/electrochemical stability.

Hole mobilities in organic materials have been widely studied,[1-5] and they have been shown to correlate with device performance.[6] The redox potential determines how easily the material is oxidized at the anode/HTL interface (reaction (1)), or how easily its radical cation is reduced at the HTL/EL interface (reaction (2) and (3)).

Redox reaction at the anode/HTL interface:

$$HTM \longrightarrow HTM^{+\cdot} + e^{-} \quad (1)$$

Redox reactions at the HTL/EL interface:

$$HTM^{+\cdot} + EM \longrightarrow HTM + EM^{+\cdot} \quad (2)$$

$$HTM^{+\cdot} + EM^{-\cdot} \longrightarrow HTM + EM^{*S} \quad (3)$$

HTM hole transport moiety
EM electroluminescent moiety

Relatively electron-rich compounds are commonly used as hole transport materials, since facile hole injection at the anode/HTL interface is believed to promote device function.[7,8] However, hole-transporting materials with a lower redox potential and a lower energetic barrier for hole injection at the anode/HTL interface also have a higher barrier for hole injection into the EL (Figure 4.1a).

Another pathway for exciton formation is the generation of the EM^{*S} emissive state through reaction of the radical cation of the hole transport material with the radical anion of the electroluminescent material[9] (reaction (3)). This process can occur if the energy difference between the LUMO of the emitter and the HOMO of the hole transport material is larger than the energy of the EM^{*S} emissive state. This reaction proceeds more readily for larger LUMO(EM)/HOMO(HTM) differences. Figure 4.1b illustrates how a lower energetic barrier for hole injection at the anode/HTL interface is associated with a smaller driving force for the EM^{*S} formation *via* this pathway.

Thus, facile hole injection from the anode appears to be counterbalanced by increased energetic barriers for the reactions at the HTL/EL interface. Therefore, it is difficult to predict which redox behavior of the hole transport material is optimal for the overall device performance. This motivated the preparation of hole transport polymers

with different redox potentials in order to study the effect of the redox potential on the characteristics of a two-layer OLED.

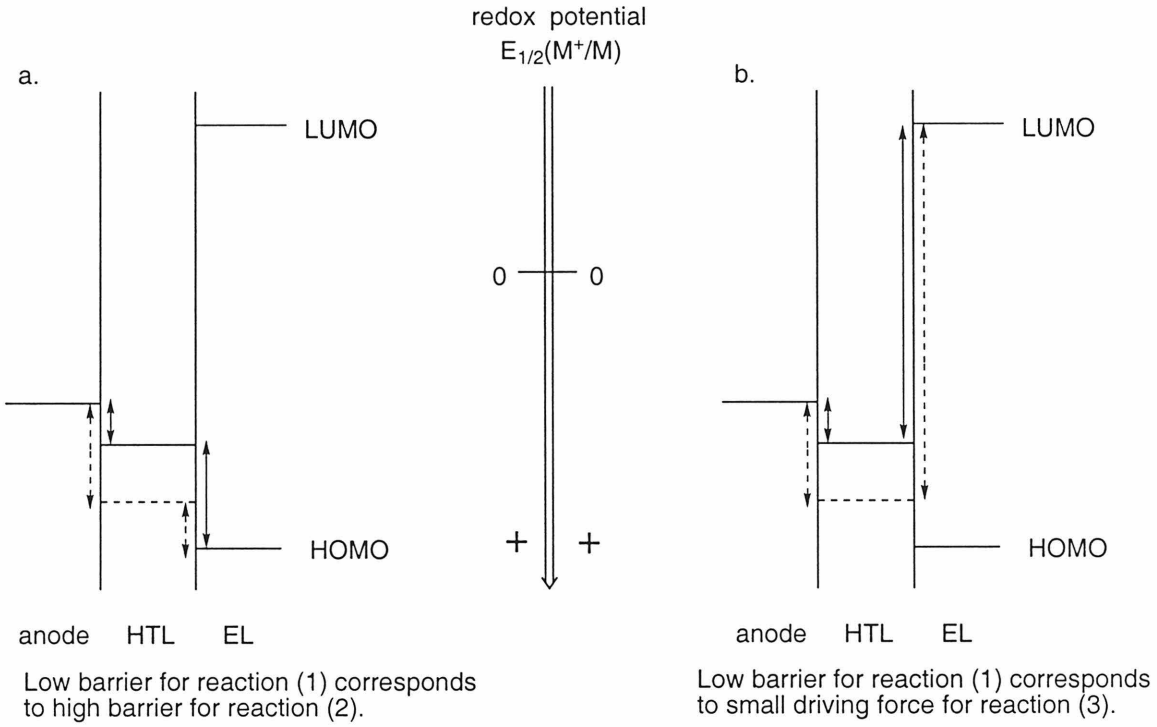

Figure 4.1: Schematic representation of the energy barriers at the anode/HTL and the HTL/EL interfaces for different redox potentials of the hole transport material.

This chapter describes the synthesis of a series of analogous hole transport polymers with systematic variation of the redox potential. The hole-transporting functionalities are derivatives of the well-studied organic hole-transporting molecules TPA and TPD[7] (see also Chapter 1, part A). Since high glass transition temperatures have been found to increase the thermal and long-term stability of the device,[10] the TPA and TPD derivatives have been incorporated into high-Tg polymers. Furthermore, by preparing a high molecular weight hole-transporting material desirable film formation properties have been achieved. The data is reported for two-layer OLEDs with indium

tin oxide (ITO) as the anode, tris(8-quinolinato)aluminum (Alq) as the electroluminescent material and magnesium as the cathode.

B. Experimental Section

General: All syntheses were carried out under argon, which was purified by passage through columns of BASF R-11 catalyst (Chemalog) and 4 Å molecular sieves (Linde). NMR spectra were recorded on GE QE-300 Plus (300 MHz for ^{1}H; 75 MHz for ^{13}C) spectrometer. Gel permeation chromatograms were obtained on a HPLC system using an Altex model 110A pump, a Rheodyne model 7125 injector with a 100 μL injection loop, American Polymer Standards 10 micron mixed bed columns, a Knauer differential refractometer and CH_2Cl_2 as eluent at a 1.0 mL/min flow rate. Cyclic voltammetry was conducted using a glassy carbon working electrode, a platinum auxiliary electrode and a AgCl/Ag pseudo-reference electrode in 0.1 M solutions of tetrabutylammonium hexafluorophosphate in methylene chloride. Redox potentials were referenced to the ferrocene/ferrocenium couple ($E_{1/2}$ (ferrocenium/ferrocene) = 0 V). Differential scanning calorimetry was carried out on a Perkin-Elmer DSC-7 with a scan rate of 10 °C/min. Thermal gravimetric analysis was performed under nitrogen at a heating rate of 10 °C/min using a Shimadzu TGA-50 device and aluminum pans. UV-VIS spectra were recorded using a Hewlett-Packard HP 8453 spectrometer. High resolution mass spectra were provided by the Southern California Mass Spectrometry Facility (University of California at Riverside) and by Mass Spectrometry Facility of

University of California at Los Angeles. Elemental analyses were performed by Midwest Microlabs.

Materials: Toluene and tetrahydrofuran were distilled from Na/benzophenone. Methylene chloride used in cyclic voltammetry measurements was dried and degassed by passage through drying columns.[11] Samples of molecular TPD derivatives were provided by Dr. Stephen Barlow and Dr. S. Thayumanavan. 1-bromo-4-(*m*-tolylphenylamino)-benzene (**4b**) was prepared as described in Chapter 3. All other reagents and starting materials were purchased from Aldrich Chemical Company or Strem Chemicals and used as received unless otherwise noted.

Preparation of 4-bromo-4'-(*m*-tolyl-*p*-methoxyphenylamino)biphenyl (1a): Tris(dibenzylideneacetone)dipalladium(0) (Pd_2dba_3) (618 mg, 0.67 mmol), 1,1'-bis(di-phenylphosphino)ferrocene (dppf) (561 mg, 1 mmol) and 3-bromotoluene (7.7 g, 45 mmol) were dissolved in 400 mL dry toluene and stirred for 15 min. Sodium *tert*-butoxide (5.2 g, 54 mmol) and *p*-methoxyaniline (5.5 g, 45 mmol) were then added. The reaction mixture was warmed to 100 °C for 3 h. Thereafter, 4, 4'-dibromobiphenyl (42 g, 135 mmol) and sodium *tert*-butoxide (5.2 g, 54 mmol) were added and the reaction mixture heated to 100 °C for 16 h. The reaction mixture was partitioned between water and ether, and the aqueous layer was extracted with ether. The combined organic fractions were dried over $MgSO_4$, and the solvent evaporated under reduced pressure. Column chromatography (silica, hexanes) afforded 19.3 g (84 %) of product **1a**. ^{1}H NMR (CD_2Cl_2) δ 7.57-7.37 (m, 6H), 7.15-6.97 (m, 6H), 6.91-6.80 (m, 4H), 3.78 (s, 3H), 2.24 (s, 3H); ^{13}C NMR (CD_2Cl_2) δ 157.1, 148.7, 148.3, 141.0, 140.2, 139.7, 132.8, 132.4, 129.6, 128.6, 128.1, 127.9, 124.9, 124.1, 122.7, 121.4, 121.1, 115.4, 56.0, 21.8; HRMS

calcd. for $C_{26}H_{22}{}^{81}BrNO$ [M^+] 445.0885, found 445.0864; Anal. calcd. for $C_{26}H_{22}BrNO$: C 69.94, H 4.46, N 3.26. Found: C 69.69, H 4.49, N 3.15.

Preparation of 4-bromo-4'-(*m*-tolylphenylamino)biphenyl (2a): **2a** was prepared by analogy to **1a** using aniline instead of *p*-methoxyaniline in 66 % yield. ^1H NMR (CD_2Cl_2) δ 7.58-7.53 (m, 2H), 7.49-7.43 (m, 4H), 7.29 (dt, J = 2.1, 7.8 Hz, 2H), 7.19 (bd t, J =7.8 Hz, 1H), 7.14-7.03 (m, 5H), 6.98 (bd s, 1H), 6.92 (bd dt, 2H, J = 1.8, 7.6 Hz, 2H), 2.24 (s, 3H); ^{13}C NMR (CD_2Cl_2) δ 147.5, 147.4, 147.2, 139.3, 139.1, 133.0, 131.5, 129.0, 128.9, 127.9, 127.2, 125.1, 124.1, 123.9, 123.2, 122.7, 121.6, 120.5, 20.9; HRMS calcd. for $C_{25}H_{20}{}^{81}BrN$ [M^+] 415.0759, found 415.0753; Anal. calcd. for $C_{25}H_{20}BrN$: C 72.47, H 4.87, N 3.38. Found: C 72.24, H 4.82, N 3.34.

Preparation of 4-bromo-4'-(*m*-tolyl-*m*-fluorophenylamino)biphenyl (3a): 3a was prepared by analogy to **1a** using *m*-fluoroaniline instead of *p*-methoxyaniline in 62 % yield. ^1H NMR (CD_2Cl_2) δ 7.60-7.42 (m, 6H), 7.25-7.12 (m, 4H), 7.02-6.67 (m, 6H), 2.24 (s, 3H), ; ^{13}C NMR (CD_2Cl_2) d 165.7, 162.4, 150.2, 150.0, 147.6, 147.4, 140.2, 140.0, 134.9, 132.4, 130.9, 130.7, 129.9, 128.8, 128.3, 126.7, 125.6, 125.1, 123.2, 121.6, 119.1, 110.5, 110.2, 109.5, 109.2, 21.8; HRMS calcd. for $C_{25}H_{19}{}^{79}BrFN$ [M^+] 433.0664, found 433.0663; Anal. calcd. for $C_{25}H_{19}BrFN$: C 69.45, H 4.43, N 3.24. Found: C 69.66, H 4.45, N 3.28.

Preparation of 4-bromo-4'-(*m*-tolyl-3,5-difluorophenylamino)biphenyl (5a): 5a was prepared by analogy to **1a** using 3,5-difluoroaniline instead of *p*-methoxyaniline in 69 % yield. ^1H NMR (CD_2Cl_2) δ 7.60-7.42 (m, 8H), 7.25-7.15 (m, 4H), 7.01 (bd m, 2H), 6.53 (m, 2H), 6.38 (m, 1H), 2.24 (s, 3H); ^{13}C NMR (CD_2Cl_2) δ 165.9, 165.7, 162.6, 162.4, 150.9, 146.8, 146.7, 140.4, 139.9, 136.0, 132.4, 130.0, 128.9, 128.4, 127.3, 126.4,

126.0, 123.8, 121.9, 121.7, 104.7, 104.6, 104.5, 104.3, 97.2, 96.8, 96.5, 21.8; HRMS calcd. for $C_{25}H_{18}{}^{79}BrF_2N$ [M^+] 449.0583, found 449.0590; Anal. calcd. for $C_{25}H_{18}BrF_2N$: C 66.68, H 4.03, N 3.11. Found: C 66.36, H 4.00, N 3.11.

Preparation of 4-(*m*-tolyl-*p*-methoxyphenylamino)-4'-(*p*-methoxybenzyl-*p*-bromophenylamino)biphenyl (1b): 1b was prepared by analogy to **1a** from **1a** and *p*-methoxyaniline followed by the addition of 1,4-dibromobenzene in 65 % yield. Purification was accomplished by column chromatography on silica gel with hexanes followed by 20 % toluene in hexanes. ^1H NMR (CD_2Cl_2) δ 7.41 (bd t, J = 8.1 Hz, 4H), 7.29 (bd d, J = 8.7 Hz, 2H), 7.06 (m, 10H), 6.87 (m, 8H), 3.78 (s, 6H), 2.24 (s, 3H); ^{13}C NMR (CD_2Cl_2) δ 157.3, 156.9, 148.5, 147.9, 146.9, 141.1, 140.5, 139.6, 135.3, 134.0, 132.5, 129.5, 128.1, 127.9, 127.7, 127.6, 124.5, 124.3, 124.0, 123.7, 123.1, 121.0, 115.4, 115.3, 114.1, 56.0, 21.8; HRMS calcd. for $C_{39}H_{33}{}^{81}BrN_2O_2$ [M^+] 642.1705, found 642.1711; Anal. calcd. for $C_{39}H_{33}BrN_2O_2$: C 73.01, H 5.18, N 4.37. Found: C 72.82, H 5.15, N 4.31.

Preparation of 4-(*m*-tolylphenylamino)-4'-(*m*-tolyl-*p*-bromophenylamino)-biphenyl (2b): 2b was prepared by analogy to **1a** from **2a** and 3-aminotoluene followed by the addition of 1,4-dibromobenzene in 63 % yield. Purification was accomplished by column chromatography on silica gel with hexanes followed by 20 % toluene in hexanes. ^1H NMR (CD_2Cl_2) δ 7.50-7.40 (m, 4H), 7.35-7.30 (m, 2H), 7.28-7.21 (m, 2H), 7.18-7.00 (m, 9H), 6.98-6.85 (m, 8H), 2.24 (s, 6H); ^{13}C NMR (CD_2Cl_2) δ 148.3, 148.1, 147.7, 147.6, 147.5, 146.9, 140.0, 139.8, 135.7, 134.8, 132.6, 129.7, 129.6, 129.5, 128.7, 127.8, 127.7, 126.0, 125.7, 125.6, 124.94, 124.87, 124.76, 124.5, 124.4, 123.3, 122.4, 122.2,

115.0, 21.8; HRMS calcd. for $C_{38}H_{31}{}^{81}BrN_2$ [M^+] 596.1650, found 596.1649; Anal. calcd. for $C_{38}H_{31}BrN_2$: C 76.63, H 5.25, N 4.70. Found: C 76.85, H 5.55, N 4.36.

Preparation of 4-(*m*-tolyl-*m*-fluorophenylamino)-4'-(-*m*-fluorophenyl-*p*-bromophenylamino)biphenyl (3b): 3b was prepared by analogy to **1a** from **3a** and *m*-fluoroaniline followed by the addition of 1,4-dibromobenzene in 63 % yield. Purification was accomplished by column chromatography on silica gel with hexanes followed by 10 % ethyl acetate in hexanes. ^{1}H NMR (CD_2Cl_2) δ 7.52 (dd, J = 8.4, 6.3 Hz, 4H), 7.41 (d, J = 8.7 Hz, 2H), 7.28-7.12 (m, 8H), 7.07-6.93 (m, 5H), 6.90-6.65 (m, 5H), 2.24 (s, 3H); ^{13}C NMR (CD_2Cl_2) δ 164.8, 161.6, 149.4, 149.3, 148.8, 148.6, 146.6, 146.2, 146.0, 145.5, 139.3, 135.7, 134.7, 132.1, 130.1, 130.0, 129.9, 129.8, 129.0, 128.7, 127.9, 127.8, 127.2, 125.8, 125.6, 124.8, 124.5, 124.4, 122.2, 118.5, 118.0, 115.5, 110.0, 109.6, 109.4, 109.1, 109.0, 108.8, 108.3, 108.0, 21.8; HRMS calcd. for $C_{37}H_{27}{}^{81}BrF_2N_2$ [M^+] 618.1305, found 618.1310; Anal. calcd. for $C_{37}H_{27}BrF_2N_2$: C 71.97, H 4.41, N 4.54. Found: C 72.13, H 4.81, N 4.73.

Preparation of 4-(*m*-tolyl-3,5-difluorophenylamino)-4'-(-3,5-difluorophenyl-*p*-bromophenylamino)biphenyl (5b): 5b was prepared by analogy to **1a** from **5a** and 3,5-difluoroaniline followed by the addition of 1,4-dibromobenzene in 62 % yield. Purification was accomplished by column chromatography on silica gel with hexanes followed by 20 % toluene in hexanes. ^{1}H NMR (CD_2Cl_2) δ 7.67-7.62 (m, 2H), 7.58-7.49 (m, 4H), 7.34-7.11 (m, 8H), 7.02-6.93 (m, 3H), 6.86-6.80 (m, 1H), 6.53-6.31 (m, 4H), 2.24 (s, 3H); ^{13}C NMR (CD_2Cl_2) δ 165.5, 165.3, 165.0, 164.9, 164.8, 150.8, 150.65, 150.5, 146.4, 145.8, 145.7, 140.3, 140.0, 136.4, 135.5, 132.7, 132.6, 130.4, 129.7, 129.2,

128.4, 128.0, 127.9, 127.8, 126.9, 125.9, 125.4, 123.4, 122.8, 121.3, 104.2, 104.1, 103.9, 103.8, 103.7, 98.0, 97.6, 96.6, 96.2, 95.9, 95.5, 95.1, 94.8, 21.8; HRMS calcd. for $C_{37}H_{25}{}^{79}BrF_4N_2$ [M^+] 652.1135, found 652.1137; Anal. calcd. for $C_{37}H_{21}BrN_2F_4$: C 68.04, H 3.24, N 4.28. Found: C 68.17, H 3.44, N 4.11.

Preparation of 4-(*m*-tolyl-*p*-methoxyphenylamino)-4'-(*p*-methoxyphenyl-*p*-vinylphenylamino)biphenyl (1): Method 1: **1b** (3 g, 4.67 mmol), palladium acetate (26.2 mg, 0.12 mmol) and tris(*o*-tolyl)phosphine were dissolved in 15 ml toluene. Diethoxymethylvinylsilane (2.25 g, 14 mmol) and tributylammoniumfluoride (21 mL of a 1M solution in tetrahydrofuran, 14 mmol) were added to the solution, and the reaction mixture was heated to 100 °C for 4 h. Method 2: **1b** (3 g, 4.67 mmol), tetrakis(triphenylphosphine)palladium(0) (136 mg, 0.12 mmol) and 2,6-di-*tert*-butyl-4-methylphenol (2-5 mg) were dissolved in 25 mL toluene. Tributyl(vinyl)tin (1.8 g, 5.6 mmol) was added to the solution, and the mixture was heated to 100 °C for 3 h. Purification of the product was achieved through column chromatography (silica, 10 % ethyl acetate in hexanes). The yields were 83 % for method 1 and 92 % for method 2. ^{1}H NMR (CD_2Cl_2) δ 7.46-7.38 (m, 4H), 7.30-7.20 (m, 2H), 7.16-6.97 (m, 12H), 6.94-6.89 (m, 6H), 6.66 (dd, J = 10.8, 17.7 Hz, 1H), 5.63 (d, J = 17.7 Hz, 1H), 5.13 (d, J = 10.8 Hz, 1H), 3.78 (s, 6H), 2.24 (s, 3H); ^{13}C NMR (CD_2Cl_2) δ 157.1, 156.9, 148.5, 148.3, 147.8, 147.6, 143.3, 141.1, 140.8, 139.6, 136.8, 134.9, 134.5, 134.2, 134.1, 131.7, 129.7, 129.5, 128.0, 127.9, 127.5, 124.5, 123.8, 123.6, 123.5, 123.4, 123.2, 122.8, 122.7, 122.5, 121.0, 115.4, 115.3, 112.1, 56.0, 21.8; HRMS calcd. for $C_{41}H_{36}N_2O_2$ [M^+]

588.2777, found 588.2787; Anal. calcd. for $C_{41}H_{36}N_2O_2$: C 83.64, H 6.16, N 4.76. Found: C 83.74, H 6.52, N 4.63.

Preparation of 4-(*m*-tolylphenylamino)-4'-(*m*-tolyl-*p*-vinylphenylamino)-biphenyl (2): **2** was prepared by analogy to **1** from **2b** in yields of 64 % for method 1 and 76 % for method 2. Purification was accomplished by column chromatography on silica gel with 5 % ethyl acetate in hexanes. ^{1}H NMR (CD_2Cl_2) δ 7.45 (dd, *J* = 2.4, 8.7 Hz, 4H), 7.32-7.22 (m, 4H), 7.18-6.97 (m, 12H), 6.95-6.85 (m, 5H), 6.66 (dd, *J* = 11.1, 17.7 Hz, 1H), 5.64 (d, *J* = 17.7 Hz, 1H), 5.13 (d, *J* = 11.1 Hz, 1H), 2.24 (s, 6H); ^{13}C NMR (CD_2Cl_2) δ 148.3, 148.1, 148.0, 147.9, 147.4, 147.1, 139.9, 139.8, 136.7, 135.3, 135.0, 134.9, 133.5, 132.3, 129.7, 129.6, 129.2, 127.7, 127.5, 125.9, 125.7, 124.8, 124.4, 124.0, 123.2, 122.4, 122.2, 112.4, 21.8; HRMS calcd. for $C_{40}H_{34}N_2$ [M^+] 542.2722, found 542.2728; Anal. calcd. for $C_{40}H_{34}N_2$: C 88.52, H 6.31, N 5.16. Found: C 88.53, H 6.58, N 4.98.

Preparation of 4-(*m*-tolyl-*m*-fluorophenylamino)-4'-(-*m*-fluorophenyl-*p*-vinyl-phenylamino)biphenyl (3): **3** was prepared by analogy to **1** from **3b** in yields of 66 % for method 1 and 92 % for method 2. Purification was accomplished by column chromatography on silica gel with 20 % toluene in hexanes. ^{1}H NMR (CD_2Cl_2) δ 7.53-7.45 (m, 4H), 7.36-7.26 (m, 2H), 7.22-7.04 (m, 9H), 6.93 (bd t, *J* = 7.8 Hz, 3H), 6.87-6.62 (m, 7H), 5.67 (d, *J* = 17.7 Hz, 1H), 5.18 (d, *J* = 11.1 Hz, 1H), 2.24 (s, 6H); ^{13}C NMR (CD_2Cl_2) δ 165.6, 162.4, 150.3, 150.1, 149.9, 149.8, 147.5, 147.2, 147.0, 146.6, 140.1, 136.6, 136.2, 136.0, 135.7, 130.6, 130.0, 129.8, 128.3, 128.0, 127.7, 126.5, 125.6, 125.4, 125.3, 125.1, 124.3, 123.0, 119.2, 118.8, 113.1, 110.6, 110.3, 110.2, 110.0, 109.9,

109.6, 109.3, 109.1, 109.0, 108.8, 21.8; HRMS calcd. for $C_{39}H_{30}N_2F_2$ [M^+] 564.2377, found 564.2397; Anal. calcd. for $C_{39}H_{30}N_2F_2$: C 82.96, H 5.35, N 4.96. Found: C 82.78, H 5.43, N 4.85.

Preparation of *m*-tolyl(*p*-vinylphenyl)phenylamine (4): **4** was prepared by analogy to **1** from **4b** in yields of 66 % for method 1 and 89 % for method 2. Purification was accomplished by column chromatography on silica gel with hexanes. ^{1}H NMR (CD_2Cl_2) δ 7.35-7.25 (m, 4H), 7.18 (bd t, *J* = 7.8 Hz, 1H), 7.13-7.01 (m, 5H), 7.18-6.88 (m, 3H), 6.70 (dd, *J* = 10.8, 17.7 Hz, 1H), 5.67 (d, *J* = 17.7 Hz, 1H), 5.13 (d, *J* = 10.8 Hz, 1H), 2.24 (s, 6H); ^{13}C NMR (CD_2Cl_2) δ 147.75, 147.70, 147.6, 139.3, 136.3, 131.7, 129.3, 129.1, 127.0, 125.3, 124.3, 124.1, 123.4, 122.9, 121.8, 111.9, 21.8; HRMS calcd. for $C_{21}H_{19}N$ [M^+] 285.1512, found 285.1517; Anal. calcd. for $C_{21}H_{19}N$: C 88.38, H 6.71, N 4.91. Found: C 88.08, H 6.85, N 4.69.

Preparation of 4-(*m*-tolyl-3,5-difluorophenylamino)-4'-(-3,5-difluorophenyl-*p*-vinylphenylamino)biphenyl (5): **5** was prepared by analogy to **1** from **5b** using method 2 in 78 % yield. Purification was accomplished by column chromatography on silica gel with 20 % toluene in hexanes. ^{1}H NMR (CD_2Cl_2) δ 7.62-7.51 (m, 6H), 7.43-7.37 (m, 2H), 7-29-7.13 (m, 6H), 7.05-6.96 (m, 3H), 6.92-6.75 (m, 2H), 6.57-6.34 (m, 4H), 5.86 (d, *J* = 17.7 Hz, 1H), 5.34 (d, *J* = 10.8 Hz, 1H), 2.24 (s, 6H); ^{13}C NMR (CD_2Cl_2) δ 165.9, 165.7, 165.2, 165.0, 163.1, 162.8, 162.7, 162.5, 161.9, 161.7, 159.8, 159.6, 151.2, 151.0, 150.9, 146.8, 146.1, 144.8, 144.7, 144.6, 141.0, 140.4, 138.3, 136.8, 135.7, 131.4, 131.1, 130.0, 129.5, 128.7, 128.2, 128.1, 127.5, 127.3, 126.3, 125.8, 123.7, 121.6, 115.2, 104.4, 104.1, 98.2, 97.9, 96.9, 96.6, 96.2, 95.7, 95.4, 95.0, 21.8; HRMS

calcd. for $C_{39}H_{28}N_2F_4$ [M^+] 600.2174, found 600.2188; Anal. calcd. for $C_{39}H_{24}N_2F_4$: C 77.99, H 4.03, N 4.68. Found: C 77.89, H 4.17, N 4.52.

General polymerization procedure: The monomer (1.5 mmol, 500 mg - 1 g) was dissolved in solvent mixture of 2 mL toluene and 0.2 mL THF. The solution was cooled to -78 °C and the polymerization was initiated through injection of *n*-butyllithium (0.075 mmol, 46.9 μL of a 1.6 M solution in hexanes). The polymerization was allowed to proceed for 1 h at -78 °C. The reaction mixture was poured into methanol to precipitate the polymer. The polymers were purified by redissolving in methylene chloride and repricipitation into methanol several times and drying *in vacuo*. **P1, P2, P3** and **P4** were prepared using this procedure. In the case of **P5**, the monomer was dissolved in 5 mL THF and 3.075 mmol of *n*-butyllithium were added to initiate. During the purification of **P5**, an insoluble fraction was removed by filtration.

P1: 96 % yield. ^{1}H NMR (CD_2Cl_2) δ 7.4 (bd), 7.1 (bd), 6.8 (bd), 6.5 (bd), 3.7 (bd), 3.4 (bd), 2.2 (bd, two overlapping signals), 1.6 (bd).

P2: 98 % yield. ^{1}H NMR (CD_2Cl_2) δ 7.4 (bd), 7.1 (bd), 6.8 (bd), 2.3 (bd), 2.2 (bd), 1.6 (bd).

P3: 98 % yield. ^{1}H NMR (CD_2Cl_2) δ 7.5 (bd), 7.2 (bd), 6.9 (bd), 6.5 (bd), 2.3 (bd), 2.2 (bd), 1.6 (bd).

P4: 96 % yield. ^{1}H NMR (CD_2Cl_2) δ 7.2-6.5 (bd), 2.2 (bd, two overlapping signals), 1.6 (bd).

P5: 65 % yield. ^{1}H NMR (CD_2Cl_2) δ 7.4 (bd), 7.0 (bd), 6.9 (bd), 6.4 (bd), 6.3 (bd), 2.2 (bd, two overlapping signals), 1.6 (bd).

Fabrication and characterization of light-emitting devices: Devices were fabricated on indium tin oxide (ITO) coated glass substrates (Donnelly Corporation) with a nominal sheet resistance of 20 ohms/sq which had been ultrasonicated in acetone, methanol and isopropanol, dried in a stream of nitrogen, and then plasma etched for 60 seconds. Polymer layers (40 nm) were formed by spin casting from chlorobenzene solutions (10 g/L). The second layer consisted of vacuum vapor deposited tris(8-quinolinato)aluminum (Alq) (60 nm), which had been purified by recrystallization and sublimation prior to deposition. Mg cathodes (200 nm) were thermally deposited at a rate of 8 Å/s through a shadow mask to create devices 3 x 5 mm^2 in area. Current-voltage and light output characteristics of the devices were measured in forward bias. Device emission was measured using a silicon photodetector at a fixed distance from the sample (12 cm). The response of the detector had been calibrated using several test devices, for which the total power emitted in the forward direction was measured with a NIST traceable integrating sphere (Labsphere). Photometric units of cd/m^2 were calculated using the forward output power and the electroluminescence spectra of the devices. Efficiencies were measured in units of external quantum efficiency (% photons/electron). Cathode deposition and device characterization were performed in a nitrogen dry box (Vacuum Atmospheres).

C. Results and Discussion

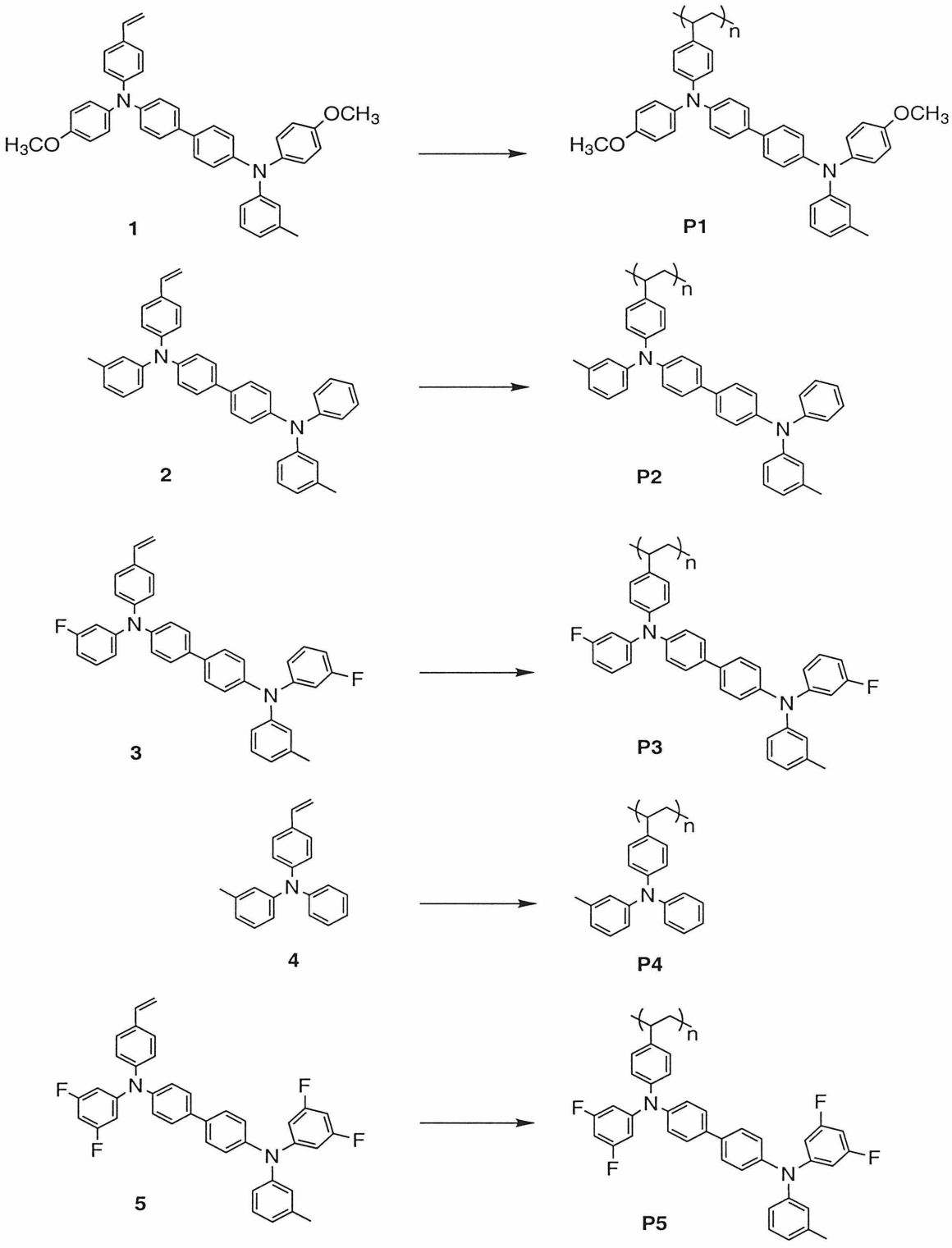

Figure 4.2: Structures of the synthesized hole-transporting polymers and the corresponding monomers.

Previous studies which are described in Chapter 3 have suggested, that polymers with non-polar compact backbones exhibit higher hole mobilities and show improved performance as hole transport layers in OLEDs.[1-6] Therefore, the monomers were designed to contain a styrene type functionality, which would permit anionic or radical polymerization yielding an all-hydrocarbon compact backbone (Figure 4.2). Electron-donating and electron-withdrawing substituents have been introduced on the TPD to vary the redox potential of the hole-transporting moiety.

Monomer Synthesis: Different asymmetrically substituted TPD derivatives have been prepared by an efficient two-step procedure based on palladium-catalyzed amination[12-15] (Scheme 4.1).

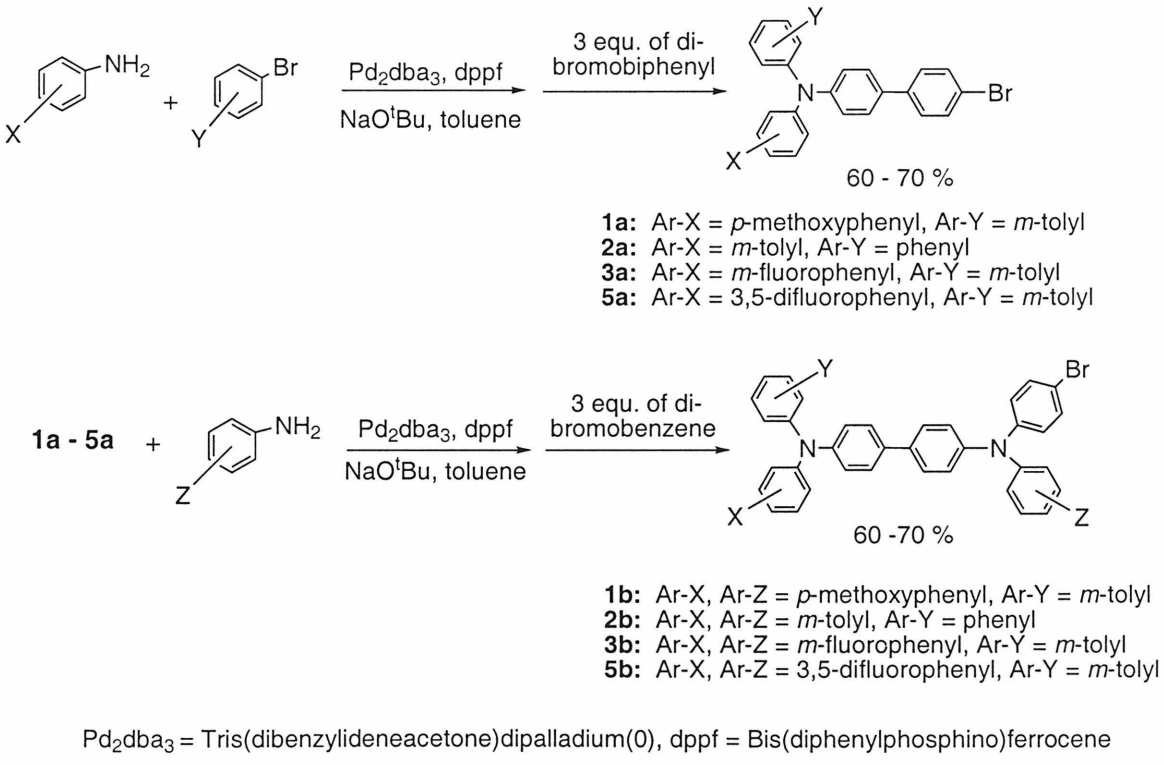

Scheme 4.1: Synthesis of asymmetrically substituted TPD.

In the first step of the reaction sequence, a substituted phenylbromide is reacted with a substituted aniline and subsequently, with an excess of 4,4'-dibromobiphenyl. The substituent patterns on the bromide and the aniline can be chosen freely. The reaction proceeds more smoothly and in higher yields, if the aniline is functionalized with electron-donating groups, and the substituents on the bromide are electron acceptors. In the second step the intermediate is reacted with another substituted aniline and another substituted bromide to yield the TPD derivative. This methodology allows for independent selection of the substituent patterns of the four outer phenyl rings. In this study, the bromide in step two is always 1,4-dibromobenzene, which is used in threefold excess. This results in TPD derivatives functionalized asymmetrically with one *para*-Br-substituent.

In the last step of the monomer synthesis, the monobromo-TPD derivatives are converted to the monovinyl compounds **1-5** by palladium-catalyzed vinylation. The desired products were prepared in high yield using the tributyl(vinyl)tin[16] or an excess of diethoxymethylvinylsilane[17] (Scheme 4.2). Nickel-catalyzed reaction of the bromo-derivatives **1b-5b** with vinyl-Grignard[18,19] did not result in formation of the desired product. Another synthetic route towards **1-5** involves substitution of the bromine in **1b-5b** by an aldehyde group via lithiation and quenching with dimethylformamide, followed by reaction of the aldehyde with the appropriate Wittig reagent or titanium reagent[20] to form the vinyl group. The transformation of **1b-5b** to **1-5** *via* the aldehyde, however, afforded considerably lower yields (approximately 40%) of the monovinyl product.

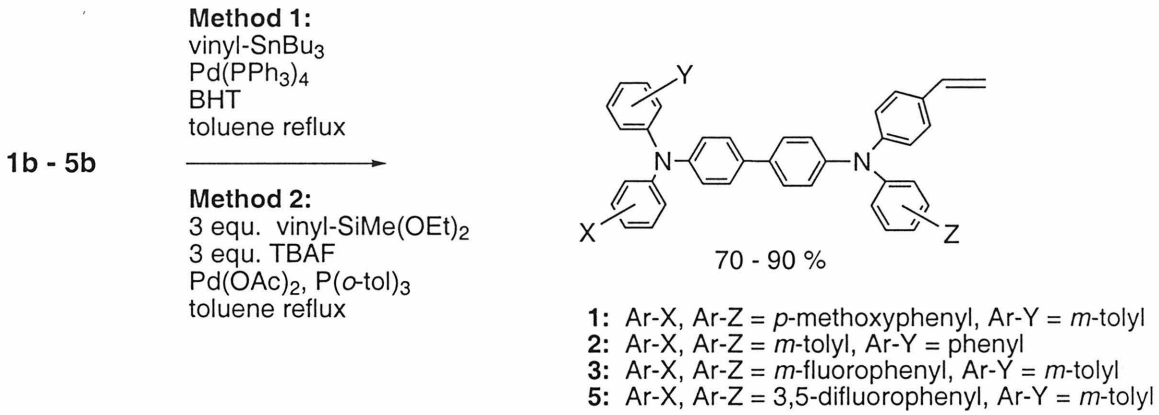

1: Ar-X, Ar-Z = *p*-methoxyphenyl, Ar-Y = *m*-tolyl
2: Ar-X, Ar-Z = *m*-tolyl, Ar-Y = phenyl
3: Ar-X, Ar-Z = *m*-fluorophenyl, Ar-Y = *m*-tolyl
5: Ar-X, Ar-Z = 3,5-difluorophenyl, Ar-Y = *m*-tolyl

BHT = 2,6-Di-*tert*-butyl-4-methylphenol, TBAF = Tributylammoniumfluoride

Scheme 4.2: Synthesis of the monovinyl-TPD derivatives.

The TPA monomer **4** was synthesized in a similar fashion to the TPD derivatives (Scheme 4.3).

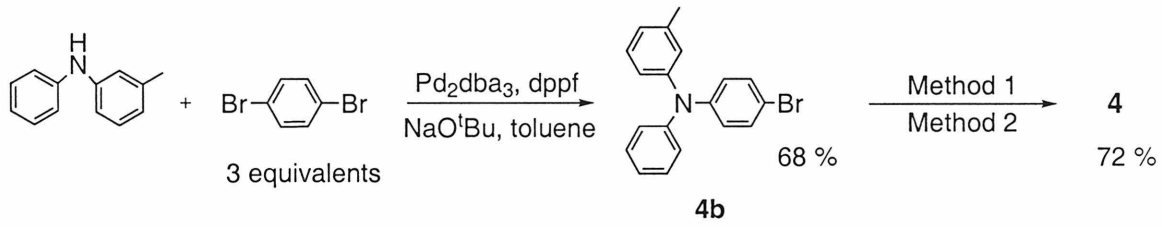

Scheme 4.3: Synthesis of the TPA-containing monomer.

Polymerization: The anionic polymerization of monomers **1-4** was initiated by 0.05 equivalents of *n*-butyllithium (*n*-BuLi) at -78°C. In the case of monomer **5**, the two fluorine substituents in the 3- and 5-position of the outer phenyl rings cause the *para*-hydrogens to be reactive toward strong bases. *n*-BuLi was observed to deprotonate the TPD core prior to initiating polymerization by a deuterium quenching experiment. The polymerization of the dianion was possible in a dilute THF solution and yielded the target polymer after quenching with methanol at -78°C. The isolated yield of polymer **P5** is

lower than the yields of polymers **P1-P4**, because an insoluble fraction had to be removed by filtration. This insoluble material is presumably caused by cross-linking during the polymerization.

Table 4.1: Polymer properties.

polymer	yield[a] [%]	M_W[b]	PDI[b]	T_g [°C]	T_{TGA}[c] [°C]	λ_{max}[d] [nm]
P1	96	15700	1.28	132	408	360, 312
P2	98	11150	1.13	151	400	358, 312
P3	98	11500	1.16	147	414	353, 312
P4	96	5000	1.09	104	397	307
P5	65	6550	1.30	140	412	338, 315

[a]isolated yield
[b]determined by gel permeation chromatography in methylene chloride versus monodispersed polystyrene standards
[c]temperature of thermal decomposition determined by thermal gravimetric analysis and reported as temperature of onset of weight loss
[d]absorption spectrum in methylene chloride solution

All of the resulting polymers exhibit high glass transition temperatures (T_g), high thermal stability (up to 400 °C by thermal gravimetric analysis) and good solubility. The polymers form high quality transparent thin films upon spin-casting, and the solutions and films display blue-violet fluorescence. The polymer properties are summarized in Table 4.1.

Cyclic Voltammetry: The redox potentials of the polymers have been determined by cyclic voltammetry in methylene chloride solution versus ferrocenium/ferrocene (Table 4.2).

Table 4.2: Redox potentials of the HTL polymers.[a]

	polymers		model small molecules	
	$^1E_{1/2}$[b] [mV]	$^2E_{1/2}$[c] [mV]	$^1E_{1/2}$[b] [mV]	$^2E_{1/2}$[c] [mV]
P1	150	355	160	400
P2	280	480	260	510
P3	390	560	360	580
P4	E_{ox} = 490, E_{red} = 380[d]		E_{ox} = 550, E_{red} = 470[d]	
P5	490	590	510	660

[a]Error of the measurement is estimated to ± 10 mV.

[b] $^1E_{1/2} = E_{1/2}(M^+/M)$

[c] $^1E_{1/2} = E_{1/2}(M^{2+}/M^+)$

[d]irreversible redox potential

The cyclic voltammograms for polymers **P1-P3** and **P5** show two sequential one-electron processes corresponding to removal of two electrons from each TPD unit. These redox potentials are similar to the redox potentials of the corresponding molecular compounds,[15] demonstrating that incorporation of TPD into the this kind of polymeric framework does not alter its redox behavior. The peak potentials in forward and reverse bias differ by approximately 59 mV, and the peak currents in forward and reverse bias are of similar magnitude. This suggests that the redox potentials are reversible.

The cyclic voltammogram for the TPA-based polymer **P4** shows an irreversible redox process at a potential, which is lower than the redox potential of the molecular TPA. Simple triarylamines without *para*-substitution are known to exhibit similar irreversible electrochemistry.[21]

The cyclic voltammetry measurements show that polymer **P1** has the lowest barrier for oxidation at the ITO/HTL interface, but its radical cation is hardest to reduce

at the HTL/Alq interface. Therefore, **P1** should readily form radical cations at the ITO/HTL interface (reaction (1)), but the reaction of these radical cations with Alq (hole injection into EL; reaction (2); Figure 4.2a) and with $Alq^{-\bullet}$ radical anion (direct formation of the Alq^{*S} emissive state at the HTL/EL interface[9]; reaction (3); Figure 2b) should be disfavored. In the case of **P5**, the hole injection at the ITO/HTL interface should be disfavored, but the relevant redox reactions at the HTL/Alq interface should occur more readily. **P2, P3** and **P4** represent intermediate cases between **P1** and **P5**.

The results of the solution phase cyclic voltammetry measurements herein expose the trends in redox behavior of the polymeric materials relative to each other. Electrochemistry has previously been shown to give qualitative estimates of energy levels in devices.[9] Photoelectron spectroscopic analysis gives quantitative solid state energies. The solid state ionization potentials have been determined for **P1** (IP = 5.06 eV), **P2** (IP = 5.38 eV) and **P3** (IP = 5.56).

Fabrication and Characterization of Light-Emitting Devices: Two-layer OLEDs of the configuration ITO/polymer/Alq/Mg have been prepared using the polymers **P1-P5** as hole transport materials. The devices show typical Alq-emission[22] resulting in green OLEDs with a peak emission of 525 nm. Table 4.3 and Figure 4.3 summarize the device data.

The current density at 9V decreases as the redox potential of the HTL increases (Table 4.3). This is consistent with an increase in the energetic barrier for hole injection from the ITO, and this same trend has been seen in previous work.[23]

Table 4.3: Device characteristics *versus* redox potential of the hole-transporting polymer for the devices ITO/HTL/Alq/Mg.

HTL-polymer	$^1E_{1/2}$[a] [mV]	current density at 9 V [mA/cm^2]	max. ext. quantum efficiency [% photons/e$^-$]	light output at 10 V [cd/m^2]
P1	150	53.4	0.61	2300
P2	280	39.7	1.09	2900
P3	390	28.7	1.25	3700
P4	435[b]	27.4	1.22	1800
P5	490	15.4	1.00	1000

[a] $^1E_{1/2} = E_{1/2}(M^+/M)$; determined by cyclic voltammetry in methylene chloride solution versus ferrocenium/ferrocene

[b] irreversible redox potential estimated from $(E_{ox}+E_{red})/2$

All of the polymers form high quality thin films upon spin-casting. To illustrate the effect of good film formation properties on the device performance, a single layer device of the configuration ITO/spin-coated **P2**/Al was compared to the analogous device with thermally evaporated small-molecule TPD instead of the polymer. Such devices behave as diodes, and current flow due to hole injection and hole transport is observed above a certain turn-on voltage. The turn-on voltage for the polymer **P2** device is approximately 8 V lower than for the small-molecule TPD device (~ 4 V vs. ~12 V). This is attributed to a difference in the interfacial contact with ITO. Spin-coating of the polymer provides better contact with the rough ITO surface. This results in a low interfacial resistance and a low operating voltage when polymers **P1 – P5** are used as HTL in an OLED.[24]

The use of a more sophisticated vacuum vapor deposition chamber with a larger source-to-sample distance and a rotating sample holder will probably provide better film

coverage and result in lower turn-on voltage for the small-molecule device. It is also possible to improve the hole injection characteristics by preparing particularly flat ITO surfaces *via* oxygen- or argon-plasma treatments.[25] However, these data illustrate the importance of the morphology for hole injection and hole transport within the OLED. It also shows that HTL films of superior morphological characteristics can be easily fabricated from polymeric materials using basic equipment, whereas small-molecule versions of the same compound yield less film coverage and require more time-consuming procedures and intricate instrumentation.

The maximum external quantum efficiency for the two-layer devices ITO/**P1-P5**/Alq/Mg increases substantially as the redox potential becomes more positive (compare **P1, P2** and **P3**, Table 4.3, Figure 4.3). Thus, this study suggests that higher external quantum efficiencies can be achieved with hole-transporting materials, which are less electron-rich than the commonly used TPD.

The most likely explanation for this trend is that increasing the ionization potential of the HTL reduces the rate of hole injection from the anode and creates a better balance between the number of holes and electrons in the device (see Chapter 1, part B, charge-balance factor γ). Another possible explanation is that that a "cross reaction" between the radical cation of the hole transport material and the radical anion of Alq at the HTL/Alq interface occurs to produce luminescence (page 50, reaction (3)). The efficiency of this luminescence increases with increasing ionization potential due to the increased driving force for the reaction (3) (Figure 4.1b). In order to test whether the cross-reaction mechanism is important in these devices, a control OLED was fabricated through evaporation of a layer of *p*-OCH_3-TPD, corresponding to **P1**, on top of polymer

P3 to yield the configuration ITO/**P3**/*p*-OCH_3-TPD/Alq/Mg. The control device did not show decreased efficiency. Therefore, cross reaction is not the dominant mechanism of light emission in these devices.

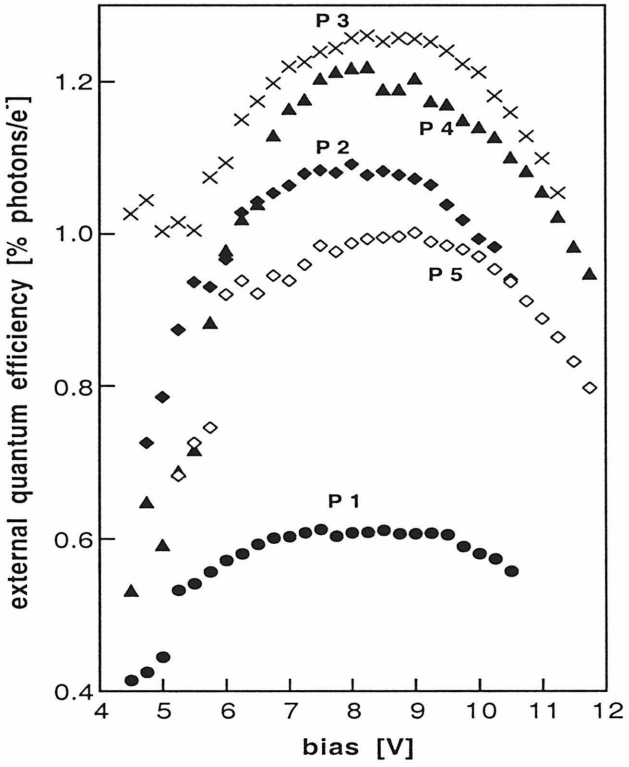

Figure 4.3: External quantum efficiency *versus* bias voltage for the two-layer devices ITO/HTL/Alq/Mg with polymers **P1 - P5** as hole transport materials.

An optimum value for the HTL redox potential appears to exist around 400 mV versus ferrocenium/ferrocene (**P3**). If the redox potential is increased further than that, the energetic barrier for the hole injection at the HTL/Alq interface is further decreased but the barrier for hole injection into the HTL form the ITO anode presumably becomes too high (Figure 4.1a). This apparently causes the external quantum efficiency to decrease again (compare **P3, P4** and **P5**). Another possible explanation for decreased external quantum efficiencies at too high redox potentials could be the following:

Electron-withdrawing substituents decrease not only the HOMO energy but also, to a lesser extent, the LUMO energy of a compound.[26] A lower LUMO level of the hole transport material could result in less efficient electron blocking at the HTL/Alq interface which would decrease device efficiency. However, the observed decrease in quantum efficiency could also be an artifact of decreased operational stability of OLEDs with high-IP hole transport materials.

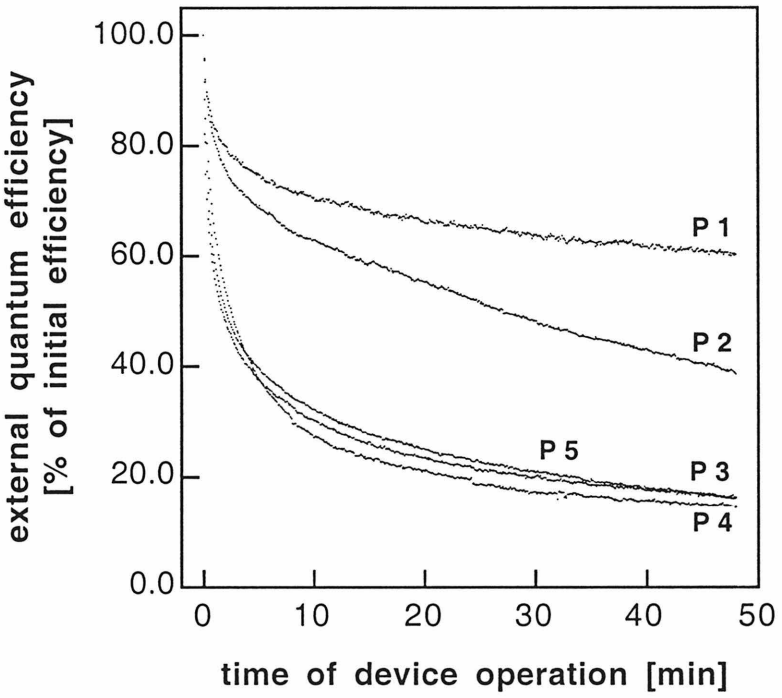

Figure 4.4: Lifetime study for the devices ITO/HTL/Alq/Mg with polymers **P1 - P5** as hole transport materials.

To test the stability of the devices, the OLEDs were operated at 6 mA constant current (corresponds to 50 mA/m^2) in a nitrogen filled dry box. Constant current, which is a common mode for testing OLED lifetimes, drives the same number of charge carriers through the devices with different HTL materials. The observed changes in external

quantum efficiency are illustrated in Figure 4.4. The device with **P1** as hole-transporting material was the least efficient at the beginning of the lifetime study, but in the end retained 60 % of its initial efficiency after 1h of continuous operation. Devices, which contained **P3, P4** and **P5,** decomposed rapidly. After 1h the trend in performance was reversed with ITO/**P1**/Alq/Mg showing the highest external quantum efficiency (Figure 6, Table 3). This observation is consistent with a previous study,[8] where it was shown that device life time is strongly dependent on the redox potential of the hole transport material.

Pursuing the results of this study, optimized devices have been fabricated using Alq doped with quinacridone as emitting layer and a bilayer of LiF/Al as cathode.[27] The device with polymer **P3** as HTL showed a luminance of 15 cd/m^2 at an applied voltage of 3.0 V, which corresponds to a luminous efficiency of 20 lm/W and an external quantum efficiency of 4.5 %. At an applied voltage of 4.0 V, the luminance is 135 cd/m^2, and the luminous efficiency is 14 lm/W.

D. Summary and Conclusions

An efficient protocol for the synthesis of a variety of soluble hole-transporting polymers, which have compact non-functionalized backbones and high glass transition temperatures, has been developed. Several hole transport materials with differences in their redox potential have been synthesized, and the effect of the redox potential on the performance of a two-layer OLED has been investigated. The device performance has

been found to depend on the redox potential of the hole-transporting material as illustrated in Figure 4.5.

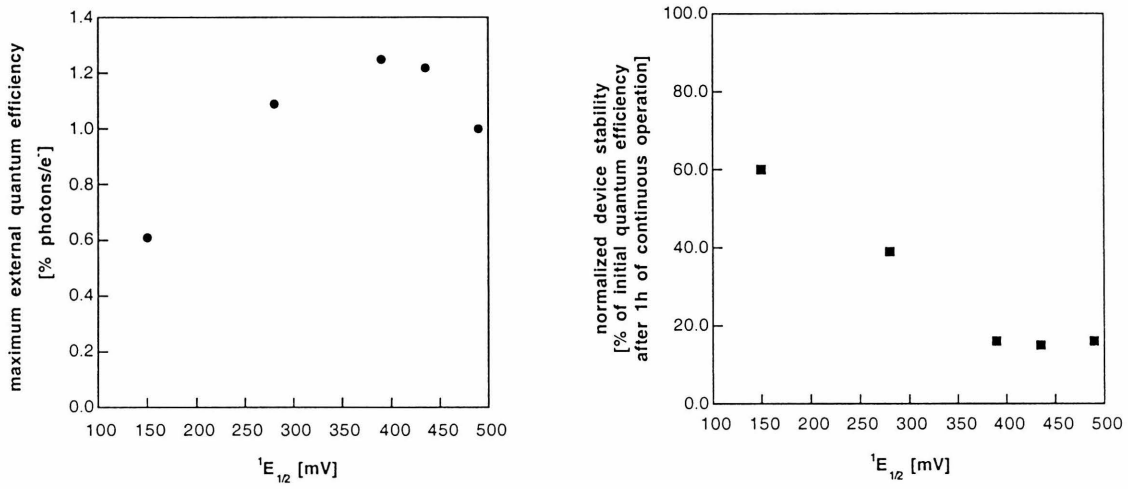

Figure 4.5: Maximum external quantum efficiency and stability of two-layer OLEDs ITO/HTL/Alq/Mg *versus* the redox potential of the hole transport polymer. ($^1E_{1/2}$ is reported relative to ferrocenium/ferrocene as measured in methylene chloride solution.)

The efficiency of the device increases with increasing redox potential, which is due to a better balance of hole and electron injection. An optimum value for the redox potential seems to exist, which could be due to decreased electron-blocking capability of high-IP hole transport materials, or to decreased operational stability of OLEDs containing high-IP HTLs. Complimentary results show that the cross reaction between the radical cations of the hole transport material and the radical anions of Alq is not the dominant mechanism of light emission in these devices. Specifically, it has been found that the redox behavior of unsubstituted TPD, which is a commonly used hole transport material, is not optimal for OLEDs with the two-layer configuration ITO/HTL/Alq/Mg. Higher quantum efficiencies have been observed for polymers containing TPA and fluoro-TPD (**P4** and **P3**), which have higher redox potentials.

Device stability also depends on the redox potential of the HTL material: more electron-rich derivatives yield devices with improved lifetimes. A possible explanation for this trend is the fact that higher amounts of Joule heat are produced in a device with a high-IP hole transport material due to the higher energetic barrier for charge injection.[8] Consequently, a device containing a high-IP hole transport material experiences more heat stress and is particularly prone to partial delamination or other thermally induced morphological changes and decomposition processes. A way to improve the operational stability of the fluoro-TPD polymer device through enhancing the polymer's adhesion to the anode is described in Chapter 5.

The polymers presented in this chapter have excellent film formation properties. A polymer-based single-layer device shows a turn-on voltage 8 V lower than a single-layer device based on the analogous small-molecule compound. This improvement is attributed to better film coverage and better morphology at the anode/HTL interface.

An optimized device showing a luminous efficiency of 20 lm/W has been fabricated using polymer **P3** as the hole transport layer.

E. References and Notes

A majority of the work in this chapter has been previously published: Bellmann, E.; Shaheen, S. E.; Grubbs, R. H.; Marder, S. R.; Kippelen, B.; Peyghambarian, N. *Chem. Mater.* **1999**, *11*, 399. b. Shaheen, S. E.; Jabbour, G. E.; Kippelen, B.; Peyghambarian, N.; Anderson, J. D.; Marder, S. R.; Armstrong, N. R.; Bellmann, E.; Grubbs, R. H. *Appl. Phys. Lett.* **1999**, *74*, 3212.

(1) Bässler, H. *Phys. Status Solidi (b)* **1993**, *175*, 15 and references therein.

(2) Van der Auweraer, M.; De Schryver, F. C.; Borsenberger, P. M.; Fitzgerald, J. J. *J. Phys. Chem.* **1993**, *97*, 8808.

(3) Borsenberger, P. M.; Pautmeier, L.; Richert, R.; Bässler, H. *J. Chem. Phys.* **1991**, *94*, 8276.

(4) Gruenbaum, W. T.; Sorriero, L. J.; Borsenberger, P. M.; Zumbulyadis, N. *Jpn. J. Appl. Phys.* **1996**, *35*, 2714.

(5) Heun, S.; Borsenberger, P. M. *Physica B* **1995**, *216*, 43.

(6) Bellmann, E.; Shaheen, S. E.;Thayumanavan, S.; Barlow, S; Grubbs, R. H.; Marder, S. R.; Kippelen, B.; Peyghambarian, N. *Chem. Mater.* **1998**, *10*, 1668.

(7) Tsutsui, T. *MRS Bulletin* **June 1997**, 39 and references therein.

(8) Adachi, C.; Nagai, K.; Tamoto, M *Appl. Phys. Lett.* **1995**, *66*, 2679.

(9) Anderson, J. D.; McDonald, E. M.; Lee, P.A.; Anderson, M. L.; Ritchie, E. L.; Hall, H. K.; Hopkins, T.; Padias, A.; Thayumanavan, S.; Barlow, S.; Marder, S. R.; Jabbour, G. E.; Shaheen, S. E.; Kippelen, B; Peyghambarian, N.; Wightman, R. M.; Armstrong, N. R. *J. Am. Chem. Soc.* **1998**, *120*, 9646.

(10) a. Tanaka, H.; Tokito, S.; Taga, Y.; Okada, A. *J. Chem. Soc., Chem. Commun.* **1996**, 2175. b. Thelakkat, M.; Schmidt, H.-W. *Adv. Mater.* **1998**, *10*, 219. c. Katsuma, K., Shirota, Y. *Adv. Mater.* **1998**, *10*, 223.

(11) Pangborn, A. B.; Giardello, M. A.; Grubbs, R. H.; Rosen, R. K.; Timmers, F. J. *Organometallics* **1996**, *15*, 1518.

(12) Wolfe, J. P.; Rennels, R. A.; Buchwald, S. L. *Tetrahedron* **1996**, *52*, 7525.

(13) Wolfe, J. P.; Wagaw, S.; Buchwald, S. L. *J. Am. Chem. Soc.* **1996**, *118*, 7215.

(14) Driver, M. S.; Hartwig, J. F. *J. Am. Chem. Soc.* **1996**, *118*, 7217.

(15) Thayumanavan, S.; Barlow, S.; Marder, S. R. *Chem. Mater.* **1997**, *9*, 3231.

(16) McKean, D. R.; Parrinello, G.; Renaldo, A. F.; Stille, *J. Org. Chem.* **1987**, *52*, 422.

(17) Hatanaka, Y.; Hiyama, T. *J. Org. Chem.* **1989**, *54*, 268.

(18) Tamao, K.; Sumitani, K.; Kumada, M. *J. Am. Chem. Soc.* **1972**, *94*, 4374.

(19) Nugent, W. A.; McKinney, R. J. *J. Org. Chem.* **1985**, *50*, 5370.

(20) Pine, S. H. *Organic Reactions* **1993**, *43*, 1.

(21) Yano, M.; Furuichi, M.; Sato, K.; Shiomi, D.; Ichimura, A.; Abe, K.; Takui, T.; Itoh, K. *Synth. Met.* **1997**, *85*, 1665.

(22) Tang, C. W.; VanSlyke, S. A. *Appl. Phys. Lett.* **1987**, *51*, 913.

(23) Okutsu, S.; Onikubo, T.; Tamano, M.; Enokida, T. *IEEE Trans. Electron Devices* **1997**, *44*, 1302.

(24) Similar ternd has been observed by Feast, W. J.; Peace, R. J.; Sage, I. C.; Wood, E. L. *Polym. Bull.* **1999**, *42*, 167.

(25) a. Kim, J. S.; Cacialli, F.; Friend, R. H.; Daik, R.; Feast, W. J. *Synth. Met.* **1999**, *102*, 1065. b. Kim, J. S.; Cacialli, F.; Granstrom, M.; Friend, R. H.; Johansson, N.; Salaneck, W. R.; Daik, R.; Feast, W. J. *Synth. Met.* **1999**, *101*, 111.

(26) Estimates of solid state LUMO levels for different TPD derivatives have been presented at the 214th ACS meeting. Thayumanavan, S.; Barlow, S.; Marder, S. R.; Lee, P.; Anderson, J. D.; Armstrong, N. R; Jabbour, G. E.: Kawabe, Y.; Morrell, M. M.; Shaheen, S. E.; Kippelen, B.; Peyghambarian, N. *ACS meeting abstract*, **1997**, 214.

(27) Jabbour, G. E.; Kawabe, Y.; Shaheen, S. E.; Wang, J. F.; Morrell. M. M.; Kippelen, B.; Peyghambarian, N. *Appl. Phys. Lett.* **1997**, *71*, 1762.

Chapter 5:

Hole Transport Polymers with Improved Interfacial Contact to the Anode Material

A. Introduction

The performance of organic light-emitting diodes (OLEDs) has greatly improved in recent years and is now approaching commercially viable levels. In particular, multilayer devices consisting of thermally deposited hole transport layer (HTL) and emission layer have shown promising properties such as high brightness and efficiency, low operating voltage, and good operational stability.[1] Additional improvements can be achieved by using hole-transporting polymers instead of the thermally deposited small-molecule materials to prepare the HTL. Polymers can be spin-casted from solution yielding a more cost-effective method for the fabrication of the hole transport layer. High glass transition temperatures and the possibility to cross-link[2,3] the polymer can potentially increase the thermal and operational stability of the device. Furthermore, excellent film formation properties of the polymeric materials have resulted in improved device performance compared to OLEDs containing the analogous small-molecule HTL.[4,5]

As described in Chapter 4, polymeric TPD derivatives have been investigated as hole-transporting materials in organic two-layer LEDs.[5,6] OLEDs with poly-TPD as HTL exhibited operating voltages 8 V lower then the analogous small-molecule-TPD devices.[5] The quantum efficiencies increased with increasing ionization potential (IP) of the HTL material.[7] The optimization of the device structure resulted in the fabrication of an OLED with 20 lm/W efficiency using the fluorinated derivative **1** (Figure 5.1).[5] However, operational stability also depended on the IP. The device lifetime decreased as the IP of the HTL increased.[6,8] Consequently, the most efficient device was less stable than OLEDs with low-IP hole transport materials.

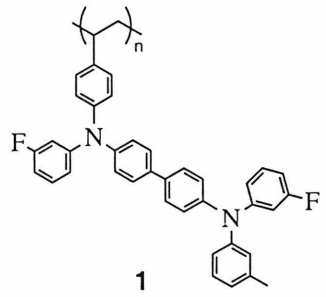

1

Figure 5.1: Structure of the fluorinated TPD derivative polymer.

Careful examination of the time-voltage curves obtained in constant-current lifetime experiments led to the belief that one of the major decomposition mechanisms is possibly due to poor adhesion of the HTL to the anode. Even though the initial interfacial contact is good, exposure to current and, consequently, heat results in partial delamination of the device causing a respective increase in contact resistance. The increased resistance is experimentally observed through a substantial increase in voltage immediately after beginning of current flow (Figure 5.3, curve D1).

This chapter reports the incorporation of trimethoxyvinylsilane into the polymer **1** and the use of these modified HT polymers in OLEDs. Upon hydrolysis, trimethoxy-silanes cross-link and form covalent bonds with oxidic surfaces (Scheme 5.1).[9] Therefore, the connection between the silanated HTL and the indium-tin-oxide (ITO) anode is based on chemical bonding and not physical adsorption, which in turn results in stronger adhesion of the HTL to the ITO. A procedure to cross-link the hole transport polymer to a glass surface is described. Improved adhesion behavior of silanated HTL under operating conditions of an OLED is demonstrated, and the dependence of device performance on the trimethoxysilane content of the HTL is investigated.

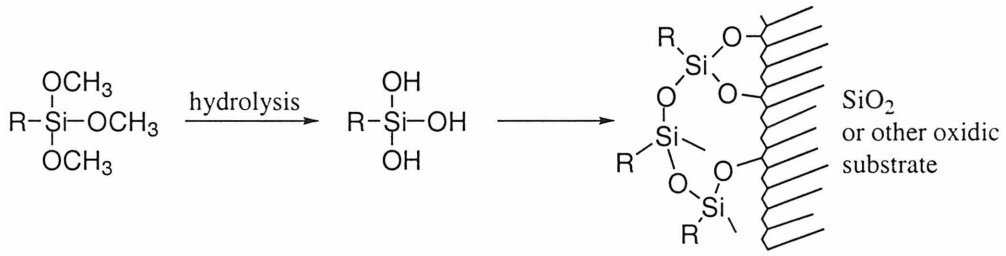

Scheme 5.1: Reaction of trimethoxysilanes with oxidic surfaces.

B. Experimental Section

General: All syntheses were carried out under argon, which was purified by passage through columns of BASF R-11 catalyst (Chemalog) and 4 Å molecular sieves (Linde). NMR spectra were recorded on a JEOL GX-400 spectrometer (399.65 MHz for ^{1}H). Gel permeation chromatograms were obtained on a HPLC system using an Altex model 110A pump, a Rheodyne model 7125 injector with a 100 mL injection loop,

American Polymer Standards 10 micron mixed bed columns, a Knauer differential refractometer and CH_2Cl_2 as eluent at a 1.0 mL/min flow rate. Differential scanning calorimetry was carried out on a Perkin-Elmer DSC-7 with a scan rate of 10 °C/min.

Materials: Toluene and tetrahydrofuran (THF) were distilled from Na/benzophenone. Deuterated methylene chloride was dried by refluxing over calcium hydride and vacuum transfer into a flame-dried Schlenk flask. Monomer **2** was synthesized as described in Chapter 4. Trimethoxyvinylsilane was obtained from Gelest, Inc. All other chemicals were obtained from Aldrich Chemical Company, and were used without further purification.

Preparation of polymer 1 by radical polymerization: A solution of monomer **2** (1 g) and 2,2'-azobisisobutyronitrile (AIBN) (20 mg) in toluene (2 mL) was heated to 80 °C for 30 h. The polymer was purified by precipitation into methanol. Yield: 80 %. PDI = 1.53. M_w = 13,000 (determined by GPC in methylene chloride relative to polystyrene standards). ^{1}H NMR (CD_2Cl_2) δ 7.5 (bd), 7.2 (bd), 6.9 (bd), 6.5 (bd), 2.3 (bd), 2.2 (bd), 1.6 (bd).

Copolymerization procedure: An excess of the co-monomer trimethoxyvinylsilane (TVS) was added to the solution of monomer **2** (1 g) and 2,2'-azobisisobutyronitrile (AIBN) (20 mg) in toluene (2 ml), and the mixture was heated to 80 °C for 30 h. The polymer was purified by precipitation into dry methanol under argon, redissolving in dry THF and reprecipitation into dry methanol. The reprecipitation was undertaken five times to ensure removal of excess co-monomer. Subsequently, the solvents were removed *in vacuo*, and the copolymer samples were stored under argon excluding air

moisture. The samples were checked for absence of monomeric TVS by NMR. Different amounts of TVS in the feed resulted in different contents of trimethoxysilane in the copolymer. The trimethoxysilane content in the polymer samples was determined by taking ^{1}H NMR with 64 scans and 10 s delay time and integration of the aromatic region versus the trimethoxysilane peak.

^{1}H NMR (CD_2Cl_2): aromatic region: δ 7.5 (bd), 7.2 (bd), 6.9 (bd), 6.5 (bd); 1 unit = 24 H. trimethoxysilane: δ 3.3 (bd); 1 unit = 9 H. methyl group on the TPD: δ 2.3 (bd). backbone: δ 2.2 (bd), 1.6 (bd), 0.9 (bd).

A determination of the PDI and the molecular weight of the copolymers was not undertaken, since the partially reactive polymer could be incompatible with the GPC columns.

Cross-linking of the copolymers on glass: Glass slides (Corning) were heated to 80 °C for 30 min in a mixture of 1 part 30 % aqueous hydrogen peroxide solution and 3 parts concentrated sulfuric acid. After rinsing with copious amounts of deionized water, the slides were sonicated in a mixture of 5 parts water, 1 part ammonium hydroxide, and 1 part 30 % aqueous hydrogen peroxide solution for 30 min. The slides were washed carefully with copious amounts of deionized water and placed in an oven to dry for 5 min at 120 °C. Solutions of the copolymers in dry THF were prepared at a concentration of 10 mg/mL, and silicon tetrachloride (20 μL/mL) was added immediately prior to the preparation of the films. The films were heated to 120 °C for 14 h.

Fabrication of light-emitting devices: Devices were fabricated on indium tin oxide (ITO) coated glass substrates (Donnelly Corporation) with a nominal sheet resistance of 40 ohms/sq which had been ultrasonicated in acetone, methanol and

isopropanol, dried in a stream of nitrogen, and then plasma etched for 60 seconds. Polymer layers (40 nm) were formed by spin casting from solutions in dry THF (10 g/L). For the fabrication of devices with cross-linked HTL, silicon tetrachloride (20 μL/mL) was added to the polymer solutions before spin casting. The HTL films were heated to 120 °C in moist air. The second layer consisted of vacuum vapor deposited tris(8-quinolinato)aluminum (Alq) (60 nm), which had been purified by recrystallization and sublimation prior to deposition. Subsequently, a layer CsF (7 - 8 Å) was evaporated, and the aluminum cathode (150 nm) was thermally deposited through a shadow mask creating devices of 0.1 cm^2 in active area. Cathode deposition and device characterization were performed in a nitrogen dry box (Vacuum Atmospheres).

Characterization of light-emitting devices: Current-voltage and light output characteristics of the devices were measured in forward bias. Device emission was measured using a silicon photodetector at a fixed distance from the sample (12 cm). The response of the detector had been calibrated using several test devices, for which the total power emitted in the forward direction was measured with a NIST traceable integrating sphere (Labsphere). Efficiencies were measured in units of external quantum efficiency (% photons/electron). The lifetime experiments were done using constant current mode of 5 mA resulting in a current density of 50 mA/cm^2.

C. Results and Discussion

Copolymer Synthesis: Polymer **1** (Figure 5.1) has originally been prepared through anionic polymerization of monomer **2** (Structure of monomer **2** is shown in Scheme 5.2. Synthesis and anionic polymerization of monomer **2** are described in Chapter 4). A copolymerization of **2** with monomers containing the trimethoxysilane group by this method is not possible since anionic initiators will decompose in the presence of trimethoxysilanes. Therefore, the polymerization of **2** was performed under radical conditions yielding polymer **1** with M_w = 18,000, PDI = 1.53 and T_g = 141°C.

To prepare a hole transport polymer, which would combine the good hole injection characteristics of **1** with improved adhesion to the anode material, incorporation of trimethoxysilane groups into **1** through copolymerization of **2** with trimethoxyvinylsilane was undertaken. Trimethoxyvinylsilane (TVS) was chosen as the co-monomer, because of its simple compact structure and commercial availability. The reactivity of TVS under radical conditions is low. The reactivity ratios for the copolymerization of styrene and TVS are 20 and 0,[10] showing that under these circumstances TVS never reacts with itself. This data suggests that a block-copolymer will not be formed, and incorporation of TVS into the backbone of the polystyrene-type polymer **1** would proceed at random and in small amounts. Such behavior is advantageous for the application since only small amounts of TVS should be present within the hole transport material, and a blocky structure containing poly-TVS segments is undesirable.

Copolymers **P1 - P6** with varying contents of trimethoxysilane were prepared by radical polymerization using large excess of TVS (Scheme 5.2, Table 5.1).

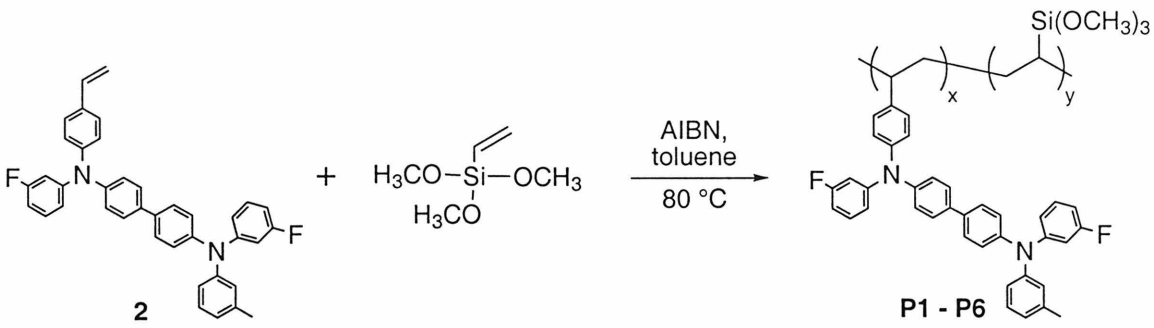

Scheme 5.2: Preparation of the copolymers.

Trimethoxy-silane contents between 0.9 and 6.8 % by weight have been achieved. The lowest content of trimethoxysilane corresponds to an FTPD/$Si(OCH_3)_3$-ratio of 28 or, in other words, to 3.4 % of the monomer units being TVS. A trimethoxysilane content of 6.8 weight % is equivalent to an FTPD/$Si(OCH_3)_3$-ratio of 3.6, or to 21.7 % of the monomer units being TVS.

Table 5.1: Preparation and composition of the trimethoxysilane-containing hole-transporting copolymers.

copolymer	equivalents of TVS in the feed	% trimethoxysilane in the copolymer[a]
P1	2	0.9
P2	5	1.6
P3	8	2.8
P4	10	4.1
P5	13	6.0
P6	16	6.8

[a]The composition was determined by integration of the ^1H NMR spectra. The percentage was calculated as % by mass taking into account the different molecular weights of monomer **2** and TVS.

Cross-linking of the Copolymers to Glass: Procedures for the reaction of trimethoxysilanes with cleaned and activated glass surfaces have previously been described.[9] In order to test the reactivity of the copolymers **P1 - P6**, films of the polymers were spin-casted on glass slides, which were pretreated with piranha solution and a mixture of ammonium hydroxide and hydrogen peroxide. Films prepared from polymer solutions in dry THF remained soluble after heating in moist air to 120 °C over night. Addition of small amounts of water or HCl to help hydrolysis of the trimethoxysilane group resulted in opaque films, which would not be suitable for application in OLEDs. Successful cross-linking has been achieved through addition of tetrachlorosilane (20 μL for 1 ml of polymer solution in dry THF) and subsequent heating of the spin-casted films to 120 °C for 14 h. The resulting films were transparent, exhibited blue-violet fluorescence and did not redissolve in THF or methylene chloride. This procedure was used to prepare hole transport layers on ITO during the fabrication of light-emitting diodes.

Fabrication and Characterization of OLEDs: Organic light-emitting diodes of the configuration ITO/HTL/Alq/CsF/Al were fabricated (ITO = indium tin oxide, Alq = tris(8-quinolinato)aluminum). The hole transport layers were prepared through spin-casting of one of the copolymers **P3, P4** and **P6** out of solutions in dry THF to which tetrachlorosilane was added. In control experiments copolymer-HTLs were prepared without $SiCl_4$, and polymer **1** was used as hole transport material with and without the additive. In all cases, the hole transport layers on ITO were heated to 120 °C for 14 h prior to thermal deposition of the emissive layer and the cathode. Table 5.2 shows the

compositions of the hole transport layers and the performance parameters of the corresponding devices.

An examination of the initial performance of the OLEDs revealed that the maximum external quantum efficiency is not affected by addition of $SiCl_4$ or incorporation of trimethoxysilane units into the hole-transporting polymer. In contrast to a previous study in which devices with a cross-linked hole transport layer showed decreased performance compared to OLEDs containing the soluble parent polymer (Chapter 3), addition of the cross-linking reagent $SiCl_4$ to the HTL polymers does not alter the external quantum efficiency of the device. The external quantum efficiency is also independent of the trimethoxysilane content of the copolymers. All of the devices **D1** through **D8** show the same external quantum efficiency within the experimental error of $\pm$0.1 % photons/e^-. In conclusion, the trimethoxysilane method is a way to modify and cross-link the HTL without reducing the external quantum efficiency of the OLED.

The operating voltage decreases significantly with increasing trimethoxysilane content of the HTL, and is lowered further if the complete cross-link procedure with addition of $SiCl_4$ is performed (Table 5.2, Figure 5.2). This is indicative of the improved interfacial contact between the hole transport layer and the anode. The presence of Si-O-moieties could not have enhanced the intrinsic charge injection and charge transport properties of the HTL, since silicon oxides are insulators. Therefore, the over-all reduction in operating voltage is to be attributed to better wetting and better surface coverage which results in a decrease of contact resistance at the ITO/HTL interface.

Table 5.2: Composition of the HTL and performance of the ITO/HTL/Alq/CsF/Al-devices.

device	HTL	ext. quant. eff. [% photons/e^-][a]	operating voltage[b] [V]	increase in voltage[c] [%][d]
D1	**1**	1.3	8.6	28
D2	**P3**	1.4	8.2	18
D3	**P4**	1.4	6.8	19
D4	**P6**	1.2	5.8	38
D5	**1** + $SiCl_4$	1.3	7.2	18
D6	**P3** + $SiCl_4$	1.5	7.4	10
D7	**P4** + $SiCl_4$	1.5	6.2	19
D8	**P6** + $SiCl_4$	1.5	6.0	26

[a]Peak external quantum efficiency as determined from the current-voltage behavior.
[b]Light output at this voltage equals 5 cd/m^2.
[c]After 3 h of continuous operation at 50 mA/cm^2.
[d]% of initial voltage at the beginning of the lifetime experiment.

Interestingly, addition of silicon tetrachloride to polymer **1** also lowers the device operating voltage, even though **1** has no functional groups to react with $SiCl_4$ or with the anode surface. The hydrolyzed silicon tetrachloride apparently acts as an adhesion promoter in this case.

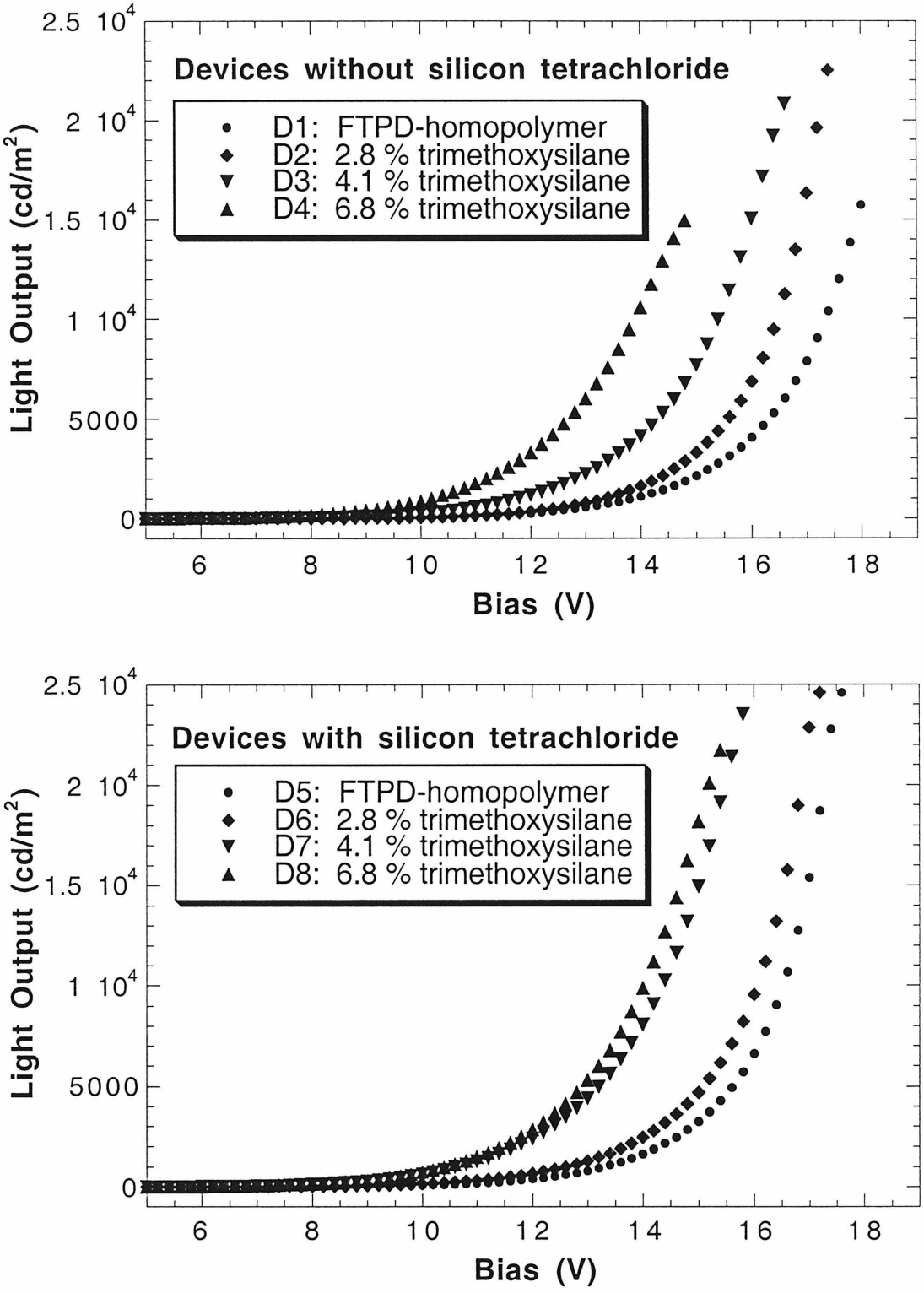

Figure 5.2: Light output *versus* voltage for the devices **D1 - D8**.

In order to characterize the operational stability of the devices **D1 - D8**, the OLEDs have been operated under constant current conditions at 50 mA/cm^2. Figure 5.3 shows the obtained voltage-time curves. A fast increase in voltage indicates a substantial increase in contact resistance presumably due to delamination. The increase in voltage over a period of three hours is reported in Table 5.2 in percent of initial voltage. Addition of $SiCl_4$ results in a slower voltage increase in all cases. The hydrolized silicon tetrachloride clearly makes the connection between the HTL film and the anode better for all of the studied polymers. It also improves the voltage-time behavior of the parent polymer **1**, which does not contain functional groups to react with the surface or $SiCl_4$.

The increase in voltage also depends on the trimethoxysilane content of the copolymers. Copolymers with low trimethoxysilane contents perform better than the parent polymer **1**. In particularly, device **D7** shows a relatively flatter voltage-time curve. Over the period of 3 h, and under such high current density, the voltage increased by only 10 % suggesting that the contact between the layers is good and device delamination is slow.

However, if the trimethoxysilane content is increased above 6 % by weight, it is no longer beneficial in terms of operational stability. Devices **D4** and **D8** show a fast increase in voltage during operation at constant current. Even though the initial operating voltage for these devices is lowest, the operational stability is less than in the case of the parent device **D1**. The specific morphology at the ITO/HTL interface after hydrolysis of trimethoxysilane and $SiCl_4$ is not known. A determination of the exact morphology at the ITO/HTL interface would be helpful in explaining why there is a change in properties at a trimethoxysilane content of around 6 %.

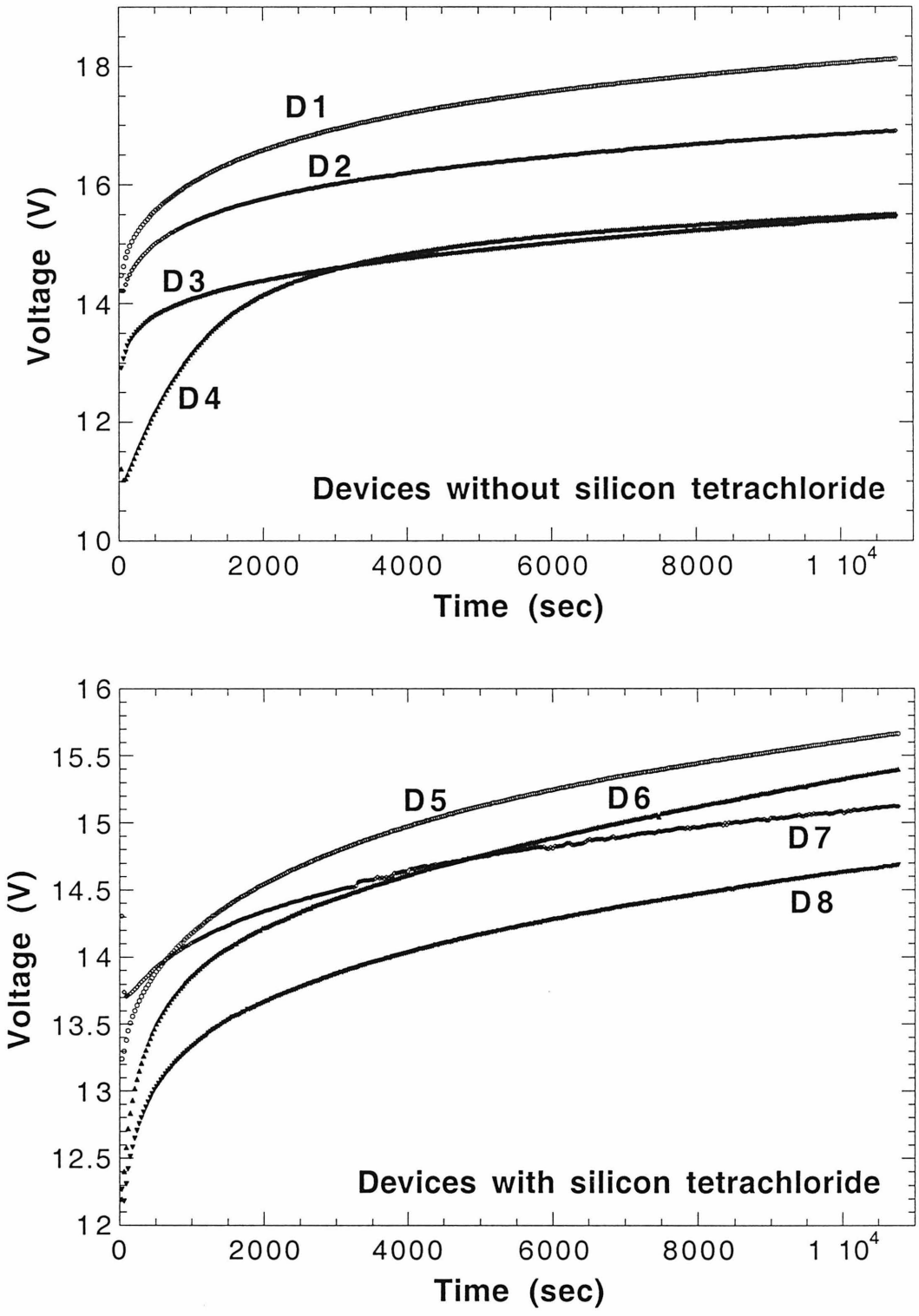

Figure 5.3: Voltage-time curves for the devices **D1 - D8** (at 50 mA/cm^2).

D. Summary and Conclusions

A series of copolymers, which contain a fluorinated TPD derivative as the hole-transporting functionality and small amounts of trimethoxysilane, has been synthesized. These copolymers can be cross-linked onto an oxidic surface through addition of silicon tetrachloride and heating in moist air.

Two-layer OLEDs containing these materials as the hole transport layer have been fabricated. The peak quantum efficiency of the devices does not depend on the trimethoxysilane content or addition of the cross-linking reagent $SiCl_4$. The HTL can be prepared through spin-casting, and the subsequent cross-linking procedure does not decrease the device efficiency.

The initial operating voltage of the devices decreases with increasing trimethoxysilane content and is lowered further through addition of $SiCl_4$. The hydrolyzed trimethoxysilane improves the bond between the anode surface and the HTL resulting in lower contact resistance and, consequently, lower operating voltage. Hydrolized silicon tetrachloride acts as an adhesion promoter since it also improves the properties of the FTPD-homopolymer **1** which does not have functional groups to chemically react with the ITO surface or $SiCl_4$.

The operational stability of the OLEDs has been studied in constant current density experiments at 50 mA/cm^2. Copolymers with low contents of trimethoxysilane show improved operational stability. The voltage increases slowly with time indicating that the contact between the layers remains good. If the trimethoxysilane content is above 6 % by weight, the voltage increase is higher compared to the parent device showing that, despite the low initial operating voltage, the operational stability is poor.

To explain this change in properties the specific morphology at the ITO/HTL interface after hydrolysis would need to be determined. Addition of silicon tetrachloride is beneficial in all cases and improves the operational stability of both the copolymer and the parent homopolymer devices.

E. References and Notes

A majority of the work in this chapter has been submitted for publication.

(1) a. Van Slyke, S. A.; Chen, C. H.; Tang, C. W. *Appl. Phys. Lett.* **1996**, *69*, 2160. b. Jabbour, G. E.; Kawabe, Y.; Shaheen, S. E.; Wang, J. F.; Morrell, M. M.; Kippelen, B.; Peyghambarian, N. *Appl. Phys. Lett.* **1997**, *71*, 1762.

(2) a. Bayerl, M. S.; Braig, T.; Nuyken, O.; Muller, D. C.; Gross, M.; Meerholz, K. *Macromol. Rapid Comm.* **1999**, *20*, 224. b. Bacher, A.; Erdelen, C. H.; Paulus, W.; Ringsdorf, H.; Schmidt, H. W.; Schuhmacher, P. *Macromolecules* **1999**, *32*, 4551.

(3) Bellmann, E.; Shaheen, S. E.; Thayumanavan, S.; Barlow, S; Grubbs, R. H.; Marder, S. R.; Kippelen, B.; Peyghambarian, N. *Chem. Mater.* **1998**, *10*, 1668.

(4) Feast, W. J.; Peace, R. J.; Sage, I. C.; Wood, E. L. *Polym. Bull.* **1999**, *42*, 167.

(5) Shaheen, S. E.; Jabbour, G. E; Kippelen, B.; Peyghambarian, N.; Anderson, J. D.; Marder, S. R.; Armstrong, N. R.; Bellmann, E.; Grubbs, R. H. *Appl. Phys. Lett.* **1999**, *74*, 3212.

(6) Bellmann, E.; Shaheen, S. E.; Grubbs, R. H.; Marder, S. R.; Kippelen, B.; Peyghambarian, N. *Chem. Mater.* **1999**, *10*, 1668.

(7) Similar trend has been shown for small-molecule HTL: a. Roitman, D. B.; Antoniadis, H.; Hueschen, M.; Moon, R.; Sheats, J. R. *IEEE J. Sel. Top. Quantum Electron.* **1998**, *4*, 58. b. Giebeler, C.; Antoniadis, H.; Bradley, D. D. C.; Shirota, Y. *J. Appl. Phys.* **1999**, *85*, 608.

(8) Similar trend has been shown for small-molecule HTL: Adachi, C.; Nagai, K.; Tamoto, M *Appl. Phys. Lett.* **1995**, *66*, 2679.

(9) Ulman, A. *Adv. Mater.* **1990**, *2*, 573 and references therein.

(10) Brandrup, J.; Immergut, E. H. (Eds.) *Polymer Handbook* John Wiley & Sons, New York, **1975**.

Appendix 1:

Synthesis of Highly Tactic Polymers by Ring-Opening Metathesis Polymerization

A. Introduction

This appendix describes the results of a project, which is not related to the general topic of synthesis and characterization of polymers for organic light-emitting diodes. Four chiral molybdenum-based catalysts have been explored with regard to their ability to produce stereoregular polymers *via* ring-opening metathesis polymerization (ROMP) of substituted norbornadienes.

For a general introduction to ROMP, please see Chapter 2, Part A. The first metathesis catalysts were heterogeneous systems containing transition metal salts or complexes and Lewis acid co-catalysts. Such heterogeneous catalysts have occasionally been found to yield highly stereoregular and tactic polymers with substituted norbornenes and norbornadienes,[1,2] however a correlation between structure and stereoselectivity has not been established. For more recently developed well-defined systems the relationship between the catalyst structure and the stereochemical outcome of ROMP is better understood.[3] The stereoregular polymerization of 2,3-bis(trifluoromethyl)norbornadiene (NBDF6) has been studied in particular, since the resulting highly tactic *cis* and highly tactic *trans* polymers show pyroelectric and ferroelectric properties.[4,5]

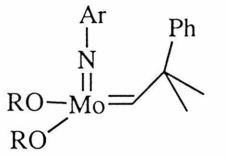

R = $C(CH_3)_3$
or $C(CH_3)_2CF_3$
or $C(CH_3)(CF_3)_2$

1

Figure A1: Structure of a molybdenum-based ROMP initiator.

For the Mo-based ROMP initiator **1** (Figure A1), it has been established, that *syn* and *anti* alkylidene rotamers are present during the polymerization. The two rotamers may or may not interconvert easily. According to references 3 and 6, the monomer coordinates to the *syn*-rotamer first. The *syn*-rotamer can rearrange to the *anti*-rotamer at a rate $k_{syn\text{-}anti}$ or propagate at a rate $k_{p,syn}$ to give a *syn* insertion product resulting in formation of a *cis* double bond in the polymer backbone. The *anti*-rotamer affords a *syn* insertion product, which corresponds to formation of a *trans* double bond (propagation rate of the *anti*-rotamer $k_{p,anti}$). The *cis/trans* ratio of the polymer is based on the ratio of the propagation rates *versus* the rate of rotamer interconversion (Figure A2).

In general, the propagation from the *anti*-rotamer is about 100 times faster than the propagation from the *syn*-rotamer and the *syn*-to-*anti* rotamer interconversion. Every formation of an *anti*-rotamer therefore leads to incorporation of a *trans* double bond into the growing polymer chain. The rate of propagation out of a *syn*-rotamer can be faster, slower or similar to the rate of rotamer interconversion. If the *syn* propagation is faster than the rearrangement, high *cis* polymer is obtained. Slow *syn* propagation leads to a

high *trans* polymer. If the rates for the two processes are similar, no stereoregularity is observed.

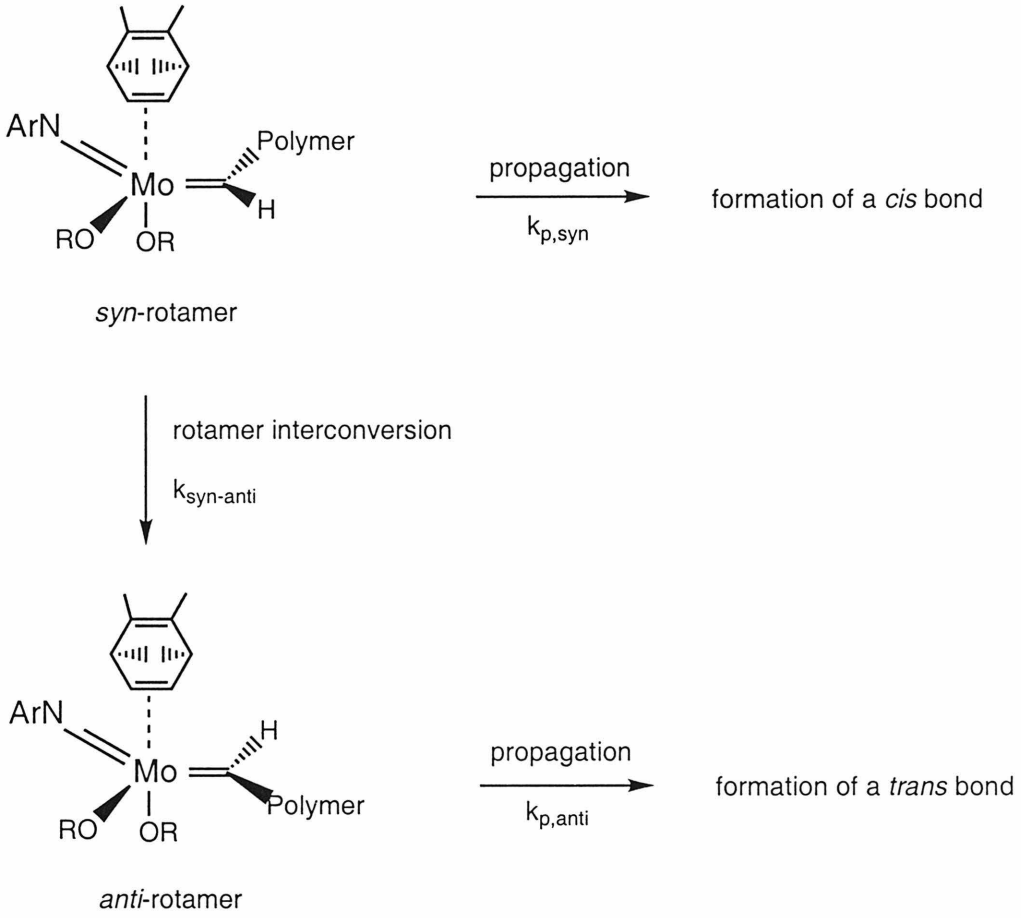

Figure A2: Rotamer interconversion *versus* propagation and the *cis/trans* ratio of the resulting polymer.

Propagation rates can be correlated with the structure of the catalyst. Bulky, electron-withdrawing R-groups on complexes from type **1** enhance catalyst activity and substantially speed up propagation. **1** with R = $C(CH_3)(CF_3)_2$ gives all *cis* poly-NBDF6, because propagation from the *syn*-rotamer is faster than rotamer interconversion. The less active analogue with R = $C(CH_3)_3$ produces all *trans* poly-NBDF6.[3,7,8]

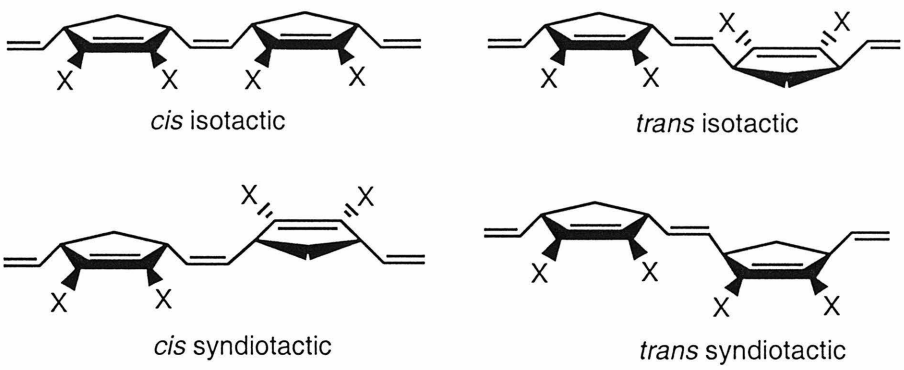

Figure A3: Stereochemistry of poly(norbornadienes).

Besides the *cis/trans* isomerism, a polynorbornadiene can be isotactic or syndiotactic. Figure A3 shows the four different stereoregular structures. Isotactic polymer is formed when the monomer always approaches from the same side of the Mo=C bond (same CNO face). If the monomer approaches alternate CNO faces sequentially, a syndiotactic structure is produced. Experiments demonstrate that chiral R-groups on the catalyst enhance the degree of isotacticity of poly-NBDF6.[9]

In the research group of Professor Robert H. Grubbs, four new chiral molybdenum-based catalysts have been developed by Osamu Fujimura and used to catalyze asymmetric ring-closing metathesis[10-12] (Figure A4). Their structures seem to fulfill all the known requirements for a highly stereoselective ROMP-catalyst. The alkoxy-ligands contain electron-withdrawing perfluoroalkyl-groups, which should provide for sufficient activation of the initiator and consequently, result in all *cis* polymer. The chirality of the ligands should contribute to formation of an isotactic structure. This appendix describes studies on ROMP of 2,3-bis(trifluoromethyl)-

norbornadiene (NBDF6) and 2,3-bis(carbomethoxy)norbonadiene (NBDC) using these four initiators.

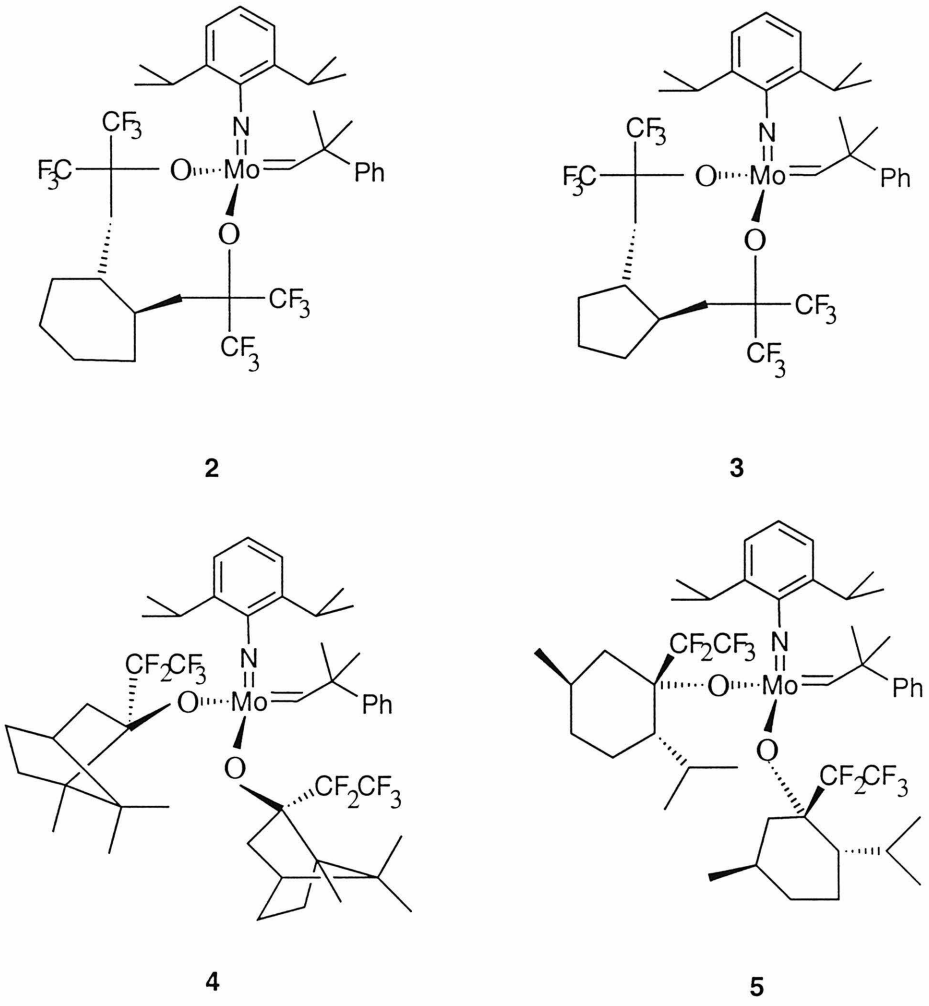

Figure A4: Structure of new ROMP-initiators with chiral ligands.

B. Experimental Section

General: Argon was purified by passage through columns of BASF R-11 catalyst (Chemalog) and 4 Å molecular sieves (Linde). NMR spectra were recorded on JEOL-GZ 400 spectrometer. Gel permeation chromatograms were obtained on a HPLC

system using an Altech model 426 pump, a Rheodyne model 7125 injector with a 100 μL injection loop, American Polymer Standards 10 micron mixed bed columns, a Viscotek differential refractometer and THF as eluent at a 1.0 mL/min flow rate.

Materials: Solvents used for polymerization were distilled from calcium hydride and degassed by repeated freeze-pump-thaw cycles. All other solvents were used without further purification unless otherwise noted. The starting materials for the synthesis of NBDF6 and NBDC were used as received from Aldrich Chemical Co. NBDF6 and NBDC were synthesized in analogy to literature procedures,[1] distilled under reduced pressure several times, dried over calcium hydride and degassed by repeated freeze-pump-thaw cycles. Compounds **2, 3, 4** and **5** were provided by Dr. Osamu Fujimura.

Typical polymerization procedure: In a glove box under nitrogen atmosphere 100 mg of a carefully purified monomer were dissolved in 1 ml of C_6D_6 or CD_2Cl_2. About 4 mg of the catalysts **3, 4, 5** or **6** (monomer : catalyst = 100 : 1) were dissolved in a few drops of the solvent and added to the stirring monomer solution all at once. The reaction mixture was placed in a sealed NMR-tube, which was taken out of the dry box to monitor the progress of the polymerization. After completion of the polymerization, the catalyst was deactivated through adding one drop of benzaldehyde to the reaction mixture. The polymer was precipitated into hexane and purified by dissolving in acetone and reprecipitating into hexane several times. The pure polymer was dried under vacuum of 10-20 mTorr over night.

Poly-NBDF6 prepared using initiator 2: ^{1}H NMR (d_6-acetone) δ 5.6 (bd, 2H), 4.2 (bd, 2H), 2.8 (bd m, 1H), 1.5 (bd m, 1H); ^{13}C NMR (d_6-acetone) δ 139.6 (m), 131.1, 125.2, 122.5, 119.7, 117.0, 43.9, 37.5, 36.8.

Poly-NBDF6 prepared using initiator 3: ^{1}H NMR (d_6-acetone) δ 5.6 (bd, 2H), 4.2 and 3.8 (bd, 2H), 2.8 (bd m, 1H), 1.5 (bd m, 1H); ^{13}C NMR (d_6-acetone) δ 139.6 (m), 132.6, 131.1, 125.2, 122.5, 119.7, 117.0, 49.1, 43.9, 37.5, 36.8.

Poly-NBDC prepared using initiator 2: ^{1}H NMR (CD_2Cl_2) δ 5.4 (bd, 2H), 3.9 (bd, 2H), 3.5 (bd, 3H) 2.2 (bd m, 1H), 1.3 (bd m, 1H); ^{13}C NMR (CD_2Cl_2) δ 165.2, 142.3, 131.5, 51.8, 44.2, 38.9, 38.5.

Poly-NBDC prepared using initiator 3: ^{1}H NMR (CD_2Cl_2) δ 5.4 (bd, 2H), 3.9 (bd, <2H), 3.5 (bd, >3H), 2.2 (bd m, 1H), 1.3 (bd m, 1H); ^{13}C NMR (CD_2Cl_2) δ 165.2, 142.3, 132.6, 131.5, 51.8, 49.0, 44.2, 38.9, 38.5.

C. Results and Discussion

The norbornodiene monomers 2,3-bis(trifluoromethyl)norbornadiene (NBDF6) and 2,3-bis(carbomethoxy)norbonadiene (NBDC) were synthesized through Diels-Alder-reactions of cyclopentadiene and substituted alkynes[1] (Scheme A1).

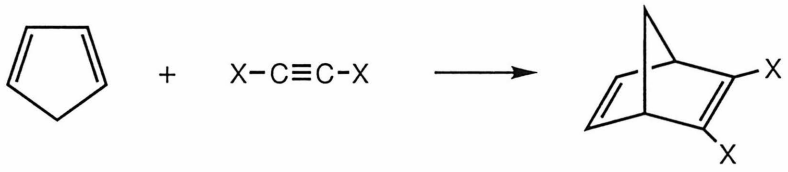

7: X = CF_3 (NBDF6)
8: X = $COOCH_3$ (NBDC)

Scheme A1: Synthesis of substituted norbornadienes.

Polymerization of NBDF6 and NBDC was initiated using complexes **2 - 5** and monitored by ^{1}H-NMR. The resulting polymers were characterized by ^{1}H-, ^{13}C-NMR. The tacticity was determined from the ^{13}C-MNR-spectrum.[13] The *cis/trans* ratio can be deducted from the ^{1}H- or the ^{13}C-NMR. Table A1 summarizes the main experimental results.

Table A1: Results of the polymerization experiments.[a]

	Poly-NBDF6	**Poly-NBDC**
3	polymerization complete in 3 h 100% cis; 95% cis isotactic PDI = 1.05	polymerization complete in 7 min 100% cis; 96% cis isotactic PDI = 1.24
4	polymerization complete in 1.5 h 90% cis; 70% cis isotactic PDI = 1.30, MN = 45600	polymerization complete in less then 2 min 88% cis; 77% cis isotactic PDI = 1.35
5, 6	polymerization very slow; poor initiation 80% cis; atactic PDI ca. 1.8	no ROMP polymer could be obtained

[a]Conditions: initial monomer concentration 100mg/ml; solvent methylene chloride; monomer/catalyst ratio 100:1; room temperature; GPC-data vs. polystyrene.

Since the properties of the initiators **2** and **3** are very different from the properties of the initiators **4** and **5**, the results will be discussed separately.

Results with initiators containing chelating chiral ligands: Catalysts **2** and **3** successfully polymerized NBDF6 and NBDC by ROMP. The progress of polymerization was monitored by ^{1}H-NMR. The carbene signal of the free initiator disappeared immediatly after starting the reaction, showing good initiation. No carbene signal for the propagating species was detected.

The polymerization using initiator **2** proceeds slower then the polymerization using initiator **3**. This is consistent with previous results,[10-12] since catalyst **2** was also found to be less active in ring-closing metathesis.

The *cis/trans* ratio of the polymers can be determined from the ^{13}C-NMR spectrum looking at the chemical shift of the signal for the carbons in position 1 and 4 or the carbons in position 5 and 6[13] (Table A2). Both initiators produced high *cis* polymers, the polymers being 100% *cis* in the case of **2** and 90% *cis* in the case of **3** as seen by ^{13}C-NMR. The different degree of stereoregularity was also apparent from the physical properties of the polymers. Polymers with lower stereoregularity produced using **3** exhibited higher solubilities in organic solvents. The bias towards *cis* was expected, since the electronwithdrawing CF_3-substituents on the alkoxy-ligands are known to enhance catalyst activity leading to fast propagation rates and preferential formation of *cis* double bonds.

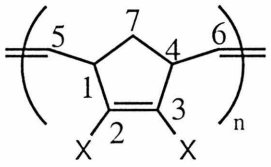

Table A2: ^{13}C-NMR data for the determination of *cis/trans* ratio.

	Poly-NBDF6	**Poly-NBDC**
3	C 1,4: δ 43.94[a] C 5,6: δ 131.14[a]	C 1,4: δ 43.94[a] C 5,6: δ 131.14[a]
4	C 1,4: δ 49.12 (90%)[a], 43.94 (10%)[b] C 5,6: δ 132.6 (90%)[a], 131.14 (10%)[b]	C 1,4: δ 44.24 (88%)[a], 49.00 (12%)[b] C 5,6: δ 131.51 (88%)[a], 132.60 (12%)[b]

[a]*cis*; [b]*trans*

The lower *cis* content of the polymer produced using **3** is surprising. **3** is obviously more active than **2**. The polymerization goes to completion twice as fast. Therefore, one would expect the *syn* propagation to compete more successfully with the rotamer interconversion resulting in an even greater possibility for *cis* bond formation.

A likely explanation for this observation is the occurrence of secondary metathesis processes. The growing polymer chain contains double bonds, which may interact with the catalyst. This interaction results in rearrangement of *cis* double bonds to thermodynamically more favored *trans* double bonds and can also lead to degradation of the polymer chains broadening the molecular weight distribution. Secondary metathesis is more likely to be found in systems containing a very active catalyst. Since **3** appears to be very active, it could react with the growing polymer chain partially transforming the initially formed *cis* bonds into *trans*, which would explain the lower *cis* content.

The coordination of polymer double bonds to the metal center of the catalyst is sterically disfavored. Secondary metathesis processes are therefore observed only at low monomer concentrations (shortly before or after completion of the polymerization). If *trans* double bonds are caused by secondary metathesis, terminating the polymerization at low conversion should result in higher *cis* content of the polymer. However, using **3** as initiator, exactly the same *cis/trans* ratio was found at 25%, 50% and 100% conversion, indicating that the *trans* double bond formation is not due to secondary metathesis processes.

The observed *cis/trans* content shows that the ratio of *syn* propagation rate *versus* the rate of rotamer interconversion is less favorable for **3** than for **2**. Since the propagation rate for **3** is faster than for **2**, the rate of rotamer interconversion must be

remarkably faster for **3** than for **2**. An experimental result to support this claim can not be presented here. *Syn*- and *anti*-rotamers have different carbene signals in the ^{1}H-NMR, but since no propagating carbene was observed, nothing can be said about the *syn/anti*-ratio during the polymerization.

The *cis/trans* ratio is solvent and temperature dependent. The reported ratios were obtained in non-coordinating solvents benzene and methylene chloride. If THF is used as solvent, the polymerization is much slower and gives a *cis/trans* ratio of 1:2. THF coordinates to the catalyst slowing down the propagation and changing the geometry of the propagating species. Furthermore, increased temperature leads to preferred formation of thermodynamically favored *trans* double bonds. The reported numbers are room temperature values. Less stereoregular polymers are obtained at higher temperatures. In case of initiator **3**, slightly improved stereoregularity was observed, when the polymerization was performed at 0 °C.

The tacticity of the polymers can be determined from the ^{13}C-NMR spectrum looking at the chemical shift of the signal for the carbon in position 7[13] (Table A3). Poly-NBDF6 and poly-NBDC prepared using **2** are highly isotactic (95 % and 96 %, Table A1), wich demonstrates, that the chelating chiral ligand efficiently blocks one side of the CNO-face of the initiator. The polymers prepared using **3** are also clearly biased towards isotacticity, showing once more the directing effect of the chelating chiral ligand.

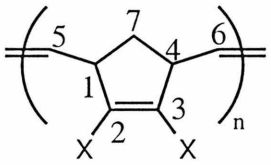

Table A3: ^{13}C-NMR data for the determination of tacticity.

	Poly-NBDF6	Poly-NBDC
3	C 7: δ 37.51 (95%)[a], 36.79 (5%)[b]	C 7: δ 38.87 (96%)[a], 38.50 (4%)[b]
4	C 7: δ 37.51 (70%)[a], 36.79 (30%)[b]	C 7: δ 38.89 (77%)[a], 38.52 (23%)[b]

[a] isotactic; [b] syndiotactic

All-*cis* isotactic poly-NBDF6 is an interesting ferroelectric material.[4,5] Compound **2** is a new initiator for the synthesis of monodispersed highly tactic poly-NBDF6. The obtained stereoregularity is very high.

Using initiator **2** a narrow molecular weight distribution (Table A1) can be obtained for poly-NBDF6, if the initiator is deactivated right after completion of the polymerization. However, the polymerization is not living. Experiments demonstrate, that chain transfer, chain termination and side reactions take place during polymerization and after 100% conversion is reached. Leaving the polymer in the presence of the active catalyst for two hours results in an increase of the PDI from 1.05 to 1.4. It is not possible to make well-defined block-copolymers and the molecular weight of the polymer does not depend linearly on the monomer to catalyst ratio.

Results with initiators containing non-chelating chiral ligands: The compounds **4** and **5** have been found to exhibit very slow initiation rates.

When **4** and **5** were added to a solution of NBDF6, ^{1}H- and ^{13}C-NMR showed no consumption of the monomer at room temperature and at 40 °C over a period of 3 days.

The observed alkylidene signals were those of the free complexes indicating that NBDF6 did not interact with **4** and **5** under the polymerization conditions. Heating to 75 °C for 5 days resulted in 40-50% monomer conversion and catalyst decomposition. The obtained polymers were 80% cis, atactic and had PDIs around 1.8.

Similar observations have been made for NBDC. A ROMP polymer could not be obtained, since heating of the reaction mixture leaded to formation of an intractable gel.

In conclusion, the compounds **4** and **5** are not suitable as initiators for ring-opening metathesis polymerization of substituted norbornadienes. In contrast to active ROMP catalysts **2** and **3**, the alkoxy-ligands on the complexes **4** and **5** have only one flourinated substituent. Thus, the complexes **4** and **5** are less electron-deficient and consequently, less activated towards olefin metathesis.

D. References and Notes

(1) Alimuniar, A.; Blackmoore, P. M.; Edwards, J. H.; Feast, W. J.; Wilson, B. *Polymer* **1986,** *27,* 1281.

(2) Thoi, H. H.; Ivin, K. J.; Rooney, J. J. *J. Mol. Cat.* **1982,** *15,* 245.

(3) Schrock, R. R.; Lee, J. K.; O'Dell, R.; Oskam, J. H. *Macromolecules* **1995,** *28,* 5933.

(4) Davies, G. R.; Almond, P. J.; Hubbard, H. V.; Ward, I. M. *Macromol. Symp.* **1996,** *102,* 73.

(5) Davies, G. R.; Hubbard, H. V.; Ward, I. M.; Feast, W. J.; Gibson, V. C.; Khosravi, E.; Marshall, E. L. *Polymer* **1995,** *36,* 235.

(6) Oskam, J. H.; Schrock, R. R. *J. Am. Chem. Soc.* **1993,** *115,* 11831.

(7) Bazan, G. C.; Khosravi, E.; Schrock, R. R.; Feast, W. J.; Gibson, V. C. *J. Am. Chem. Soc.* **1990,** *112,* 8378.

(8) Feast, W. J.; Gibson, V. C.; Khosravi, E.; Marshall, E. L. *J. Chem Soc. Chem. Commun.* **1994,** 9.

(9) McConville, D. H.; Wolf, J. R.; Schrock, R. R. *J. Am. Chem. Soc.* **1993,** *115,* 4413.

(10) Fujimura, O.; Grubbs, R. H. *J. Am. Chem. Soc.* **1996,** *118,* 2499.

(11) Fujimura, O.; de la Mata, J.; Grubbs, R. H. *Organometallics* **1996,** *15,* 1865.

(12) Fujimura, O.; Grubbs, R. H. *J. Org. Chem.* **1998,** *63,* 824.

(13) O'Dell, R.; McConville, D. H.; Hofmeister, G. E.; Schrock, R. R. *J. Am. Chem. Soc.* **1994,** *116,* 3414.